NOTE TO USERS

Study of Elliptically Symmetrical Two-dimensional Digital Filters Possessing Separable Denominator Transfer Functions

Keerthi Chandra Lavu

A Thesis

in

The Department

of

Electrical and Computer Engineering

Presented in Partial Fulfillment of the Requirements

for the Degree of Master of Applied Science at

Concordia University

Montréal, Québec, Canada

June 2004

Your file Votre référence
ISBN: 0-612-94704-1
Our file Notre référence
ISBN: 0-612-94704-1

ABSTRACT

Study of Elliptically Symmetrical Two-dimensional Digital Filters Possessing Separable Denominator Transfer Functions

Keerthi Chandra Lavu

Two-dimensional digital filters are being widely used in modern image processing software for various types of analysis. The main objective of this thesis has been to implement two-dimensional filter functions using simple design procedures such that the presence of elliptical symmetry in such designed filters are obtained by parameter modifications. In keeping with the simple design criteria, the two-dimensional filters studied in this thesis have been designed starting from a product of two one dimensional filters. Only IIR Filters have been considered for this purpose due to their flexibility in terms of altering filter parameters to obtain new filters. The filters have been checked for stability before analysis. The design has made use of the fact that varying the feedback factor 'k' in an IIR filter produces a near-elliptical symmetric response for certain values of 'k_1' and 'k_2' having specific magnitude ranges.

Algorithms have been obtained to check the extent of elliptical symmetry under specific magnitude ranges and to correct the feedback factors 'k_1' and 'k_2' in order to obtain the maximum proximity to elliptical symmetry. The lowpass filter has been primarily chosen to illustrate the objective of the thesis. The stability conditions for different order filters have been analyzed. Both Butterworth and Chebyshev filters have been studied. This study has also focused on the effect of changing the pole- parameters (polar angles) in two-dimensional lowpass filter functions and its contribution to elliptical symmetry.

The common filter types namely lowpass, bandpass, bandstop and highpass, as well as their combinations of lower order (fourth) in two dimensions have been studied and analyzed for elliptical symmetry.

Considerable success has been achieved in obtained near-elliptical symmetry especially among the two-dimensional lowpass filters and also in other types of filters. It has also been found that there exists numerous possibilities to achieve near elliptical symmetry based on parameter modifications (values of k_1 and k_2) and magnitude range of the filter under study.

Dedicated to my parents, brother and uncle

ACKNOWLEDGEMENTS

At the outset, I would like to express my sincere gratitude to my supervisor Dr. Venkat Ramachandran for providing the guidance and support that made this work possible. I am grateful for his extremely careful and thorough review of my thesis, and for his inspiration throughout the course of this work. I feel privileged for having the opportunity to work with him.

I would like to express my gratitude and appreciation to Dr. Anjali Agarwal and Dr. Henry Hong for their valuable suggestions to improve this Thesis. I would also like to thank all my teachers who were of great support throughout my academic life.

I am heartily grateful to my parents, brother and grandmother for their love, support and sacrifices that they made in bringing me up. I would like to express my deepest gratitude for my uncles, aunts and cousins who supported me with their love and understanding.

Finally, I would like to thank all my friends for their help and advice.

TABLE OF CONTENTS

LIST OF TABLES

LIST OF FIGURES

LIST OF AND ABBREVIATIONS AND SYMBOLS

z_1, z_2	Z-domain parameter in first and second dimensions.
s_1, s_2	Laplace domain parameter in first and second dimensions.
ω_1, ω_2	Frequencies in radians in the analog domain parameter in first and second dimensions.
H	Frequency response of a filter.
T	Transfer function of a filter.
k	Stability Condition of an IIR filter.
k_1, k_2	Feedback factors in an IIR Transfer Function in first and second dimensions.
S_1, S_2, S_3	Pole locations in a Lowpass filter.
α	Gain of a transfer function in decibels.
β	Polar angle in degrees.
$\beta_1, \beta_2, \beta_3$	Poles of a transfer function.
ε	Ripple width of a chebyshev filter.
ω_{pk}, θ_{pk}	Magnitude and angle (in degrees) of a pole-phasor.
Q	Q-factor.
ω_n	Natural frequency of a Butterworth filter in the analog domain (radians).
MDS	Multi-dimensional System.
2-D	Two-dimensional.
FIR	Finite Impulse Response.
IIR	Infinite Impulse Response.

VSHP	Very Strictly Hurwitz Polynomial.
NFSK	Non-essential Singularity of First Kind.
NSSK	Non-essential Singularity of Second Kind.
BIBO	Bounded Input Bounded Output.
VCTF	Variable Characteristics Transfer Function.
CPP	Complementary Pole Pairs.
LPF	Low Pass Filters.
BPF	Band Pass Filters.
BSF	Band Stop Filters.
HPF	High Pass Filters.

Chapter 1

Introduction

The topic of Multidimensional system (MDS) analysis and design has attracted considerable attention during recent years and is still receiving increased attention by theorists and practitioners. Multi-dimensional signal processing has many applications in modern-day devices, softwares and many practical systems, because of which, this subject is still being investigated in important areas such as facsimile, television, sonar, bio-medicine, remote sensing, underwater acoustics, moving-objects recognition, robotics and so on. Problems of different aspects have been thoroughly studied and these include modeling, stability, structure analysis and realizations, digital filter design, multi-dimensional signal processing, reconstruction and so on. Many important results have been obtained [1].

Specifically, interest has been directed by researchers into the area of two-dimensional(2-D) digital systems due to several reasons: high efficiency due to high-speed computations, permitting high quality image processing and analysis, great application flexibility and adaptivity, decreasing cost of software or hardware implementations due to the large expansion and evolution of standard computers, microcomputers, microprocessors, and high-integration digital circuits. In this respect, digital systems have taken over in implementation [1]. Two-dimensional signal processing and analysis has evoked a lot of interest among researchers due to their

numerous advantages in areas such as image processing.

The two-dimensional digital systems perform important operations which include: 2-D digital filtering, 2-D digital transformations, local space processing, data compression, and pattern recognition. Digital filtering, digital transformations, and local space operators play important roles in preprocessing of images, performing smoothing, enhancement, noise reduction, extracting boundaries and edges before pattern recognition, data compression operations permitting the reduction of large number of data representing the images in digital form and solving or minimizing transmission and storage problems. Pattern recognition operations permit the extraction of significant information and configurations from the images for final interpretation and utilization [1], [2].

Over the past decade, researchers have shown particular interest in two-dimensional (2-D) filters, both recursive and non-recursive, These 2-D filters find increasing applications in many fields, such as image processing and seismic signal processing. In many of these applications, the signal does not have any preferred spatial direction, and so the required filter functions, possessing circular, elliptical and other symmetric frequency response characteristics are finding great importance. Also 2-D filters find increasing applications in image restoration and enhancement [1]. As an example, two dimensional highpass filtering removes the unwanted background noise from an image so that the details contained in the higher spatial frequencies are easier to perceive.

1.1 Two-Dimensional Digital filters

In general, similar to one-dimensional (herewith referred to as 1-D) digital filters, 2-D filters can be classified into two main groups. The first group comprises a finite sequence transfer function and so the filters in this group are called Finite Impulse Response(FIR) filters. The second group comprises infinite sequence transfer function and so the filters in this group comprises an infinite sequence transfer function

and so the filters in this group are called Infinite Impulse Response(IIR) filters.

1.1.1 Finite Impulse Response Filters(FIR Filters)

The transfer function of 2-D FIR filters can be described by using 2-D z-transform as follows [1]:

$$H(z_1,\, z_2) = \sum_{n_1=0}^{M} \sum_{n_2=0}^{N} A_{n_1 n_2} z_1^{-n_1}\, z_2^{-n_2} \tag{1.1}$$

Eqn.(1.1) implies that some of the 1-D design methods can be directly extended to two (2-D) or more dimensions (m-D) by appropriate modifications in the design procedures. It should also be noted that a straight extension of 1-D technique to 2-D design may not always be possible. In the 2-D FIR filters, problems of stability do not occur since the impulse response is bounded and exists only for finite time duration or the stability of $h(z_1,\, z_2)$ is guaranteed. Therefore

$$\sum_{n_1=0}^{M} \sum_{n_2=0}^{N} |h(z_1,\, z_2)| < \infty \tag{1.2}$$

for all finite values of M and N.

1.1.2 Infinite Impulse Response Filters(IIR Filters)

The transfer function of 2-D IIR filters can be described by using 2-D z-transform [1] and can be expressed as a ratio of two variable polynomials as follows:

$$H(z_1,\, z_2) = \frac{N(z_1,\, z_2)}{D(z_1,\, z_2)} = \frac{\sum_{i=0}^{I} \sum_{j=0}^{J} a_{ij} z_1^{-i} z_2^{-j}}{\sum_{k=0}^{K} \sum_{l=0}^{L} b_{kl} z_1^{-k} z_2^{-l}} \tag{1.3}$$

where $b_{00} = 1$, $a_{ij}\, and\, b_{kl}$ are real coefficients.

For any input signal $X(z_1,\, z_2)$, the output $Y(z_1,\, z_2)$ of the filter is given by,

$$Y(z_1,\, z_2) = H(z_1,\, z_2) \cdot X(z_1,\, z_2) \tag{1.4}$$

In the 2-D IIR filters, one important problem to be dealt with is stability. According to the stability theorem [2], [3], the 2-D IIR filter is guaranteed to be stable in the bounded-input bounded-output(BIBO) sense, if there exists no value of z_1 and z_2 for which

$$D(z_1, z_2) = 0 \, for \, both \, |z_1| \geq 1 \, and \, |z_2| \geq 1 \tag{1.5}$$

exists [1]. This means it is highly preferable that the given analog transfer function must have Very Strictly Hurwitz Polynomial(VSHP) denominator [3], [4]. In the Laplace domain, the polynomial $D(s_1, s_2)$ is said to be VSHP if $(1/D(s_1, s_2))$ does not possess any singularities in the region (s_1, s_2) with $Re(s_1) \geq 0$ and $Re(s_2) \geq 0$. Therefore , the design of a 2-D IIR filter requires obtaining the coefficients a_{ij} and b_{kl} in Eqn.(1.3) so that $H(e^{j\omega_1 t_1}, e^{j\omega_2 t_2})$ approximates a given response $G(j\omega_1, j\omega_2)$ where ω_1 and ω_2 are horizontal and vertical spatial frequencies respectively, which also ensures the stability of the filter. If we obtain a transfer function whose denominator is a VSHP and then obtain a corresponding digital transfer function by using the double bilinear transformation given by

$$s_i \rightarrow \frac{z_i - 1}{z_i + 1}, \; i = 1, 2 \tag{1.6}$$

then we can guarantee stability in the digital domain also.

1.2 Symmetry Types associated with 2-D Transfer Functions

Two and higher dimensional systems may possess different types of symmetries. These symmetries have been used to reduce the complexity of the design and implementation of systems [5].

To understand how symmetry concept is extended to mathematical functions, consider a real function $f(x_1, x_2)$ of two independent variables x_1 and x_2. The function $f(x_1, x_2)$ assigns a unique value to each pair of values of x_1 and x_2 and so may be represented by a three dimensional object having the (x_1, x_2) plane as

the base and the value of the function at each point in the plane as the height. We may say that a function possesses a symmetry, if a pair of operations, performed simultaneously, one on the base of the function object (i.e.,(x_1, x_2) plane), and the other on the height of the object(function value) leaves the function undisturbed.

In other words, existence of symmetry in a function implies that the value of the function at (x_{1T}, x_{2T}) meets a certain requirement or condition, where (x_{1T}, x_{2T}) is obtained by some operation on (x_1, x_2) and this condition being satisfied for all points in the region.

Most of the applications require that a 2-D digital filter shall have a certain symmetry in its magnitude response. This symmetry property can be used in the reduction of the number of multiplications in the implementation of these filters and also in the reduction of the number of variables in the optimization procedure. The following gives a brief review of the different symmetry constraints [5].

1.2.1 Displacement(Identity) Symmetry

If a function possesses displacement identity symmetry with a displacement of d, the symmetry conditions on the function can be expressed as

$$f(x+d) = f(x) \ \vee x \in X \tag{1.7}$$

1.2.2 Rotational Symmetry

Choosing the rotational center as the origin ant the rotation angle as $\pi/2$ radians, we get the four-fold rotational symmetry condition as

$$f(x_1, x_2) = f(-x_2, x_1) \bigvee x \in X \tag{1.8}$$

following which we have

$$f(x_1, x_2) = f(-x_2, x_1) = f(-x_1, -x_2) = f(x_2, -x_1) \tag{1.9}$$

1.2.3 Centro-Symmetry

In the two-variable case, twofold rotational symmetry(rotation by π radians) is called centro-symmetry. The required condition for centro-symmetry is

$$f(-x_1, -x_2) = f(x_1, x_2) \bigvee x \in X \tag{1.10}$$

1.2.4 Centro-Anti Symmetry

In the two-variable case, the required condition for centro-anti symmetry is

$$f(-x_1, -x_2) = -f(x_1, x_2) \bigvee x \in X \tag{1.11}$$

1.2.5 Centro-Conjugate Symmetry

In the two-variable case, the required condition for centro-conjugate symmetry is

$$f(-x_1, -x_2) = [f(x_1, x_2)]^\star \bigvee x \in X \tag{1.12}$$

1.2.6 Centro-Conjugate Anti Symmetry

In the two-variable case, the required condition for centro-conjugate anti symmetry is

$$f(-x_1, -x_2) = [-f(x_1, x_2)]^\star \bigvee x \in X \tag{1.13}$$

1.2.7 Reflection Symmetry

Reflections about the x_1 axis, the x_2 axis, and the diagonals $x_1 = x_2$ and $x_1 = -x_2$ line, respectively, result in reflection symmetries which could be anyone of the following:

$$x_1 \, axis \, reflection \rightarrow f(x_1, -x_2) = f(x_1, x_2) \tag{1.14}$$

$$x_2 \, axis \, reflection \rightarrow f(-x_1, x_2) = f(x_1, x_2) \tag{1.15}$$

$$x_1 = x_2 \, line \, intersection \rightarrow f(x_2, x_1) = f(x_1, x_2) \tag{1.16}$$

$$x_1 = -x_2 \, line \, intersection \rightarrow f(-x_2, -x_1) = f(x_1, x_2) \tag{1.17}$$

$$180^\circ \, rotation \, about \, the \, origin \rightarrow f(-x_1, -x_2) = f(x_1, x_2) \tag{1.18}$$

$$90^\circ \, rotation \, about \, the \, origin \rightarrow f(x_2, -x_1) = f(x_1, x_2) \tag{1.19}$$

1.2.8 Quadrantal Symmetry

The condition on the function to possess quadrantal identity symmetry is

$$f(x_1, x_2) = f(-x_1, x_2) = f(-x_1, -x_2) = f(x_1, -x_2) \tag{1.20}$$

It is easy to verify that the four quadrants of the X-plane correspond to the four symmetry regions. Hence this symmetry is called quadrantal symmetry.

1.2.9 Diagonal Fourfold reflection Symmetry

Similar to the quadrantal case, if the function possesses reflection symmetry with respect to the $x_1 = x_2$ line and the $x_1 = -x_2$ line simultaneously, it is supposed to possess diagonal fourfold reflection symmetry

$$f(x_1, x_2) = f(x_2, x_1) = f(-x_2, -x_1) = f(-x_1, -x_2) \tag{1.21}$$

As in quadrantal symmetry, the function possesses two-fold rotational symmetry when it possesses diagonal fourfold reflection symmetry.

1.2.10 Octagonal Symmetry

In this case the function possesses quadrantal symmetry and diagonal symmetry simultaneously. The conditions for a function to posses octagonal symmetry are given by

$$f(x_1, x_2) = f(x_1, -x_2) = f(-x_1, x_2) = f(x_2, x_1)$$

$$= f(-x_2, -x_1) = f(-x_1, -x_2) = f(x_2, -x_1) = f(-x_2, x_1) \tag{1.22}$$

1.2.11 Circular Symmetry

Mathematically, circular symmetry in 2-D filter responses can be defined as the filter response being able to satisfy the general equation of a circle, according to which,

$$\omega_1^2 + \omega_2^2 = M \tag{1.23}$$

where ω_1 and ω_2 are the frequencies in the two dimensions, and M is the magnitude response which needs to be a constant in order to satisfy the circular symmetry property.

The function relation for circular symmetric response in ω plane is given by[6]

$$\widehat{H}_1(\omega_1^2)\widehat{H}_2(\omega_2^2) = H_s(\omega_1^2 + \omega_2^2) \tag{1.24}$$

where $\widehat{H}(\omega_1^2)$ and $\widehat{H}(\omega_2^2)$ are the transfer functions of both the dimensions.

1.2.12 Elliptical Symmetry

Similar to the circular case, elliptical symmetry in 2-D filter responses can be defined as the filter response being able to satisfy the general equation of an ellipse, according to which,

$$\frac{\omega_1^2}{a_1^2} + \frac{\omega_2^2}{a_2^2} = M \tag{1.25}$$

where ω_1 and ω_2 are the frequencies in the two dimensions, and M is the magnitude response which needs to be a constant in order to satisfy the elliptical symmetry property.The Magnitude 'M' takes both the axes(major and minor) into account when a constant value for it is chosen and a_1 & a_2 corresponding to a magnitude M.

By replacing ω_1 by $\alpha\omega_1$ and ω_2 by $\beta\omega_2$ in Eqn.(1.24), we obtain the function relation for elliptic symmetric separable functions.

Thus an ideal elliptical symmetric 2-D magnitude squared function is given by [6]

$$H(\omega_1^2,\, \omega_2^2) = \lambda \exp(\alpha\omega_1^2 + \beta\omega_2^2) \tag{1.26}$$

In order to approximate elliptical symmetry, a product separable function given by,

$$H(s_1,\, s_2) = h_1(s_1)h_2(s_2) \tag{1.27}$$

is considered.

From the above, the following can be deduced:

(1)Any separable function $H(s_1,\, s_2) = h_1(s_1) \times h_2(s_2)$ is quadrantally symmetric.

(2)When $h_1(.) = h_2(.)$, $H(s_1,\, s_2)$ is also octagonally symmetric, where $h_1(.)$ is a single variable function.

(3)For the magnitude of elliptical symmetry being the main criterion, $|h_1(j\omega_1)|^2$ should approximate $\lambda e^{\alpha\omega_1^2}$ for suitable values of λ and α.

(4) When stable, all-pole 2-D transfer functions are constrained to possess quadrantal symmetry, they turn out to be separable.

(5) $H(s_1,\, s_2)$ is said to possess elliptical(rectangular) symmetry if its magnitude is invariant on a set of specified elliptical(rectangular) paths around the origin in the ω plane.

1.3 Realization of the 2-D Filter Functions

The realization of the filter networks from the transfer function can be accomplished using the following important methods:

1.3.1 Direct Method

All 2-D transfer functions can be realized using this method. This realization follows from the algorithm given by Shank [7].

It can be shown that Eqn.(1.3) can be written as

$$Y(z_1, z_2) = \left(\sum_{i=0}^{I} \sum_{j=0}^{J} a_{ij} z_1^{-i} z_2^{-j} \star X(z_1, z_2) \right) - \left(\sum_{k=1}^{K} \sum_{l=1}^{L} b_{kl} z_1^{-k} z_2^{-l} \star Y(z_1, z_2) \right) \tag{1.28}$$

The above equation can be directly realized using different approaches [8]. However, one main limitation of direct realization is that it results in high round-off errors.

1.3.2 Parallel Realization

In this case the given 2-D transfer function is to be expanded, where possible, into partial fractions. Each of such function is realized suitably and they are connected in parallel.

1.3.3 Cascade Realization

Here, it is required that the given 2-D transfer function is expressed as a product of several lower order 2-D transfer functions which may not always be possible since a 2-variable polynomial, in general, is not factorizable. It is noted here that when the 2-D function may be expressed as a product of realizable low-order functions, then a cascade type of realization can be used.

1.3.4 Wave Realization

This realization starts from a given analog network which is transformed into digital domain by a double bilinear transformation. As is evident, exact realizations of the product separable transfer functions are not possible [9].

1.4 Scope of the Thesis

Finite impulse frequency response (FIR) filter functions possessing nearly elliptical symmetric responses can be generated from 1-D FIR functions [10]. This procedure cannot, however, be used to generate 2-D infinite impulse response (IIR) functions approximating elliptical symmetry, as the application of such a transformation to a 1-D IIR function results in a 2-D IIR function which is not, in general, factorizable into a set of quarter-plane or half-plane stable functions without further effort [11].

It has been recently proved that if a quarter plane filter possesses quadrantal symmetry in its magnitude response, then its denominator can be expressed as a product of two 1-D polynomials [6], [12]. It can be readily verified that the presence of elliptical symmetry implies the presence of octagonal, and hence, quadrantal symmetries. Therefore it is reasonable to constrain the desired function to possess octagonal symmetry in its magnitude response and to choose the filter function with a product separable denominator. The main scope of this thesis is to choose and study such filter functions. A choice of such type eliminates the necessity for checking the stability of the filter during the approximation stage of the design. The denominator product separable constraint restricts the domain of functions for filters which do not possess quadrantal symmetry in their frequency responses over which approximation is carried out and results in suboptimal solutions. Since there is no constraint on the numerator polynomials, the types of responses one can approximate using separable denominator filter functions seems to be practically unlimited. Also, in order to obtain good elliptical symmetry and frequency selective

characteristics, one may opt for non-separable functions.

In this thesis, the common types of filter responses namely lowpass, highpass, bandpass and bandstop have been considered in detail with respect to the above mentioned theory are used. In all the above cases, separable denominator transfer functions are being considered. So, the 2-D filters will be studied as an extension to the 1-D counterpart. All the 2-D filter designs considered in this thesis work will therefore be derivations from two 1-D filters. This is also the simplest of all conventional 2-D filter designs in effect and therefore gives a lot of scope for future work.

In Chapter-2, lowpass filters obtained from Butterworth, Chebyshev and pole parameter transformations have been utilized in-order to design 2-D filters of approximate elliptical symmetry. First the stability conditions for all the orders of with different shifts in the poles of Butterworth filters are tabulated using the "Very Strict Hurwitz Polynomial(VSHP)" concept [3]. Also the elliptical symmetry conditions which fall under the stability regions are obtained for the corresponding filters. The lowpass filter will be chosen as the basis of comparison for the distinctly different types of filters, studied in this chapter. The effect of pole-parameter transformation and its effect on performance of the filter will then be studied. In this respect, first we point out that the pole vectors of the Butterworth filters(of order $n = 2^k$) can be subjected to "prescribed symmetrical swinging"[13], such that certain symmetry properties present in the original pole-pattern can be maintained invariant. Here we discuss the family of filters called "2-D Complementary Pole-Pair Filters(2-D CPPF's)", generated by exploiting the symmetry invariant property as mentioned above. The performance of the new filters obtained are studied. The effect of this symmetrical swinging affecting the elliptical symmetry of these types of filters will also be studied.

In Chapter-3, transformations of the highpass, bandpass and bandstop Butterworth filters will be implemented and their approximation to near elliptical symmetry for each case will be studied. The Chebyshev filter design for these types of filters and their comparison to the Butterworth counterpart will be left as a scope for future study.

In Chapter-4, we will investigate the possibilities of combining different 2-D Butterworth filters to form unique transfer functions and therefore unique filter responses. The possibility of elliptical symmetry after the combination of two transfer functions will be studied. It is possible to obtain user specific responses by such combination filters. In this chapter, three different designs of combination filters will be considered and studied.

The basic goal, underlying in all of the above study, is to emphasize on the possibility of near elliptical symmetry starting with filters possessing separable denominators and their combinations. Elliptical symmetry will also be one of the most important aspect of commonly used filters, in emerging fields. The main goal of this thesis is obtain the nearest approximation of such filters with the simplest design methods possible.

Chapter-5 gives the summary, conclusions and some directions for future investigations.

Chapter 2

Generation of Stable Lowpass IIR 2-D Transfer Functions Possessing Near-elliptical Symmetry

2.1 Introduction

In order to design a filter having required specifications, one can suitably choose a transfer function with no common factors between the numerator and the denominator. Specifically in 1-D systems in the s-domain(analog domain), let

$$H_a(s) = \frac{N_a(s)}{D_a(s)} \tag{2.1}$$

be transfer function with $N_a(s)$ and $D_a(s)$ being relatively prime. For the above function to be stable, we must have $D_a(s)$ to be a Strictly Hurwitz Polynomial(SHP). A strictly Hurwitz polynomial is one which contains its zeros strictly in the left-half of s-plane. In a similar manner, if

$$H_d(z) = \frac{N_d(z)}{D_d(z)} \tag{2.2}$$

is a transfer function in the discrete domain with $N_d(z)$ and $D_d(z)$ being relatively prime, then $D_d(z)$ should be a Schur polynomial in order that $H_d(z)$ shall be stable

[3]. A Schur polynomial contains its zeros strictly within the unit circle.

A simple method to generate a 2-D transfer function is to combine two 1-D transfer functions as a product. In other words, the eventual 2-D sequence is separable as two 1-D sequences that can be expressed as

$$h(x_1, x_2) = f(x_1)g(x_2) \tag{2.3}$$

where $f(x_1)$ and $g(x_2)$ are 1-D functions of independent variables x_1 and x_2 respectively. Such sequences are a special class of 2-D sequences. The 2-D sequence $h(x_1, x_2)$ of this type has $(N_1 - 1)(N_2 - 1)$ degrees of freedom where

the region of support of $f(x_1)$: $0 \leq x_1 \leq N_1 - 1$ and

the region of support of $g(x_1)$: $0 \leq x_2 \leq N_2 - 1$

In the 2-D analog case in the s-domain, the transfer function may be expressed as

$$H_a(s_1, s_2) = \frac{N_a(s_1, s_2)}{D_a(s_1, s_2)} = \frac{m_n(s_1, s_2) + n_n(s_1, s_2)}{m_d(s_1, s_2) + n_d(s_1, s_2)} \tag{2.4}$$

where $m_n = even\ part\ of\ N_a(s_1, s_2)$,

$n_n = odd\ part\ of\ N_a(s_1, s_2)$,

$m_d = even\ part\ of\ D_a(s_1, s_2)$ and

$n_d = odd\ part\ of\ D_a(s_1, s_2)$,

The numerator $N_a(s_1, s_2)$ and the denominator $D_a(s_1, s_2)$ are polynomials in s_1 and s_2 with both even and odd terms. It may be possible that both the even and the odd parts of the polynomial become zero at specified sets of points, but not in their neighborhood. If this occurs in the denominator of the transfer function, it is called a non-essential singularity of the first kind(NSFK). If in the 2-D transfer functions both the numerator and denominator polynomials become zero simultaneously at a given set of points, it is known as non-essential singularity of the second kind(NSSK) [3].

The above two cases may be expressed as follows:

(a)$D_a(s_1, s_2) = 0$ and $N_a(s_1, s_2) \neq 0$ constitute non-essential singularity of the first kind at (s_1, s_2).

(b)$D_a(s_1, s_2) = 0$ and $N_a(s_1, s_2) = 0$ constitute non-essential singularity of the second kind at (s_1, s_2).

In the case of 2-D discrete or digital systems, a similar situation exists.

A well known method of designing digital filters is to start from the analog filter transfer function and then apply bilinear transformations $s_i \rightarrow \frac{z_i - 1}{z_i + 1}$, $i = 1, 2$, to obtain the corresponding digital filter transfer function [14]. In 1-D systems, such a transformation does not pose any problems. However in 2-D systems, this could pose problems concerning stability. In such cases, the denominator polynomial may cause problems because of non-essential singularities of first or the second kind. The occurrence of non-essential singularity of the first kind always results in an unstable filter [4]. The occurrence of non-essential singularity of the second kind could result in instability. However, it is not possible to determine, by inspection, if such a transfer function is stable or not [4], [15]. The next section discusses on the stability issue of filters.

2.2 Stability

As mentioned above, 2-D filters can be classified into two main categories namely the Finite Impulse Response Filters(FIR) and the Infinite Impulse Response Filters(IIR).

The Finite Impulse Response Filters have transfer functions resulting from a finite sequence and the Infinite Impulse Response Filters have transfer functions resulting from an infinite sequence.

One important issue concerning both the above types of Filters is the stability of the filter. Now it is known that Finite Impulse Response Filters are inherently stable. Infinite Impulse Response Filters may or may not be stable depending upon

the transfer function.

The most commonly used definition for stability is based on the bounded-input bounded-output(BIBO) criterion. This criterion states that a filter is stable if its response to a bounded input is also bounded. Mathematically, it is possible to show that for a causal linear shift-invariant systems, this corresponds to the condition that

$$\sum_{n_1=0}^{\infty} \sum_{n_2=0}^{\infty} |h(n_1, n_2| < \infty \tag{2.5}$$

where $h(n_1, n_2)$ is the impulse response of the filter.

The above definition points out an important observation that the stability criterion is always verified if the number of terms of the impulse response is finite which is the case with FIR Filters. However, the above condition does not prove feasible to the test of stability of IIR filters. In the 1-D case, it is possible to relate the BIBO stability condition to the positions of the z-domain transfer function poles which have to be within the unit circle and it is possible to test the stability by determining the zeros of the denominator polynomial. Similarly, in the 2-D case, a theorem establishing the relationship between the stability of the filter and the zeros of the denominator polynomial, can be formulated. This theorem states that [7], for causal quadrant filters, if $B(z_1, z_2)$ is a polynomial in z_1 and z_2, the expansion of $1/B(z_1, z_2)$ in the negative powers of z_1 and z_2 converges absolutely if and only if

$$B(z_1, z_2) \neq 0 \; for \; \{|z_1| \geq 1, |z_2| \geq 1\} \tag{2.6}$$

The above theorem has the same form as in the 1-D case, i.e., it relates the stability of the filter to the singularities of the z-transform. However, in the 2-D case such a formulation for stability condition does not produce an efficient method for stability test, as in 1-D, due to the lack of appropriate factorization theorem of algebra. Therefore, it is necessary in principle, to use an infinite number of steps to test the stability. Also, even if it is possible to find methods to test conditions

equivalent to Eqn.(2.6) in a finite number of steps [16], computationally it is not easy to incorporate them in a design method and there is a problem of stabilizing the filters which may become unstable.

From the point of view of stability tests, there can be two different approaches that can be considered, in designing an IIR filter. One method is to carry out the stability test in every stage of the filter design so that eventually the filter is stable. In the second method, stability is not considered as a part of the design and a magnitude squared transfer function is first designed. Then a stable filter is obtained, by choosing the poles in the stability region. Such an approach is convenient, because squared magnitude functions can be in a simple form ant it is easy to find the poles of the filter.

However, in the 2-D case, poles in the stability cannot be substituted for poles in the instability regions. This is because, unlike in the 1-D case, it is not possible to substitute the 2-D pole-pair combination by taking the inverse pole-pair transformation. Therefore different methods have to be used in arriving at a solution.

One possible solution can be obtained by considering this as a deconvolution problem. In the quadrant filter case, a filter $H(z_1, z_2)$ can be divided as a product of four filters ${}^{++}H(z_1, z_2)$, ${}^{+-}H(z_1, z_2)$, ${}^{--}H(z_1, z_2)$, ${}^{-+}H(z_1, z_2)$, each of which correspondingly represents their transfer function in the first, second, third and fourth quadrant, respectively, and each of which is stable, if computed through suitable sequence of computation. In view of the property that multiplication in the z-domain corresponds to a convolution in the space domain, the problem corresponds to the reconstruction of the four sequences. Similar procedures may be applied for two unsymmetrical half plane sequences. Thus it is possible to decompose the sequence into two half plane filters. However in both the above cases there are problems which can arise, as the cepstrum obtained using the above procedure are not finite in extent and some amount of truncation is necessary. This again modifies the transfer

function and also the minimum phase property cannot be guaranteed after truncation. It is possible to observe that half-plane filters, each being stable if a suitable sequence of computation is chosen, can give a direct method of obtaining linear phase filtering with IIR implementation. This is especially important when visual images have to be processed, because the shape of the object is related primarily to the phase information.

In addition to ensuring stability, it may be required to add some symmetry constraints as well. We discuss one type of symmetry, namely Elliptical symmetry below.

2.3 Elliptical Symmetry: Importance and Significance

Of the various types of symmetry that we have discussed in Chapter-1, the symmetry that is of interest to us in this thesis is the elliptical symmetry of 2-D filters. In many of the applications such as image processing and seismic signal processing, the signal does not possess any preferred spatial direction. Therefore it is desirable to process images with filters whose frequency response is approximately elliptically symmetric. As mentioned earlier, FIR filter functions possessing nearly elliptically symmetric frequency response can be generated using 1-D FIR functions [10]. But the same is not possible in the case of IIR functions, since the 2-D IIR function is not in general, factorable into a set of quarter-pane or half-plane functions. Moreover, the incorporation of the stability constraints in the approximation procedure, is yet another difficulty experienced in the design of IIR Filters. As a solution to this problem, it has been proved that if a quarter-plane filter possesses quadrantal symmetry in its magnitude response, then its denominator can be expressed as a product of 2-D polynomials [6], [12]. It can be readily verified that the specification of elliptical symmetry, implies the presence of the lower order symmetries namely, octagonal

and hence, quadrantal symmetries. Therefore it may be reasonable to constrain the desired transfer function of the filter to posses octagonal symmetry(say) and choose the filter function with a product separable denominator. In cases where the filter function is not even quadrantally symmetric, the separable denominator constraint restricts the domain of functions over which approximation is carried out and results in sub-optimal solutions. But since the elliptical symmetry condition must also include quadrantal symmetry, the separable denominator condition does not prevent us from attaining optimal solutions. One another important aspect is that there is no constraint over the numerator polynomials in any of the above designs. Hence the types of responses that can be obtained using separable denominator filter function is practically endless. FIR Filters can be designed by various methods as given by [10], [17], [18], [19], [20], [21]. The following sections gives a brief overview of the general design method of IIR Filters following which the design method adopted in obtaining elliptical symmetry of lowpass filters is described in detail.

2.4 Design Methods for 2-D IIR Digital Filters

IIR Filters have transfer functions resulting from an infinite sequence. In general, it is more difficult to design a 2-D IIR filter than a 1-D IIR filter. 1-D techniques normally depend on the factor-ability of one-variable polynomials, resulting in simple algorithms for the stability test and stabilization of unstable filters. Such techniques, unfortunately are not directly generalizable to the 2-D case.

From the 2-D IIR filter function in Eqn.(1.3), it can be seen that the coefficients a_{kl} and b_{kl} have to be chosen to approximate the desired frequency response with a stable recursive implementation. Different design methods have been proposed, of which two design methods are the most common.

The first method involves spectral transformation from one-dimension to two-dimensions. The second method is based on parameter optimization, using classes of

filter structures, as for example the cascade connection of second order filter sections, wherein stability of the filter is introduced using approximation algorithms.

The first method, as proposed in [7], involves a mapping operation from 1-D to 2-D, with a rotation operation. Given a 1-D continuous filter in the factored form, its transfer function can be seen as one of a 2-D filter varying in one direction only:

$$H(s_1,\, s_2) = H_1(s_2) = H_0 \left[\frac{\Pi_{i=1}^{m}(s_2 - q_i)}{\Pi_{i=1}^{m}(s_2 - p_i)}\right] \tag{2.7}$$

where q_i and p_i are the zeros and poles of the filter.

As was mentioned before, a rotation operation, needs to be performed with the transformation operation. A rotation of the $(s_1,\, s_2)$ axes by an angle β may be performed by means of the transformation.

$$s_1 = s_1' \cos\beta + s_2' \sin\beta \qquad s_2 = -s_1' \sin\beta + s_2' \cos\beta \tag{2.8}$$

Thus we obtain a filter whose frequency response is a function of s_1 and s_2 and corresponds to a rotation by an angle $-\beta$ of Eqn.(2.8). From this a digital filter can be obtained by applying bilinear z-transforms to both the continuous variables. This method has been used to obtain simple rotated blocks which can be combined to obtain the design of elliptically symmetric recursive filters [22]. Here the conditions of stability have also been proved.

Another method in the similar sense, involves transformation of the squared magnitude function of a 1-D filter to the 2-D domain, followed by a suitable decomposition of the resulting filter.

Given a causal filter(first quadrant filter), it is possible to define the corresponding second, third and fourth quadrant filters, according to the relations given by

$$h_1(k,\, l) = h_2(k,\, -l) = h_3(-k,\, -l) = h_4(-k,\, l) \tag{2.9}$$

with the following transfer functions given by

$$H_1(z_1,\, z_2) = H_2(z_1,\, z_2^{-1}) = H_3(z_1^{-1},\, z_2^{-1}) = H_4(z_1^{-1}, z_2) \tag{2.10}$$

If the above four filters are cascaded, we obtain a zero-phase digital filter whose frequency response is defined by the coefficients $p(k,\ l)$ and $q(k, l)$ determined through the convolution of the coefficients of the four filters and is of the following form

$$G(\exp^{j\omega_1},\ \exp^{j\omega_2}) = \frac{\sum_{k=0}^{N}\sum_{l=0}^{N} p(k,\ l)\cos(k\omega_1)\cos(l\omega_2)}{\sum_{k=0}^{K}\sum_{l=0}^{K} q(k,\ l)\cos(k\omega_1)\cos(l\omega_2)} \tag{2.11}$$

If we take a squared magnitude function of a 1-D IIR filter, and apply the following transformation

$$\cos(\omega) = A\cos\omega_1 + B\cos\omega_2 + C\cos\omega_1\cos\omega_2 + D \tag{2.12}$$

to its numerator and denominator, then the above equation can be obtained. The squared magnitude function obtained has to be factorized to obtain stable recursive filters.

Based on the review given so far, in what follows, we consider the generation of 2-D filters having elliptical symmetry. Although it has been clearly proved in [6], [23] that it is not possible to obtain exact elliptically symmetric filters, we consider the extent to which such filters can be designed by using separable 1-D transfer functions. In this Chapter we only consider the design of elliptically symmetric lowpass filters. The design of other filters namely highpass, bandpass and bandstop filters will be dealt with in the subsequent chapters.

2.5 Generation of Stable 2-D IIR Product Separable Denominator Transfer Functions and Test for Elliptical Symmetry

In order to obtain a required symmetry, the magnitude response of the filter has to be varied. One way to do it is to vary the coefficients of the filter. This necessarily perturbs the pole-zero locations of the filter in each dimension and thus varies the

filter characteristics. But there is possibility that the filter may become unstable as a result. If FIR filters are used, then we do not have to worry about stability, as it is known fact that FIR filters are inherently stable. However FIR may require high order filters to satisfy the change in magnitude characteristics and thus implementation could be difficult. If however, we use an IIR filter, by using one or more feedback paths in the design, we may achieve the above purpose. But we need to take care of the stability of the filter. In the case of 2-D systems, the complexity of testing the stability of the system is quite high. Therefore it is necessary to obtain the bounds of one or more coefficients, in order to ensure that the designed filter is stable. In this section, we design a filter transfer function possessing variable characteristics in their frequency response depending upon certain assigned variables.

The basic structure that will be used to explain this, is shown by a signal flow graph in the Fig.(2.1)

From Fig(2.1), the overall transfer function can be deduced as

$$T_{ac} = \frac{V_c}{V_a} = \frac{T_{ab}T_{bc}}{1 - T_{bc}T_{cb}} \tag{2.13}$$

From Eqn.(2.13)(Mason's formula), it can be seen that any change in T_{ab} will result in a scale change in the magnitude response of the filter. Also, it has to be ensured that the eventual transfer function T_{ac} is stable. Now in order to change the magnitude characteristics of the transfer function, one of the transmittance should be changed. This is always possible by using T_{cb} as a variable quantity. This results in a Variable Characteristic Transfer Function(VCTF) [3].

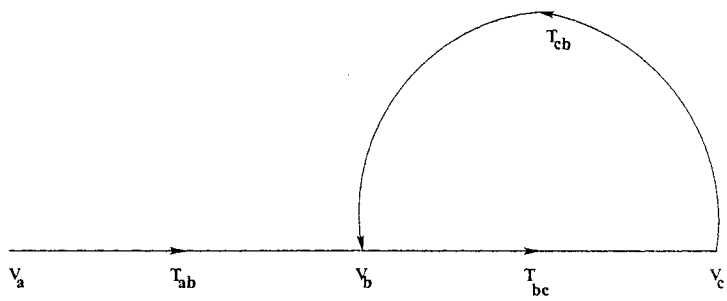

Figure 2.1: Basic structure for the 2-D transfer function expressed as a signal flow graph

2.6 Generation of Transfer Function when no poles in a Butterworth filter are shifted

One of the simplest ways to generate a 2-D IIR VCTF is to obtain it as a product of two stable 1-D Strictly Hurwitz Polynomials(SHP), one in the s_1 domain and the other in the s_2 domain, and from this we can obtain the denominator polynomial. The numerator polynomial can either be product separable or non-product separable. Then the application of bilinear transformation results in a transfer function which is stable in the discrete domain.

Here the transfer function obtained has none of the poles shifted in the Butterworth filter.

For our case, let us consider a 2-D transfer function $T(s_1,\ s_2)$ given as a product of two 1-D functions $T_1(s_1)$ and $T_2(s_2)$ each having the form as shown in Eqn.(2.13)

Therefore,

$$T_3(s_1,\ s_2) = T_1(s_1)T_2(s_2) \tag{2.14}$$

Let $T_1(s_1) = \frac{1}{g_1(s_1)+f_1(s_1)}$ where $g_1(s_1)$ is a third order Butterworth polynomial given by

$g_1(s_1) = s_1^3 + 2s_1^2 + 2s_1 + 1$ and $f_1(s_1) = k_1$.

Similarly for $g_2(s_2)$ and $f_2(s_2)$ in the second dimension, the expressions to obtain

$T_2(s_2) = \frac{1}{g_2(s_2)+f_2(s_2)}$ are given by

$g_2(s_2) = s_2^3 + 2s_2^2 + 2s_2 + 1$ and $f_2(s_2) = k_2$.

A third order polynomial is considered for purposes of illustration. The transfer function can be of any order.

Let $k_1 = k_2 = k$

In order to determine the range of k over which the filter is stable, we apply the stability condition [24]. According to this condition if $Q_a(s) = m(s) + n(s)$ where $m(s)$ is an even polynomial and $n(s)$ is an odd polynomial and if $m_1(s)$ is an even polynomial, then $Q_a(s) + m_1(s)$ is a strictly Hurwitz polynomial if and only if, in the partial fraction expansion,

$$\frac{m(s) + m_1(s)}{n(s)} = k_\infty s + \sum_{i=1} \frac{k_i s}{s^2 + \beta_i^2} + \frac{k_0}{s} \tag{2.15}$$

with $\beta_i^2 < \beta_{i+1}^2 (\beta' s$ being real), we have the conditions

$(i)\ k_\infty \geq 0,\ (ii)\ k_i > 0$ for all values of i and $(iii)\ k_0 > 0$.

From the above condition we have, in our present case, letting $m = 2s^2 + 1$, $m_1 = k$ and $n = s^3 + 2s$,

$$\frac{m(s) + m_1(s)}{n(s)} = \frac{2s^2 + 1 + k}{s^3 + 2s} = \frac{\frac{1+k}{2}}{s} + \frac{\frac{3-k}{2}s}{s^2 + 2} \tag{2.16}$$

Evaluating the above conditions from Eqn.(2.16), we have $k = 3$ or $k = -1$.

Therefore the range of k is $-1 < k < 3$.

A program in "Matlab" is written for the above procedure followed to determine the stability conditions and the range of k for different orders of the Butterworth Filter.

The Matlab Program A1 is shown in Appendix.

The results tabulated for "stability conditions of k" for different orders are shown in Table {2.1}.

Order of Filter	*Stability Conditions of k*
Third	$-1 < k < 3$
Fourth	$-1 < k < 1.4142$
Fifth	$-1 < k < 1.0900$
Sixth	$-1 < k < 1.0319$
Seventh	$-1 < k < 1.014$
Eighth	$-1 < k < 1.0001$

Table 2.1: Stability Conditions of "k" when no poles are shifted

2.7 Elliptical Symmetry Observation

The basic structure of a 2-D Transfer function as a product of two 1-D functions with k_1 & k_2 is shown in Fig.(2.2). From Eqn.(2.14) we have

$$T_3(s_1,\, s_2) = \left(\frac{1}{s_1^3 + 2s_1^2 + 2s_1 + 1 + k_1}\right)\left(\frac{1}{s_2^3 + 2s_2^2 + 2s_2 + 1 + k_2}\right) \tag{2.17}$$

Substituting $s_1 = j\omega_1$ and $s_2 = j\omega_2$ in the above equation and simplifying the transfer function by eliminating all the higher powers of ω_1 and ω_2 and retaining only the second degree powers, we have in two dimensions, the relationship to be satisfied as [25]

$$\left\{2\omega_1^2(k_2+1) + 2\omega_2^2(k_1+1) = 4\omega_1^2\omega_2^2 - 4\omega_1\omega_2 + k_1 + k_2 + k_1k_2 - \epsilon\right\} \tag{2.18}$$

where $\epsilon = response\ of\ the\ transfer\ function.$

Simplifying the above Eqn.(2.18) further, we obtain the relationship as

$$\left\{\frac{4k_2\omega_1^2}{(1+k_1)^2} + \frac{4k_1\omega_2^2}{(1+k_2)^2} = 1 - \epsilon\right\} \tag{2.19}$$

Plotting a direct response for Eqn.(2.19) for values of $k_1 = 0.35$ and $k_2 = 0.70$, we have the magnitude and contour plots as shown in Fig.(2.3).

As we notice from Fig.(2.3), it is an elliptical symmetric response corresponding to the Eqn.(2.19) which, in general terms, is the equation of an ellipse. The contour plots of $T_3(s_1,\, s_2)$ are drawn after bilinear transformation for $k_1 = -0.45$ and $k_2 = -0.20$, $k_1 = -0.75$ and $k_2 = -0.50$, $k_1 = -0.58$ and $k_2 = -0.35$,

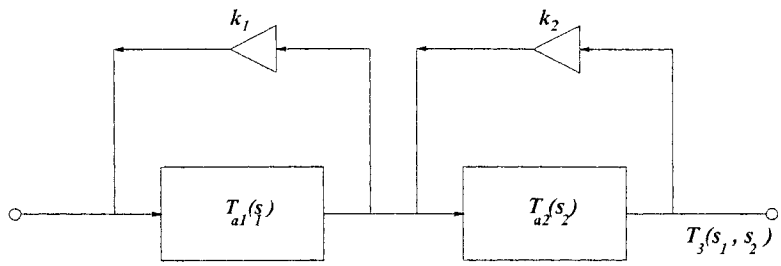

Figure 2.2: Basic structure of a 2-D transfer function

$k_1 = -0.30$ and $k_2 = -0.12$. We obtain the results as shown in Figs.(2.4), (2.5) and (2.6). It can be seen that elliptically symmetric response is possible only in a limited frequency range, since the contribution due to higher frequencies is not considered.

From Figs.(2.4), (2.5) and (2.6), it can be deduced that for a certain range of k_1 and k_2, in and around $k_1 = -0.45$ and $k_2 = -0.20$, the filter exhibits close to elliptical symmetry.

It should be noted that when $k_1 = k_2$(for some value), we get the response close to circular symmetry [21].

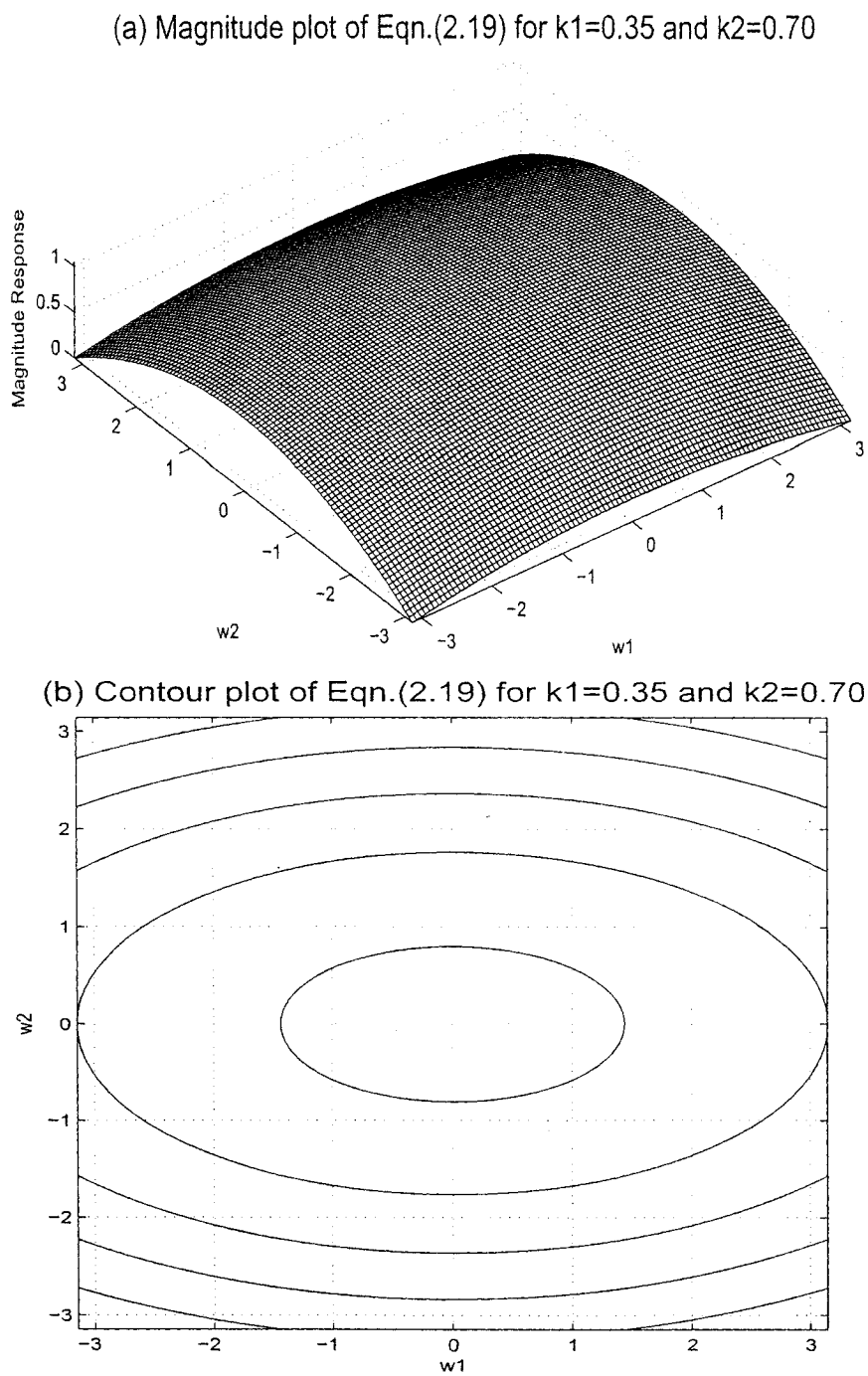

Figure 2.3: Plot of Eqn.(2.19) for k1=0.35 and k2=0.70 (a) Magnitude Plot (b) Contour Plot.

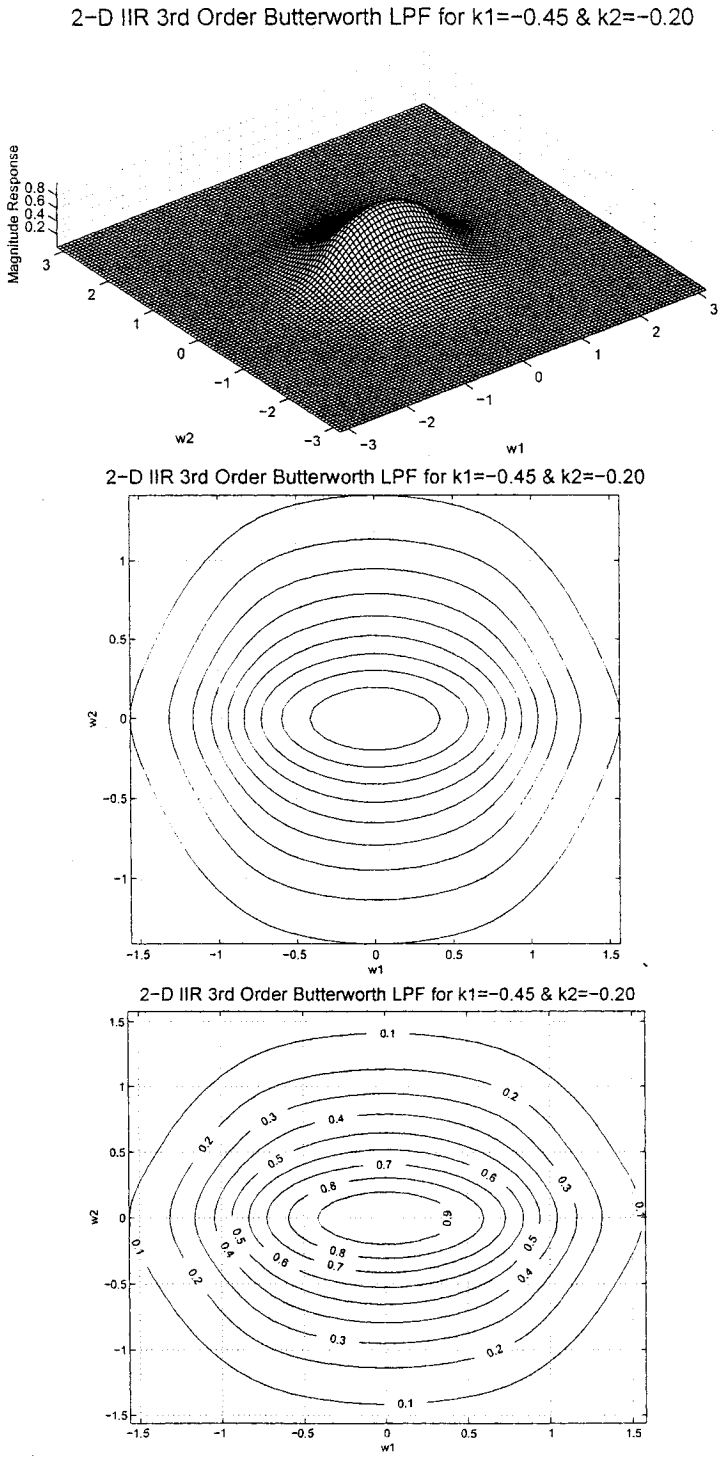

Figure 2.4: Plots for 2-D IIR Butterworth LPF (a) Magnitude Plot (b) Contour plot (c) Magnitude values for contours

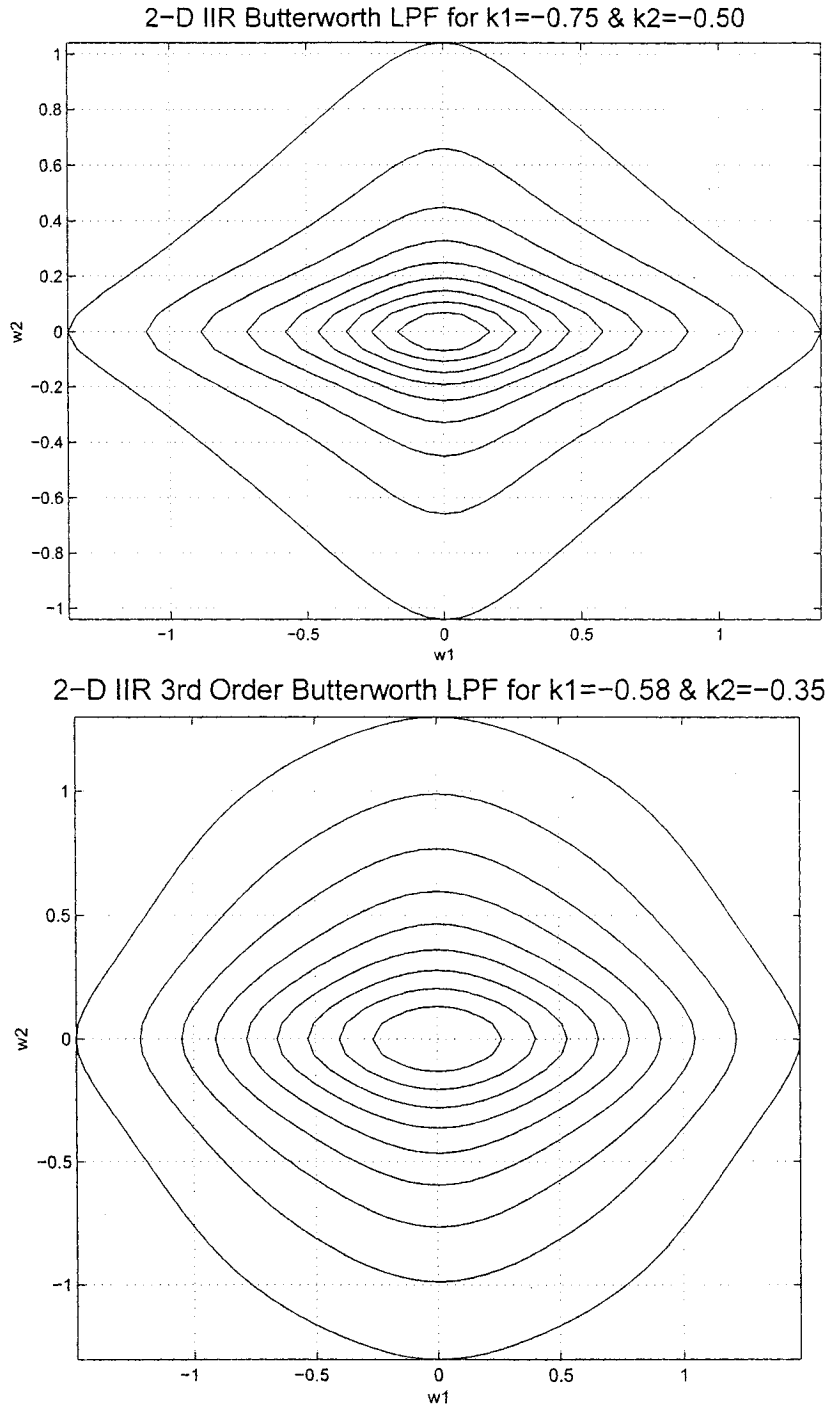

Figure 2.5: Contour plots for 2-D IIR Butterworth LPF for (a) k1=-0.75 and k2=-0.50 (b) k1=-0.58 and k2=-0.35

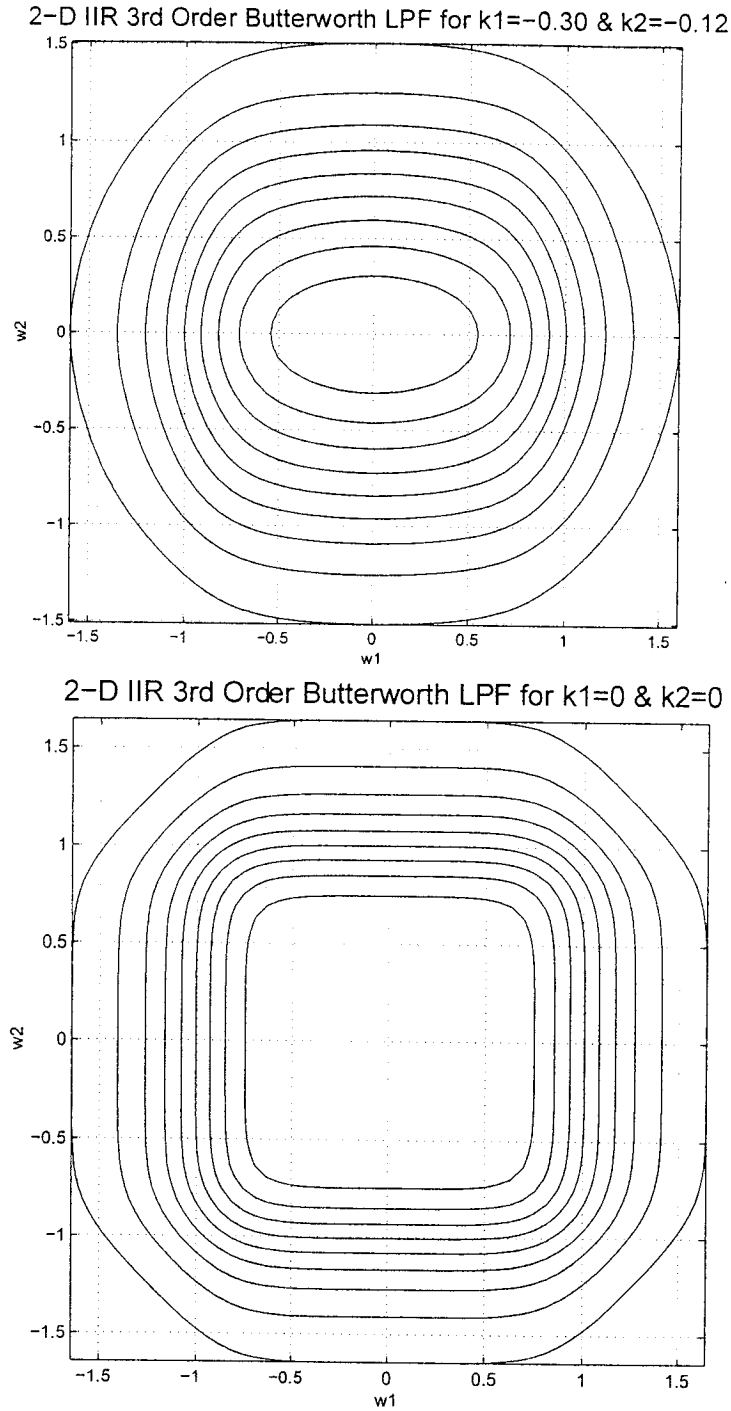

Figure 2.6: Contour plots for 2-D IIR Butterworth LPF for (a) k1=-0.30 and k2=-0.12 (b) k1=0 and k2=0

The program to determine the transfer function of the filter for a given k_1 and k_2 for Figs.(2.4), (2.5) and (2.6)(Program A2) is as follows. This program also outputs the contours with magnitudes of the corresponding ellipses.

Program A2

```
%%Function to determine the transfer function of the filter for
    %%a given k1,k2(kerthproga2.m)-for Figs.(2.4),(2.5),(2.6)
    k1=-0.45;
    B1=[1];
    A1=[1 2 2 1];
    B2=B1;
    [R,C]=size(A1);
    A1(C)=A1(C)+k1;
    A2=[1 2 2 1];
    [R,C]=size(A2);
    k2=-0.20;
    A2(C)=A2(C)+k2;
    %%Bilinear transformation of transfer function
    [N1,D1]=bilinear(B1,A1,1);
    [N2,D2]=bilinear(B2,A2,1);
    %%To determine the 2-D transfer function of the IIR Filter
    for m=1:1:size(N1,2)
    for n=1:1:size(N2,2)
    N(m,n)=N1(m)*N2(n);
    end
    end
    for m=1:1:size(D1,2)
    for n=1:1:size(D2,2)
    D(m,n)=D1(m)*D2(n);
    end
    end
    lim=pi;
    interval=pi/50;
    c1=0;
    for w1=-lim:interval:lim
    c2=0;
    c1=c1+1;
    for w2=-lim:interval:lim
    c2=c2+1;
```

```
for col=1:1:size(N2,2)
NRow(1,col)=(cos(w2)+j*sin(w2))^(size(N2,2)-col);
end
for row=1:1:size(N2,2)
NCol(row,1)=(cos(w1)+j*sin(w1))^(size(N1,2)-row);
end
NR=NRow*N'*NCol;
a=real(NR);
b=imag(NR);
for col=1:1:size(D2,2)
DRow(1,col)=(cos(w2)+j*sin(w2))^(size(D2,2)-col);
end
for row=1:1:size(D2,2)
DCol(row,1)=(cos(w1)+j*sin(w1))^(size(D1,2)-row);
end
DR=DRow*D'*DCol;
c=real(DR);
d=imag(DR);
MOD(c1,c2)=(sqrt((a*c+b*d)^2+(b*c-a*d)^2))/(c^2+d^2);
end
end
%%To plot the frequency response plots
w1=-lim:interval:lim;
w2=-lim:interval:lim;
[ww1,ww2]=meshgrid(w1,w2);
%%Normalizing the max value of magnitude to 1
zz=MOD/(max(max(MOD)));
%%Mesh plot
mesh(w1,w2,zz);
axis('image');
xlabel('w1');
ylabel('w2');
zlabel('Magnitude Response');
title('2-D IIR 3rd Order Butterworth LPF for k1=-0.45 & k2=-0.20','Fontsize',16);
grid on;
figure;
%%Contour plot
contour(w1,w2,zz)
axis('image');
xlabel('w1');
ylabel('w2');
zlabel('Magnitude Response');
grid on;
```

```
figure;
%to plot the magnitude values of contours
[C,h] = contour(w1,w2,zz);
clabel(C,h)
colormap cool
xlabel('w1');
ylabel('w2');
zlabel('Magnitude Response');
grid on;
%%End of Program
```

2.8 Algorithm to Check the Extent of Elliptical Symmetry for a Given Magnitude Range

From the above study, it is seen that, for given values of k_1 and k_2, it becomes necessary to determine whether at a certain value of magnitude range, the filter exhibits elliptical symmetry. An iterative algorithm has been written in MATLAB, to check the extent of elliptical symmetry under a given magnitude range and if required, alter the value of the variable quantity(in this case k_1 and k_2) so as to obtain the elliptical symmetric condition.

As a particular case, for the third order Butterworth IIR Filter, the initial value of k_1 and k_2 have been taken as $k_1 = -0.80$ and $k_2 = -0.60$. The magnitude range under check is the value what we choose to give at the input(in this case it is 0.49<Mag<0.51.

A program in Matlab is written to determine the magnitude range upto which elliptic response is possible with an error of $\alpha\%$ when k_1 and k_2 are selected.

The algorithm has been written as follows

(1) Program A3 is the main program showing the inputs to be given for Elliptical symmetry test. The filter is first designed given the transfer function in terms of numerator and denominator polynomials.

(2) The transfer function of the 2-D filter is determined using a separate subroutine(same as program A2) which is called from the main program. This subroutine returns the 2-D transfer function of the filter.

(3)The subroutine for determining the Magnitude range upto which Elliptical symmetry is possible is then called(Program A3-b).

(4)The basic idea underlying Program A3-b is explained as follows. The magnitude range for the Elliptical symmetry check for the derived frequency response is given at the input or defined. In this case this value is between (0.49, 0.51). The magnitude value can be of any value chosen between 0 and 1.

(5)The magnitude values falling under this range is isolated into a separate matrix and their frequency positions with respect to both the dimensions are noted.

(6)To check if these isolated values of magnitude fall under an ellipse, their individual magnitude values are noted and a percentage error of 5% is used to include the points into a ellipse. If desired, any other percentage value can also be chosen.

(7)If all the values fall under this limit then the given magnitude range is considered to be fairly elliptically symmetric and if this is not the case, the values of k_1 and k_2 are increased by a value of 0.05 and the whole process is carried out from the beginning.

Thus this algorithm is highly useful in determining the extent of elliptical symmetry in 2-D Filters. It is noted that this procedure can be used for testing the elliptical symmetry of any filter by looking at the shape of the ellipse what we get at the output, given the transfer function. In cases where elliptical symmetry is not very obvious, the value of the percentage error inside the program can be varied in order that the best match for elliptical symmetry can be obtained.

For this particular case, the algorithm gave an elliptical symmetry result for the order $n = 3$, values of $k_1 = -0.45$ and $k_2 = -0.20$.The program for the above procedure(Program A3,A3-b) has been written in the MATLAB and is shown as follows:

Program A3

```
%%Program to design a filter and check the extent of elliptical symmetry
    %%for a specific filter transfer function that is input by the user.
    %%(kerthproga3.m)for Figs.(2.7),(2.8),(2.9)
    %%This program calls two subroutines.
    %%Define the numerator(B1) and denominator(A1) polynomials of the transfer function
    %%for which elliptical symmetry is to be tested
    B1=[1];A1=[1 2 2 1];
    %% Increment the value of k1 & k2 and output the result for each k1 & k2.
    for k1=-0.8:0.05:0
    for k2=-0.6:0.05:0
    %%This defines the range of k1 & k2 that is to be tested.
```

```
%%Calls the sub-routine to design the filter for a specific k1 & k2(same as Program A2)
Mag=kerthproga2(B1,A1,K1);
%%Calls the subroutine to test extent of elliptical symmetry(Program A3-b)
[output]=garg_rama_ellip(Mag)
end
%%End of program
```

Sub-routine A3-b

```
%%Program to check the extent of elliptical symmetry for a designed filter.
    %%given the Magnitude transfer function
    function [output]=gar_rama_ellip(Mag);
    j1=0;Mag=zz;
    m=input('Input the value for magnitude=')
    for i=1:size(Mag,1)
    for j=1:size(Mag,2)
    if Mag(i,j)>(m-m*5/100) & Mag(i,j)<(m+m*5/100)
    j1=j1+1;points(1,j1)=Mag(i,j);
    else
    Mag(i,j)=0;
    end
    end
    end
    lim=pi;
    interval=pi/50;
    w1=-lim:interval:lim;
    w2=-lim:interval:lim;
    [ww1,ww2]=meshgrid(w1,w2);
    figure;
    contour(ww1,ww2,Mag);
    axis('image');xlabel('w1');ylabel('w2');zlabel('Magnitude Response');grid on;
    title(['Test for elliptic symmetry for 5% change in magnitude, Mag=',num2str(n)],'Fontsize',14);
    %%To get the w1, w2 values for the non-zero elements of Mag
    count=0;
    for i=1:size(Mag,1)
    for j=1:size(Mag,2)
    if Mag(i,j)~=0
    count=count+1;
    x(count)=ww1(i,j);y(count)=ww2(i,j);
    end
    end
    end
```

```
%%Check for radius
count1=0;clear Radius;
for i=1:size(x,2)
x1=x(i);y1=y(i);
a=max(x(i));b=max(y(i));z1=sqrt((x1^2/a^2)+(y1^2/b^2));
count=count+1;Radius(count1)=z1;
end
max_Radius=max(Radius);min_Radius=min(Radius);
Radius_vector=(max_Radius-min_Radius)/max_Radius;
%%Output the result of test for elliptical symmetry
if Radius_vector<0.05
output=char('elliptically Symmetric');
else
output=char('Not elliptically symmetric');
end
%%End of program
```

The results are plotted as shown in Figs.(2.7), (2.8) and (2.9) for different values of k_1 and k_2. The magnitude range under study is varied between the lowest to the highest value within ranges of 10% of the magnitude. From this, the region of interest (where the filter is approximately elliptically symmetric) is found and further simulations are carried on with a 2% magnitude range within the reduced region of interest and eventually, after repeated simulations of Program A3, results show that for a value of $k_1 = -0.45$ & $k_2 = -0.20$ for this specific transfer function, optimum elliptical symmetry is achieved. Going beyond these values of k_1 and k_2 has resulted in degradation of elliptical symmetry. Figs.(2.7), (2.8) and (2.9) show the final plots of the filter for different values of k_1 and k_2. The magnitude values under study in these figures are in the range $0.49 < Mag < 0.51$.

Fig.(2.7) shows the plots for $k_1 = -0.75$, $k_2 = -0.50$ and $k_1 = -0.58$, $k_2 = -0.32$. Here we see that with higher value of k_1 and k_2, the plot tends to an ellipse.

Fig.(2.8) shows a plot for $k_1 = -0.45$ and $k_2 = -0.20$ for which, it is clear that we have elliptical symmetry existing between the magnitudes under study.

Fig.(2.9) shows that as the value of k_1 and k_2 increase beyond $k_1 = -0.45$ and $k_2 = -0.20$ elliptical symmetry ceases to exist, under the given magnitude range

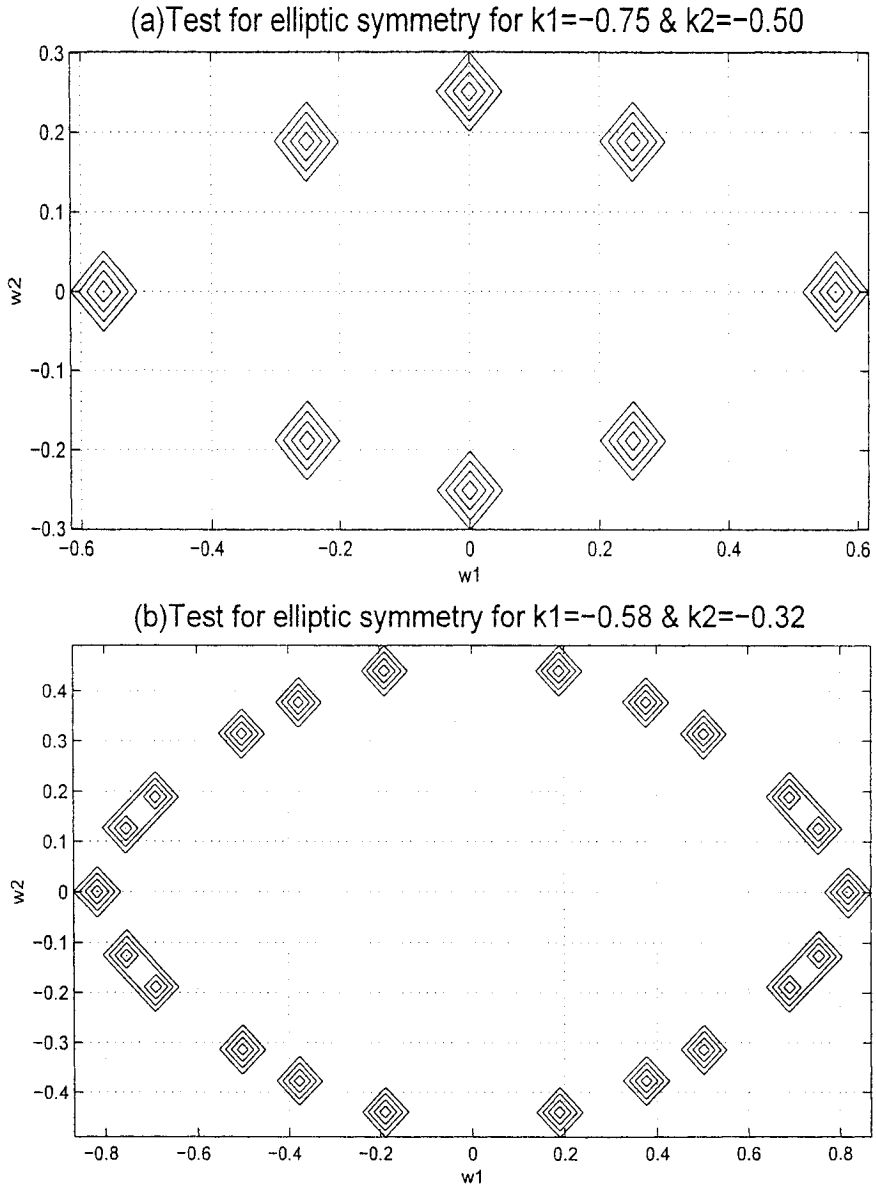

Figure 2.7: 2-D IIR Butterworth LPF response and test for elliptical symmetry under magnitude range 0.49<Mag<0.51 for (a) k1=-0.75 and k2=-0.50 (b) k1=-0.58 and k2=-0.32

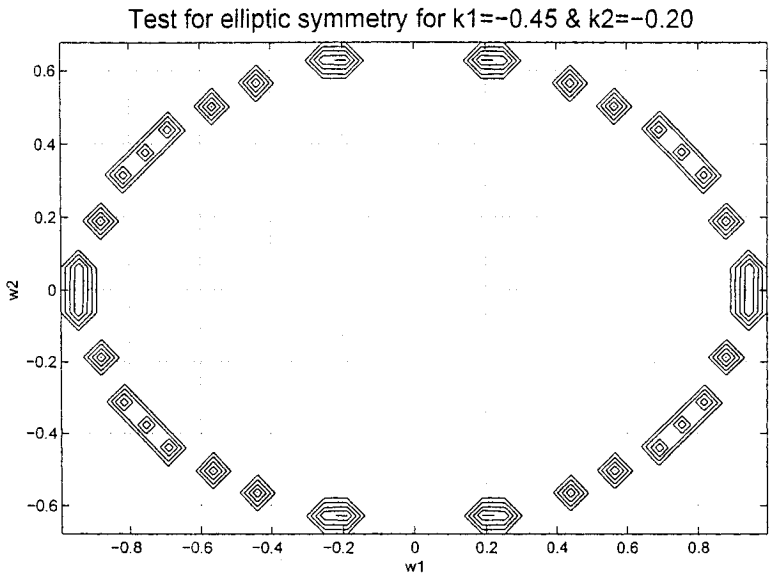

Figure 2.8: 2-D IIR Butterworth LPF response and test for elliptical symmetry under magnitude range 0.49<Mag<0.51 for k1=-0.45 and k2=-0.20

under study.

We have considered, by and far, filters of third order. In a similar manner, simulations can be extended to higher order filters. However with higher order filters, the computations become more complex.

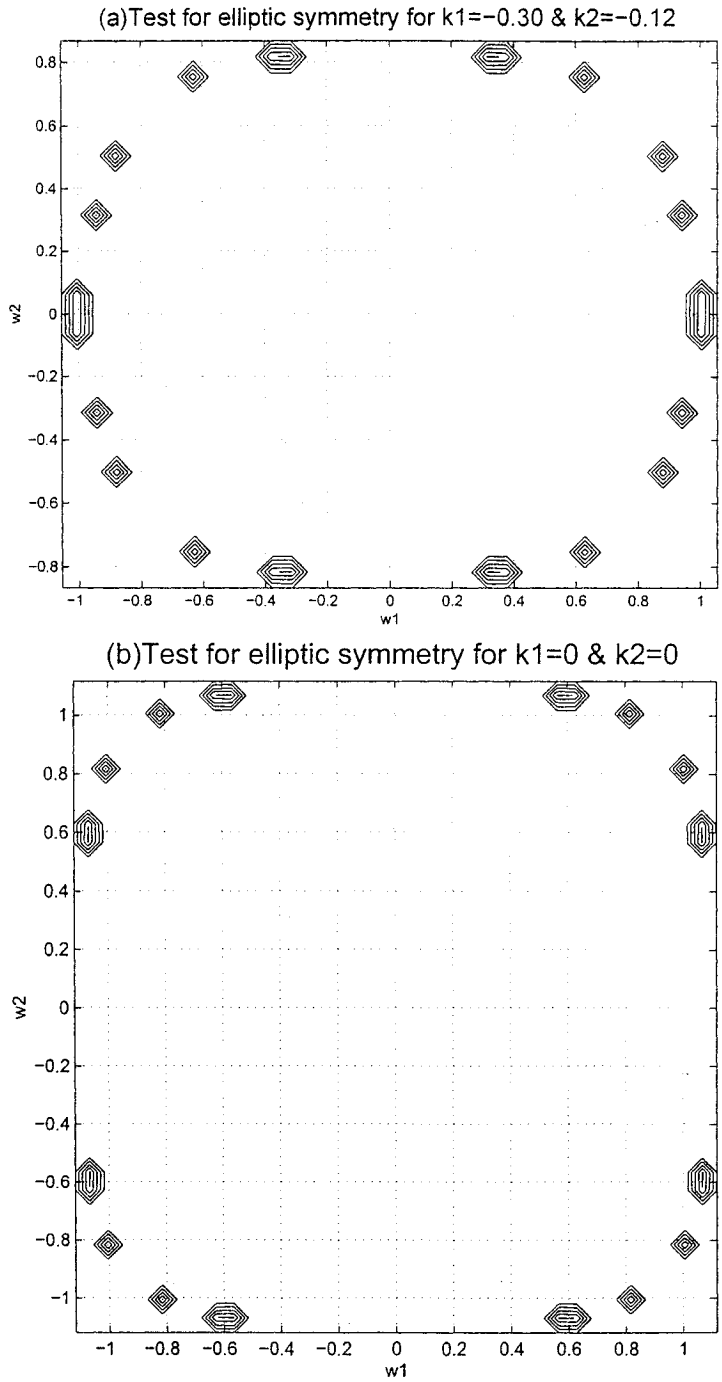

Figure 2.9: 2-D IIR Butterworth LPF response and test for elliptical symmetry under magnitude range 0.49<Mag<0.51 for (a) k1=-0.30 and k2=-0.12 (b) k1=0 and k2=0

2.9 Design of 2-D IIR Chebyshev Lowpass filter

We have discussed, so far, in detail about the implementation of 2-D Lowpass Butterworth filter design and specifically, its contribution to elliptical symmetry. In this section, we will discuss about the 2-D lowpass Chebyshev filter design and its approximation to elliptical symmetry.

The Chebyshev lowpass filter makes use of the Chebyshev polynomial [26]. It is well known that Chebyshev characteristics has an equi-ripple variation in the passband and a fast monotonic decrease in gain, outside the pass-band. In order to design a 2-D Chebyshev lowpass filter from the 1-D design, as before in the Butterworth design, we will consider it as a product of two 1-D transfer functions.

2.9.1 The Chebyshev Lowpass Characteristics

For the lowpass characteristics, we chose the value of the transfer function within the range, such that $\omega \leq 1$.

We know that $|C_n(\omega)| \leq 1$ for $\omega \leq 1$. Therefore we chose a small number ϵ such that

$F(\omega^2) = \epsilon^2 C_n^2(\omega)$.

Therefore we will have

$$|H(j\omega|^2 = \frac{1}{1+\epsilon^2 C_n(\omega)} \tag{2.20}$$

Eqn.(2.20) will have its values that fall between 1 and $\frac{1}{(1+\epsilon^2)}$ in the range $0 \leq \omega \leq 1$.

For $\omega \gg 1$, and from Eqn.(2.20)

$$|H(j\omega)|^2 \approx \frac{1}{\epsilon^2 2^{2(n-1)}\omega^{2n}} \tag{2.21}$$

Therefore the gain $\alpha(\omega)$ can be calculated as

$$\alpha(\omega) \approx -10\log(\epsilon^2 2^{2(n-1)}\omega^{2n}) = -20\log\epsilon - 20(n-1)\log 2 - 20n\log\omega \tag{2.22}$$

2.9.2 2-D Chebyshev Lowpass Characteristics and Test for Elliptical Symmetry

As it has been discussed before in the 2-D IIR Butterworth filter function derivation, the simplest way to obtain a 2-D filter function for Chebyshev filter is to cascade the transfer function of two 1-D filter functions.

As we have discussed in Section 2.6, let us consider a 2-D transfer function given as a product of two 1-D functions.

$$C_3(s_1, s_2) = C_1(s_1)\, C_2(s_2) \tag{2.23}$$

Let $C_1(s_1) = \frac{1}{g_1(s_1)+f_1(s_1)}$ where $g_1(s_1)$ is a third order Chebyshev polynomial given by [26].

$g_1(s_1) = s_1^3 + 1.9388s_1^2 + 2.6294s_1 + 1.6380$ and $f_1(s_1) = k_1$.

Similarly for $g_2(s_2)$ and $f_2(s_2)$ the expressions to obtain $T_2(s_2)$ are given by

$g_2(s_2) = s_2^3 + 1.9388s_2^2 + 2.6294s_2 + 1.6380$ and $f_2(s_2) = k_2$.

These functions have a ripple width ϵ=0.1526.

According to the stability condition of Eqn.(2.15) we determine the range of k for which the 1-D transfer function is stable.

From Eqn.(2.15) it is found that this range of is $-1.6380 \leq k \leq 4.0978$.

Plotting the response for the above range of k gives nearly elliptical symmetric response between the ranges $-0.85 < k_1 < -0.75$ and $-0.50 < k_2 < -0.40$. The plots corresponding to the above range are shown in the Figs.(2.10), (2.11), and (2.12) and these correspond to a ripple width of $\epsilon = 0.1526$. These have been plotted using the same program A2 but with different input values.

The figures also show a plot for $k_1 = -0.45$ and $k_2 = -0.20$. Using Program A3 the values of k_1 and k_2 mentioned in the figures, are tested for elliptical symmetry within the magnitude range $0.49 < Mag < 0.51$. This magnitude range essentially depends upon the necessity of the specific user and it may be chosen based on the magnitude study of interest. The same study can also be carried out

for other magnitude ranges. In this specific case of the magnitude range, it is found that,elliptical symmetry is obtained for a value of $k_1 = -0.80$ and $k_2 = -0.45$. This result has been achieved after extensive simulations of Program A3. The plots shown in Figs.(2.13) and (2.14) show the results of applying Program A3 to the transfer function achieved for the above case of Chebyshev filter.

Fig(2.12) also shows the plot for $k_1 = 0.45$ & $k_2 = 0.20$. This plot shows that, a Chebyshev type response analogous to its 1-D counterpart, can be achieved for values of k_1 and k_2 beyond 0.45 and 0.20 respectively and within stability limits.

As an example, another value of ripple width ϵ=0.3493 has been considered. In this case the equations for $g_1(s_1)$ and $g_2(s_2)$ are given by

$$g_1(s_1) = s_1^3 + 1.2529s_1^2 + 1.5349s_1 + 0.7157$$

$$g_2(s_2) = s_2^3 + 1.2529s_2^2 + 1.5349s_2 + 0.7157$$

The rest of the expression being the same, it has been found that for the above equation, the stability range of k is given by$-0.7157 < k < 0.9230$. Contour plots are obtained for the above range and the plots for which near elliptical symmetry is obtained, are shown as in Figs.(2.15) and (2.16). These have been plotted using Program A2 with appropriate input values.

Applying Program A3 to this case of transfer function, the extent of elliptical symmetry is calculated between the range $0.49 < k < 0.51$. The plots in Figs.(2.17) and (2.18) show these results.

Comparing the above two cases where the plots have shown for two different cases, it can be seen that , the values of k_1 and k_2 change for near elliptical symmetry(in the second case being $k_1 = -0.30$ and $k_2 = -0.10$). It is noted that this is the closest one can approach to elliptical symmetry for test under the specified magnitude range. It is possible that for another range better symmetry can be obtained.

Table{2.2} summarizes the above two cases. From Table{2.2} it can be noted that, depending on the value of ϵ and therefore the transfer function, the value of k

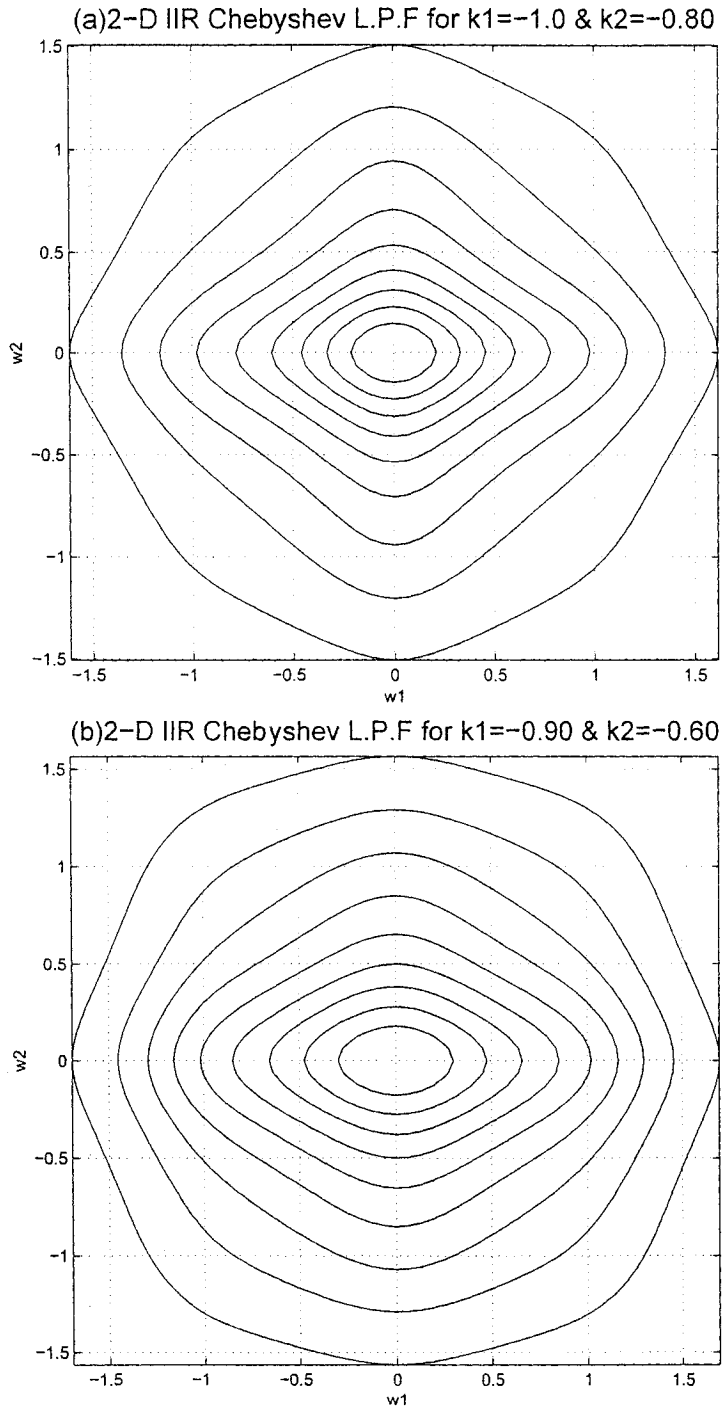

Figure 2.10: 2-D Chebyshev LPF characteristics for (a) k1=-1.0 and k2=-0.80 (b) k1=-0.90 and k2=-0.60

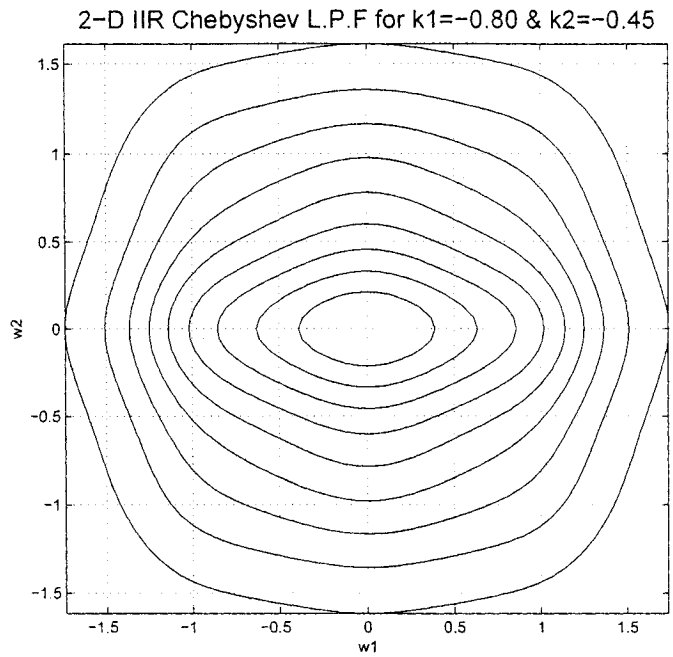

Figure 2.11: 2-D Chebyshev LPF characteristics for k1=-0.80 and k2=-0.45

Ripple Width(ϵ)	Stability range of k	Value of k_1, k_2 for near elliptical symmetry
0.1526	$-1.6380 < k < 4.0978$	$k_1 = -0.80$, $k_2 = -0.45$
0.3493	$-0.7157 < k < 0.9230$	$k_1 = -0.30$, $k_2 = -0.10$

Table 2.2: Analysis results for the extent of elliptical symmetry in 2-D Chebyshev lowpass transfer functions for two different values of ripple width. The magnitude range under study for both the above cases is 0.49<Mag<0.51.

changes for elliptical symmetry for a chosen value of magnitude range and the same can be obtained by Program A3. The 2-D Chebyshev lowpass filter characteristics have thus been analyzed and its approximation to elliptical symmetry has been studied and shown in this section.

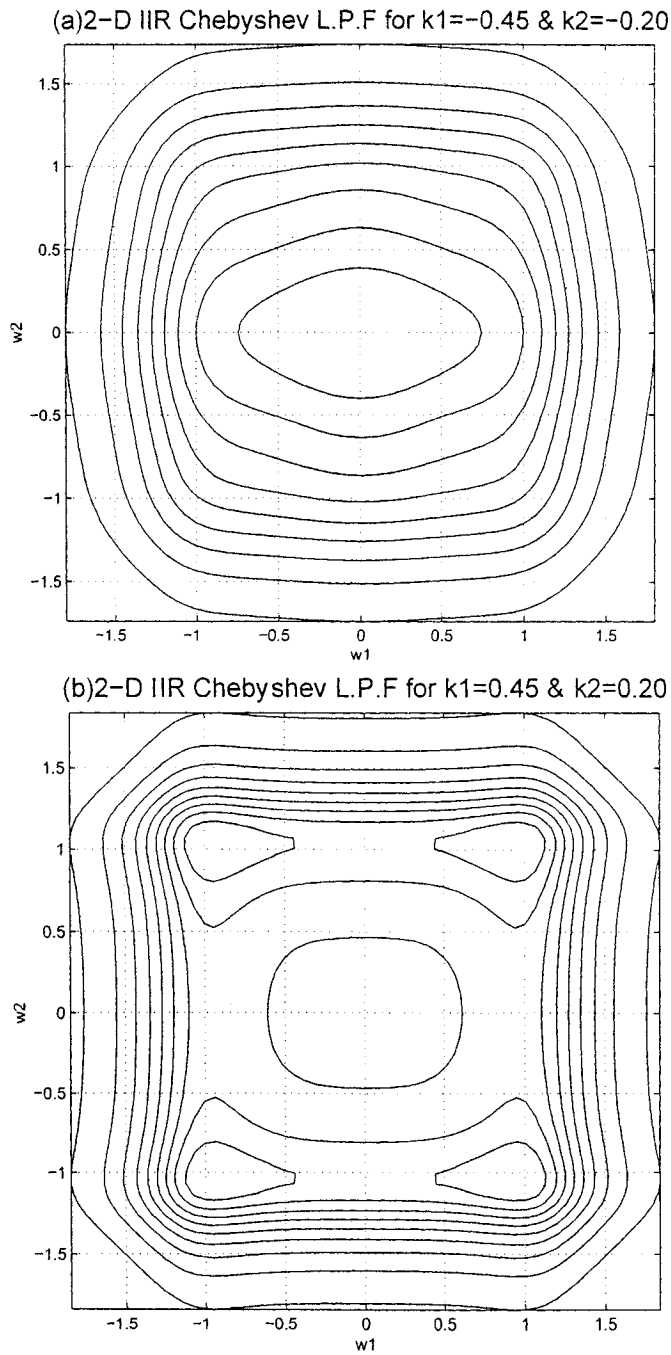

Figure 2.12: 2-D Chebyshev LPF characteristics for (a) k1=-0.45 and k2=-0.20 (b) k1=0.45 and k2=0.20

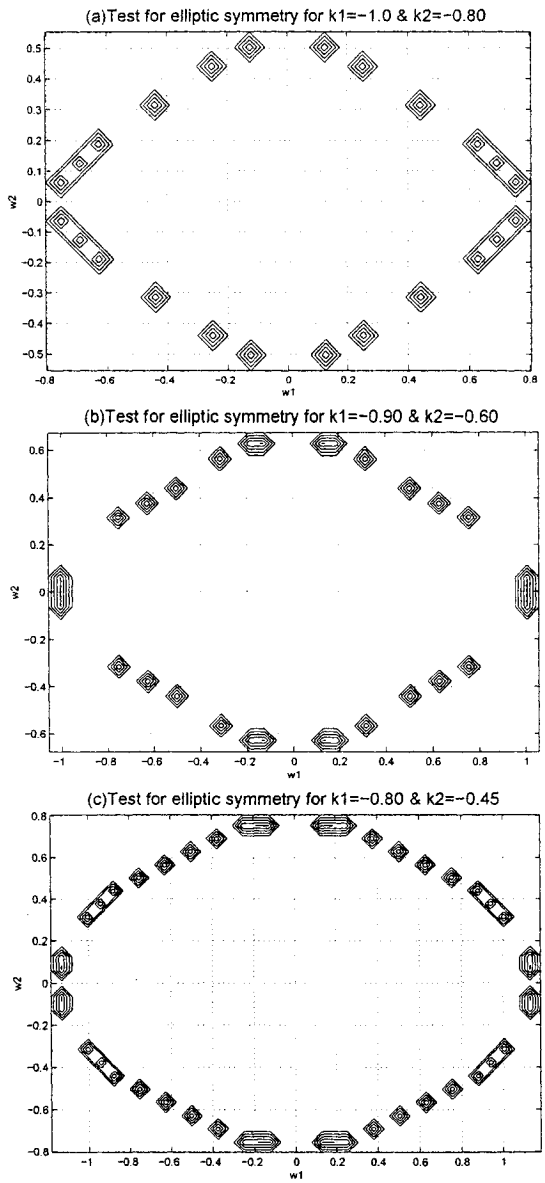

Figure 2.13: Plots showing the extent of elliptical symmetry for the case where ϵ=0.1526, for (a) k1=-1.0 and k2=-0.80 (b) k1=-0.90 and k2=-0.60 (c) k1=-0.80 and k2=-0.45 in the magnitude range 0.49 < Mag <0.51

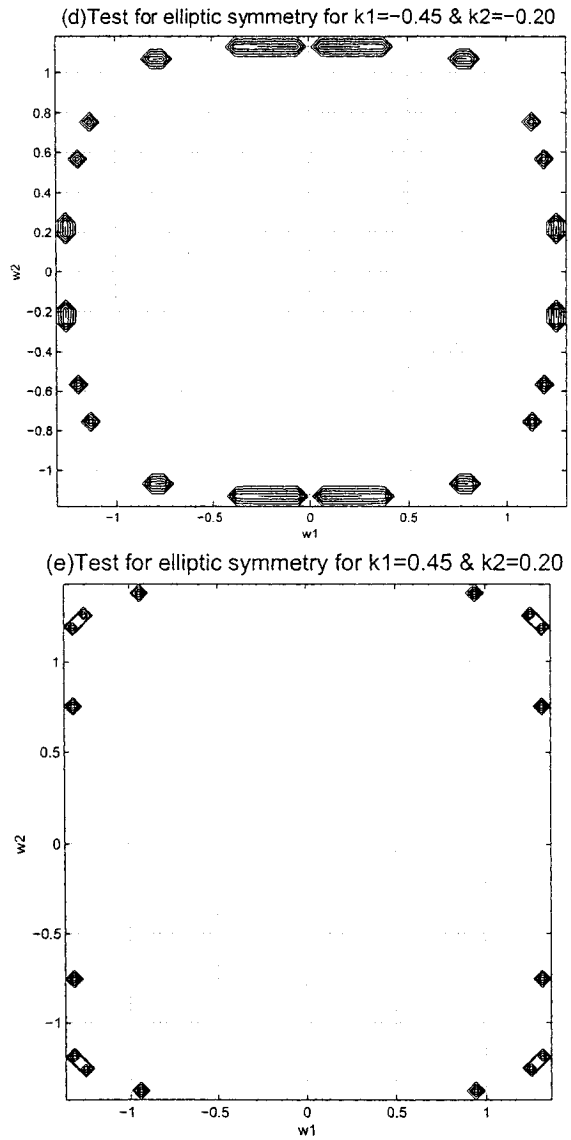

Figure 2.14: Plots showing the extent of elliptical symmetry for the case where ϵ=0.1526, for (a) k1=-0.45 and k2=-0.20 (b) k1=0.45 and k2=0.20 in the magnitude range 0.49 < Mag <0.51

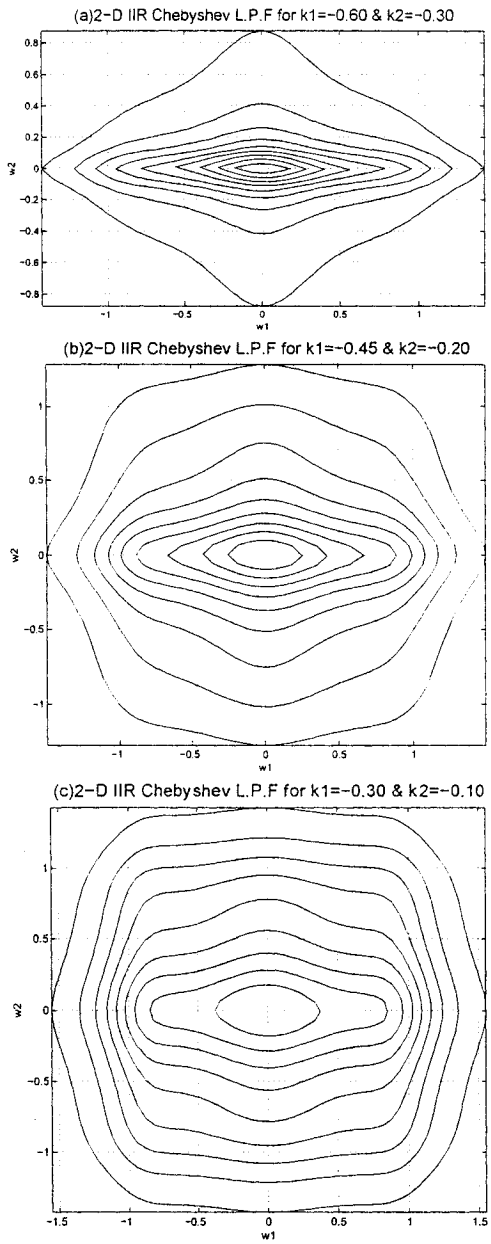

Figure 2.15: *2-D* Chebyshev LPF characteristics for the second case considered for ripple width ϵ=0.3493 for (a) k1=-0.60 and k2=-0.30 (b) k1=-0.45 and k2=-0.20 (c) k1=-0.30 and k2=-0.10

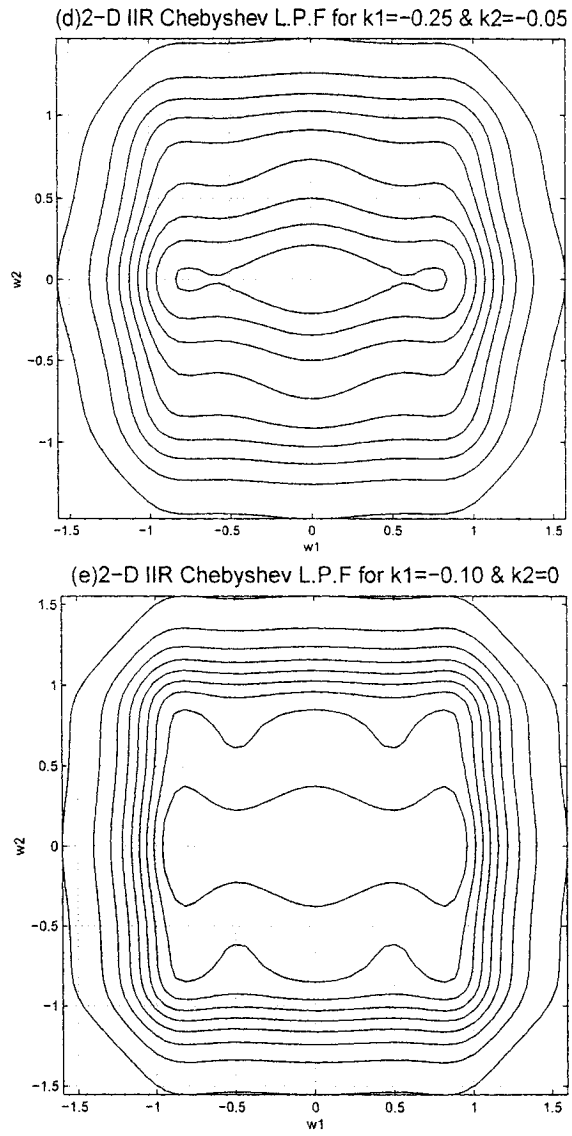

Figure 2.16: 2-D Chebyshev LPF characteristics for the second case considered for ripple width ϵ=0.3493 for (a) k1=-0.25 and k2=-0.05 (b) k1=-0.10 and k2=0.

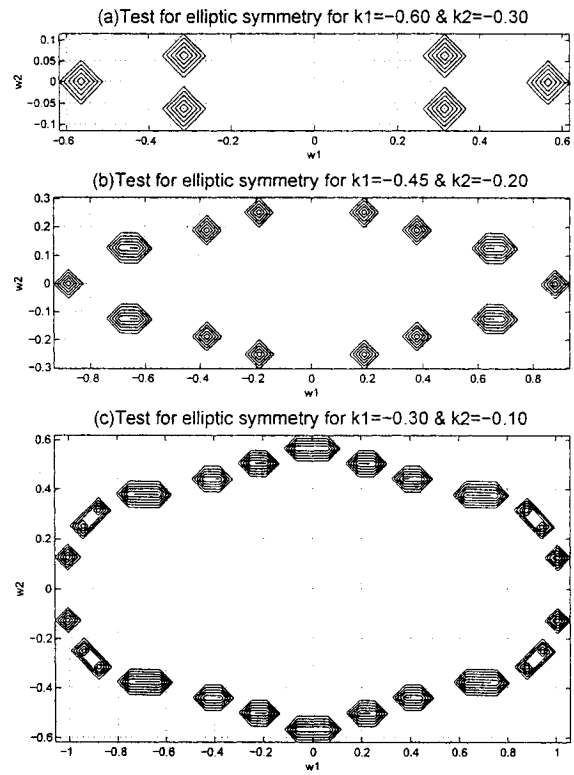

Figure 2.17: Plots showing the extent of elliptical symmetry for the case where ϵ=0.3493, for (a) k1=-0.60 and k2=-0.30 (b) k1=-0.45 and k2=-0.20 (c) k1=-0.30 and k2=-0.10 in the magnitude range 0.49 < Mag <0.51

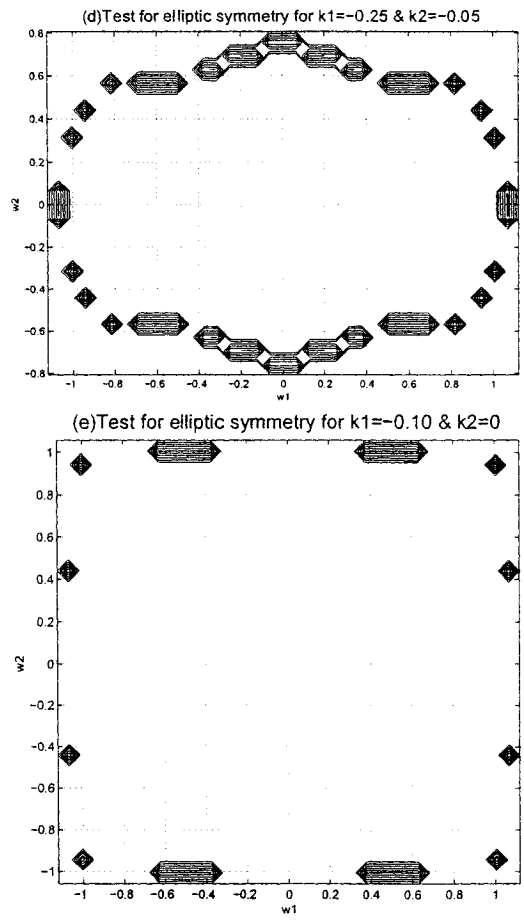

Figure 2.18: Plots showing the extent of elliptical symmetry for the case where ϵ=0.3493, for (a) k1=-0.25 and k2=-0.05 (b) k1=-0.10 and k2=0 in the magnitude range 0.49 < Mag <0.51

2.10 Analysis of Lowpass Complementary Pole Pair Filters Obtained from Butterworth Filters

2.10.1 Introduction

Having discussed in detail the implementation of filters possessing separable denominator 2-D filter transfer functions for the Butterworth and Chebyshev filters, we now proceed to study another interesting aspect of filter design namely the pole-parameter transformation [13] and their analysis. In this respect, we will discuss this topic with respect to the lowpass Butterworth filter design in particular. A brief review of this topic is as follows [13].

The Butterworth filter approximation is based on the fact that all the poles of the filter are uniformly placed on the unit circle in the s-plane.This section deals with a new family of transitional filters, whose design is based on the judicious positioning of the poles in the s-plane. The transitional feature of the new family, dealt with here, is between two Butterworth filters of specific even orders. The poles of these filters constitute a specific reference pole pattern. They lie along the arc of a circle between the reference poles of two specific Butterworth filters. The pole-phasors of each member of the family are of equal magnitude ω_p, not necessarily of unit radius. If the order of the Butterworth filter is a binary power(i.e.,$n = 2^k$, k being an integer), then the pole locations of the filter exhibit interesting symmetry properties. The pole locations are such that they are symmetric about the horizontal axis reference such that a single quadrant pole-parameter synthesis is representative of all the poles of the filter.A new family of transitional Butterworth filters can now be formed by what is called "prescribed symmetrical swinging" of the poles of the filter by specific angles such that the symmetry constraint of the original pole-pattern is not altered. Also, various performance characteristics such as selectivity of magnitude response, sensitivity or critical Q factor, can be smoothly varied by

changing the polar angles appropriately.

The transitional family of filters following this method have the same bandwidth and hence comparison among the various members of the family is more realistic [13].

2.10.2 Pole-parameter Representation

It is well known that the poles of a Butterworth filter of a specific order, are located uniformly on the unit circle in the s-plane. The line joining any pole with the origin of the coordinates is called the pole-phasor having a magnitude ω_p or the "pole frequency" and angle θ_p or the polar-angle as shown in Fig.(2.19).

The pole parameters shown in Fig.(2.19) correspond to the negative real pole (s_r) and a complex-conjugate pole-pair (s, s^*). There is a high degree of geometrical symmetry exhibited by the pole-phasors of a Butterworth filter of even order which is being exploited in the synthesis of a filter family by pole-parameter variation

2.10.3 Complementary Symmetry

For a Butterworth filter of specified order, the poles located on the left-half of s-plane, on the second and third quadrant, are symmetrical about the horizontal axis and hence exhibit a mirror image symmetry. Therefore all the poles on the left-half of the s-plane can be represented just by the poles on the second quadrant only, i.e., the second quadrant poles are representative of all the poles on the left-half of the s-plane.

Let us consider a n^{th} order Butterworth filter. The pole parameters corresponding to the second quadrant poles are given by

$$\omega_{pk} = 1 \begin{cases} k = 1, 2, ..., \frac{n}{2}, & for\, n\, even \\ k = 0, 1, ..., \frac{n-1}{2} & for\, n\, odd \end{cases} \tag{2.24}$$

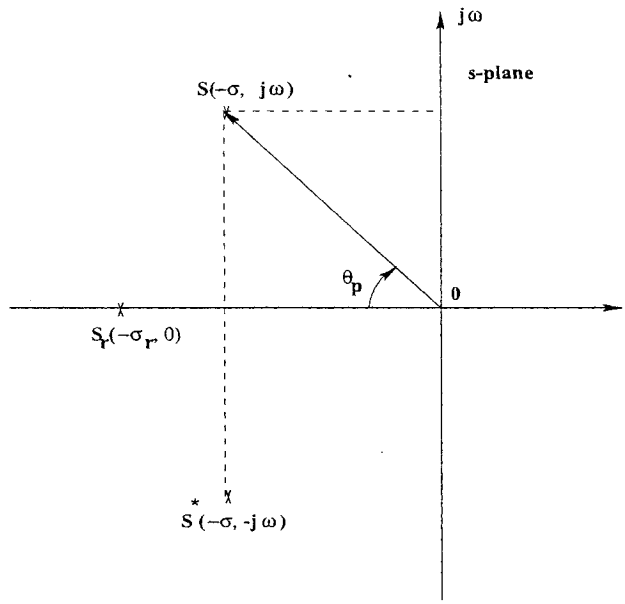

Figure 2.19: Pole parameter representation

and

$$\theta_{pk} = \begin{cases} \frac{(2k-1)\pi}{2n}, \ k = 1, 2, ..., \frac{n}{2} \ \ for\, n\, even \\ \frac{k\pi}{2n}, \ k = 0, 1, ..., \frac{n-1}{2} \ \ for\, n\, odd \end{cases} \tag{2.25}$$

For example, if the order of the filter is 8, i.e., $n = 8$, then there will be be 4 pole phasors of magnitude unity and angles $\pi/16$, $3\pi/16$, $5\pi/16$, $7\pi/16$.

Let us consider the general case, in which all pole-phasors have a magnitude equal to ω_p(not necessarily unity), and the polar angles retained at values as given by Eqn.(2.25). Normalizing the d.c value of the transfer function $A(\omega)$ to unity such that $A(\omega)$ at $\omega = 0$ is independent of ω_p, we can write the squared magnitude expression of the transfer function as follows:

$$A^2(\omega) = \frac{\omega_p^n}{\omega_p^{2n} + \omega^{2n}} \tag{2.26}$$

From the above expression, the pole locations can be written as

$$s_k = \omega_p exp\left[\frac{j(2k-1)\pi}{2n}\right], \ \ for\, k = 1, 2, ..., \frac{n}{2}, \bigvee n\, even \tag{2.27}$$

and

$$s_k = \omega_p exp\left[\frac{jk\pi}{n}\right], \quad for\, k = 0, 1, 2, ..., \frac{n-1}{2}, \bigvee n\, odd \tag{2.28}$$

In general, for any Butterworth filter of a given odd or even order, the Butterworth poles exhibit very interesting symmetry properties with respect to both real as well as the imaginary axis. In addition, if the Butterworth filter is of even order, then the filter displays varying degrees of symmetry. These additional symmetry properties are exploited in designing the new family of transitional filters.

Here, we consider only those filters whose order is a binary power, i.e., $n = 2^k$, k being integers greater than 2 only. This is because, filters of such order possess the highest degree of symmetry and therefore it is easy to deal with such a case although it is possible to extend the same case to filters of various orders. For such class of filters, whose order is a binary power, in addition to half-plane symmetry along the real or imaginary axis, which is common to all Butterworth filters, it is also symmetric with respect to the $\pi/4$ axis, in each quadrant of the s-plane.

To discuss our case, let us consider the order of the filter to be 16, i.e., n=16. Therefore we have 16 poles on the left half of the s-plane, symmetric about the real axis. Now in general, a Butterworth filter with $n = 2^k$ will have $n/2$ poles in the second quadrant given by

$$\theta_k = \frac{(2k-1)\pi}{2n}, \bigvee k = 1, 2, ..., \frac{n}{2} \tag{2.29}$$

This is illustrated in the Fig.(2.20) for n=16.

Fig.(2.20) shows eight poles on the second quadrant. Since the pole positions are symmetric about the real axis, the eight poles on the second quadrant are representative of all the poles of the filter. The eight poles designated as $s_1, s_2, s_3, ..., s_8$ make angles $\theta_1, \theta_2, ...\theta_8$ respectively to the real axis. Within the second quadrant, it is evident that the poles are symmetric about the $\pi/4$ axis and the symmetrical

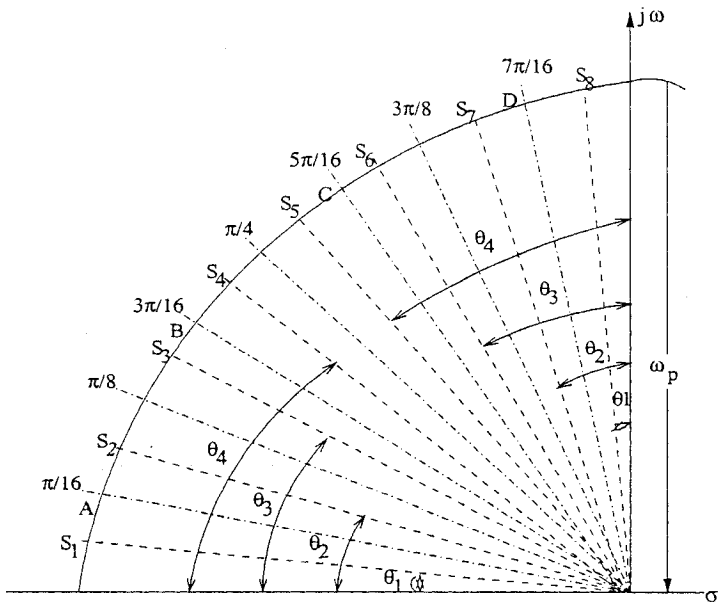

Figure 2.20: Pole plot for a 1-D filter of order n=16

pole pairs are given as follows.

$$\begin{aligned}
&\left[\theta_1 = \frac{\pi}{32} \qquad \theta_8 = \frac{15\pi}{32}\right] \\
&\left[\theta_2 = \frac{3\pi}{32} \qquad \theta_7 = \frac{13\pi}{32}\right] \\
&\left[\theta_3 = \frac{5\pi}{32} \qquad \theta_6 = \frac{11\pi}{32}\right] \\
&\left[\theta_4 = \frac{7\pi}{32} \qquad \theta_5 = \frac{9\pi}{32}\right]
\end{aligned} \tag{2.30}$$

Also, it is clear that the polar angles of each of the above four symmetrical pole-pairs add up to $\pi/2$. In general we may write this as follows

$$(\theta_1 + \theta_8) = (\theta_2 + \theta_7) = (\theta_3 + \theta_6) = (\theta_4 + \theta_5) = \frac{\pi}{2} \tag{2.31}$$

Such pole-pairs, whose θ_p values add upto $\pi/2$ can thus be designated as " Complementary Pole Pairs(CPP's)". It can be seen that each pair of poles with θ_l

and $\theta_{(n/2)-l+1}$, located symmetrically on either side of the $\pi/4$ axis, exhibit the CPP property since

$$(\theta_1 + \theta_{(n/2)-l+1}) = \frac{\pi}{2}, l = 1, 2, ..., \frac{n}{4} \tag{2.32}$$

2.10.4 Symmetrical Swinging

We shall now consider a modification in the Butterworth filter pole-pattern, which will still preserve the CPP property. Before we consider the modification, it is interesting to note that the adjacent Butterworth poles in the second quadrant possess another symmetry, this time, the adjacent pole-pairs (s_1, s_2), (s_3, s_4), (s_5, s_6) and (s_7, s_8) being symmetrical about the lines OA, OB, OC and OD which make an angle of $\pi/16$, $3\pi/16$, $5\pi/16$ and $7\pi/16$ respectively.

By varying the value of θ_0, a family of transitional filters can be obtained. Therefore, in general, for a Butterworth filter of order $n = 2^k$ the modified polar angles can be given by the following general expression.

$$\theta_k^{'} = \frac{(2k-1)\pi}{2n} + (-1)^{k-1}\theta_0, \quad \bigvee k = 1, 2, ..., \frac{n}{2} \tag{2.33}$$

It can also be seen that the modified pole-pattern as given by the Eqn.(2.33) still possesses the CPP property as we get

$$(\theta_l^{'} + \theta_{(n/2)-l+1}^{'}) = \frac{\pi}{2}, \quad \forall l = 1, 2, ..., \frac{n}{4} \tag{2.34}$$

from Eqn.(2.32). Thus it is seen that, the symmetrical swinging of the pole-phasors, equally on both sides conserves the net angle contributed by the adjacent pole-phasors, the net angle being $\pi/2$. This symmetrical swinging of adjacent pole-phasors can be both in the positive or negative direction, being towards or away from the respective axes of symmetry, such that $\theta_0 > 0 \, or \, \theta_0 < 0$ and $|\theta_0|_{max} = \frac{\pi}{2n}$. These family of filters obtained by modifications in the pole-pattern may be referred to as the CPP Filters.

The squared magnitude function of an n^{th} order CPPF can now be obtained as a product of the component squared magnitudes of each CPPF. The second order transfer function corresponding to the complex conjugate pole-pair given by the pole parameters w_{pk} and $\pm\theta_{pk}$ can be written as follows:

$$T_k(s) = \frac{\omega_{pk}^2}{s^2 + 2\omega_{pk}\cos(\theta_{pk})s + \omega_{pk}^2} \tag{2.35}$$

From Eqn.(2.35) the squared magnitude function is thus written as

$$A_k^2(\omega) = T_k(s)T_k(-s) = \frac{\omega_{pk}^4}{\omega^4 + 2\omega_{pk}^2\cos(2\theta_{pk})\omega^2 + \omega_{pk}^2} \tag{2.36}$$

From Eqn.(2.36), the squared magnitude function of each CPPF can be obtained individually and the final squared function can be obtained by taking the product of all the individual magnitude expressions.

For our case say n=16, we know that all the CPP's have the same polar magnitude $\omega_{pk} = \omega_p$. Also from the CPP property, within the 2nd quadrant the adjacent pole-pairs are symmetrical. Therefore

$$(\theta_1' + \theta_4') = (\theta_2' + \theta_3') = \frac{\pi}{4} \tag{2.37}$$

Another symmetry property is that

$$(\theta_1' + \theta_2') = \frac{\pi}{8} \tag{2.38}$$

Using Eqn.(2.36) the squared magnitude function for the poles (s_1', s_8'), (s_2', s_7'), (s_3', s_6') and (s_4', s_5') can be written individually and using the above symmetry properties, they can be eventually combined as follows

$$A^2(\omega) = \left[A_{1,8}^2(\omega).A_{4,5}^2(w)\right] . \left[A_{2,7}^2(\omega).A_{3,6}^2(\omega)\right] \tag{2.39}$$

$$= \frac{\omega_{pk}^{32}}{\omega^{32} - 2\omega_p^{16}\cos(16\theta_1')\omega^{16} + \omega_p^{32}}$$

From Eqn.(2.39), it is possible to deduce the final expression for the magnitude function for a general order $n = 2^k$ as

$$A^2(\omega) = \frac{\omega_{pk}^{2n}}{\omega^{2n} - 2\omega_p^n \cos(n\theta_1')\omega^n + \omega_p^{2n}} \tag{2.40}$$

The value θ_0 is a free parameter, offering another additional degree of freedom. It affects all the θ_p''s and hence the Q_p's including the critical one of the new family of filters we have designated as the Complementary Pole Pair Filters(CPPF's).

Low-Q filters (LQF) [13] are CPPF's corresponding to $\theta_1' > \frac{\pi}{2n}$. This swings the CPP's of the Butterworth filters towards the $\pi/4$ axis in the second quadrant. All the coefficients of $A^2(\omega)$ as in Eqn.(2.40) will be positive, since $\cos(n\theta_1') < 0$. Therefore the denominator expression increases monotonically with respect to ω and therefore $A^2(\omega)$ becomes monotonically decreasing, although not maximally flat. The analysis is more clear if we compare it with a Butterworth filter of the same order.

High-Q filters (HQF) [13] are CPPF's corresponding to $\theta_1' < \frac{\pi}{2n}$. This swings the CPP's of the Butterworth pole-phasors away from the $\pi/4$ axis in the second quadrant. Due to the above condition, $\cos(n\theta_1') > 0$ and the denominator expression of Eqn.(2.40) exhibits maxima and minima at certain values of ω.

2.10.5 Butterworth Filters preserving CPP Property

Here we can apply the technique developed in Section 2.5 to obtain some more properties for these type of filters. The complementary pole pairs for different orders(even) of Butterworth filters are obtained from the transfer functions depending on whether the order of the filter is even or odd. The transfer function can also be determined even when the poles corresponding to filter order 'n' are shifted to a certain angle, provided the filter is stable. We can thus determine the range of 'k'.

If either of the poles when shifted in a Butterworth filter cross over their neighboring poles, then the filter is unstable [13]. Also if the poles are not present

in the Second Quadrant, then the filter is unstable.

A program in "Matlab"(Program A1) is written for the above procedure followed to determine the stability conditions of(range of) 'k' for different orders of Butterworth filters.

When the order of the Butterworth filter 'n'(from 3 to 8) and the shift in corresponding angles of the poles (t_1, t_2.....$t_{(n-1)/2}$ for 'n' odd and t_1, t_2.....$t_{n/2}$ for 'n' even) are given at the input, then the program outputs the stability condition of (range of) 'k' where the corresponding filter exists.

The Matlab Program A1 is shown in Appendix. The analysis for different orders of Butterworth Filter is as follows:

(a) Third order Complementary Pole Pair Filter

For a third order Butterworth filter the transfer function obtained is given by

$$T_3(s) = \frac{1}{(s+1)(s^2 + 2\cos(\frac{\pi}{3} + \phi)s + 1)} \tag{2.41}$$

The above transfer function in Eqn.(2.41) for order n= 3(odd) has its poles having an angle $\theta_1 = (\frac{k \times \pi}{n}) = (\frac{1 \times \pi}{3}) = \frac{\pi}{3}$

The poles s_1 and $s_1^{'}$ are mirror image with each other(complex conjugate pair) and are located at angles $\pi/3$ and$-\pi/3$ respectively as shown in the Fig.(2.21)

The pole s_0 is located at the zero axis and is a negative real pole which is similar to $s_r(-\sigma_r\ ,\ 0)$ as shown before in Fig.(2.19).

The poles s_1 and $s_1^{'}$ can be shifted by any angle ϕ either way, provided which the filter should be stable in all means. i.e the pole s_1 should lie with in the second quadrant in the range between 0 and $\pi/2$. Also the pole s_0 remains stable on the negative real axis.

The simplified transfer function of the above Eqn.(2.41) is as given below

$$T_3(s) = \frac{1}{s^3 + 2s^2 + 2s + 1} \tag{2.42}$$

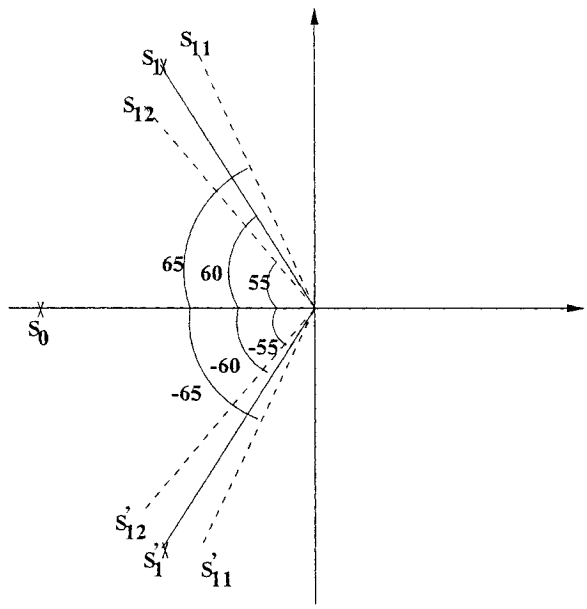

Figure 2.21: Third order Butterworth Filter

Modifying further the above transfer function [24] gives

$$T_3(s) = \frac{1}{g(s) + f(s)} \tag{2.43}$$

where $g(s) = s^3 + 2s^2 + 2s + 1$ is a third order Butterworth polynomial and $f(s) = k$ (a constant).

For our case when no poles s_1 *and* s_1' are shifted, $\phi = 0$ we have the range of k to be $-1 \leq k \leq 3$.

Like wise the stability conditions for any shift in ϕ can be determined by the Program A1 till the shift where the filter is stable.

The results tabulated below in Table{2.3} show the stability conditions (range of) k for a shift of 5° each [25].

Shift in angle ϕ	*Stability Condition*
$-65°$	*UNSTABLE*
$-60°$	$-1 \leq k \leq 8$
$-55°$	$-1 \leq k \leq 7.9544$
$-50°$	$-1 \leq k \leq 7.8186$
$-45°$	$-1 \leq k \leq 7.5958$
$-40°$	$-1 \leq k \leq 7.2909$
$-35°$	$-1 \leq k \leq 6.9108$
$-30°$	$-1 \leq k \leq 6.4641$
$-25°$	$-1 \leq k \leq 5.9606$
$-20o$	$-1 \leq k \leq 5.4115$
$-15°$	$-1 \leq k \leq 4.8284$
$-10°$	$-1 \leq k \leq 4.239$
$-5°$	$-1 \leq k \leq 3.6100$
$0°$	$-1 \leq k \leq 3$
$5°$	$-1 \leq k \leq 2.4049$
$10°$	$-1 \leq k \leq 1.8360$
$15°$	$-1 \leq k \leq 1.3032$
$20°$	$-1 \leq k \leq 0.8152$
$25°$	$-1 \leq k \leq 0.3790$
$30°$	*UNSTABLE*

Table 2.3: Stability conditions for third order Butterworth LPF when the pole s_1 is shifted by an angle ϕ

(b) Fourth order Complementary Pole Pair Filter

For a fourth order Butterworth filter, the transfer function obtained is given by

$$T_4(s) = \frac{1}{(s^2 + 2\cos(\frac{\pi}{8} + \phi_1)s + 1)(s^2 + 2\cos(\frac{3\pi}{8} - \phi_2)s + 1)} \tag{2.44}$$

The above transfer function for order n= 4(even) has its poles having at angles $\theta_1 = \left(\frac{(2k-1)\times\pi}{2n}\right) = \left(\frac{(2\times1-1)\times\pi}{2\times4}\right) = \frac{\pi}{8}(22.5°)$ and $\theta_2 = \left(\frac{(2\times2-1)\times\pi}{2\times4}\right) = \frac{3\pi}{8}(67.5°)$.

The pole pairs s_1 and s_2 are Complementary Pole Pairs(CPP's) as their corresponding angles $\theta_1$and θ_2 add upto $\pi/2$ when there is no shift in ϕ_1 and ϕ_2.

$$i.e.\ \theta_1 + \theta_2 = \pi/8 + 3\pi/8 = \pi/2. \tag{2.45}$$

Here the poles s_1 and $s_1^{'}$are mirror image with each other and are located at

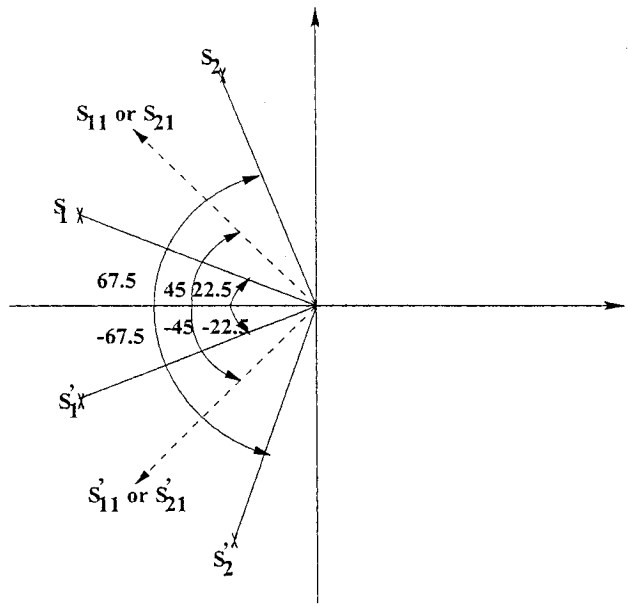

Figure 2.22: Fourth order Butterworth(CPP) Filter

angles $\pi/8$ and $-\pi/8$ respectively and the poles s_2 and $s_2^{'}$ are located at angles $3\pi/8$ and $-3\pi/8$ respectively as shown in the Fig.(2.22).

The poles s_1 and $s_1^{'}$ can be shifted by any angle ϕ_1 and similarly the poles s_2 and $s_2^{'}$ can also be shifted by an angle ϕ_2 provided which the filter should be stable in all means. i.e the pole s_1 should lie with in the second quadrant in the range between 0 and s_2, while s_2 should lie with in second quadrant in the range between s_1 and $\pi/2$.

The simplified transfer function of the above Eqn.(2.24) when $\phi_1 = \phi_2 = 0$(no shift in angles) is as given below.

$$T_4(s) = \frac{1}{s^4 + 2.613s^3 + 3.4142s^2 + 2.613s + 1} \tag{2.46}$$

Modifying further the above transfer function [24] gives

$$T_4(s) = \frac{1}{g(s) + f(s)}$$

where $g(s) = s^4 + 2.613s^3 + 3.414s^2 + 2.613s + 1$ is a fourth order Butterworth polynomial and $f(s) = k$ (a constant).

Shift in angle ϕ_1	*Shift in angle* ϕ_2	*Stability Condition*
0°	0°	$-1 \leq k \leq 1.4142$
0°	5°	$-1 \leq k \leq 1.7064$
0°	−15°	$-1 \leq k \leq 1.9856$
0°	45°	$-1 \leq k \leq 3.4142$
0°	−5°	$-1 \leq k \leq 1.1113$
35°	5°	*UNSTABLE*
35°	−15°	$-1 \leq k \leq 0.3796$
35°	−15°	$-1 \leq k \leq 0.1102$
35°	20°	*UNSTABLE*
−15°	0°	$-1 \leq k \leq 1.2445$
−15°	20°	$-1 \leq k \leq 1.9710$
−15°	40°	$-1 \leq k \leq 2.4521$
−15°	50°	$-1 \leq k \leq 2.6095$
−15°	−5°	$-1 \leq k \leq 1.0025$
−15°	−15°	$-1 \leq k \leq 0.3271$
−25°	0°	$-1 \leq k \leq 1.3041$
−25°	15°	$-1 \leq k \leq 1.8928$
−25°	35°	$-1 \leq k \leq 2.4418$

Table 2.4: Stability conditions for fourth order Butterworth LPF when the poles s_1 and s_2 are shifted by angles ϕ_1 & ϕ_2

For our case when none of the poles s_1, $s_1^{'}$, $s_2 \, and \, s_2^{'}$ are shifted, i.e when $\phi_1 = \phi_2 = 0$, we have the range of k to be $-1 \leq k \leq 1.414$.

Like wise the stability conditions for any shift in ϕ_1 and ϕ_2 can be determined by the Program A1 till the shift where the filter is stable.

The results tabulated below in Table{2.4} show the stability conditions (range of) k for different shifts in angles $\phi_1 \, and \, \phi_2$(in degrees).

(c) Fifth order Complementary Pole Pair Filter

For a fifth order Butterworth filter, the transfer function obtained is given by

$$T_5(s) = \frac{1}{(s+1)(s^2 + 2\cos(\frac{\pi}{5} + \phi_1)s + 1)(s^2 + 2\cos(\frac{2\pi}{5} - \phi_2)s + 1)} \tag{2.47}$$

The above transfer function for order n= 4(even) has its poles having an angle $\theta_1 = \left(\frac{k \times \pi}{n}\right) = \left(\frac{1 \times \pi}{5}\right) = \frac{\pi}{5}(36°)$ and $\theta_2 = \left(\frac{2 \times \pi}{5}\right) = \frac{2\pi}{5}(72°)$

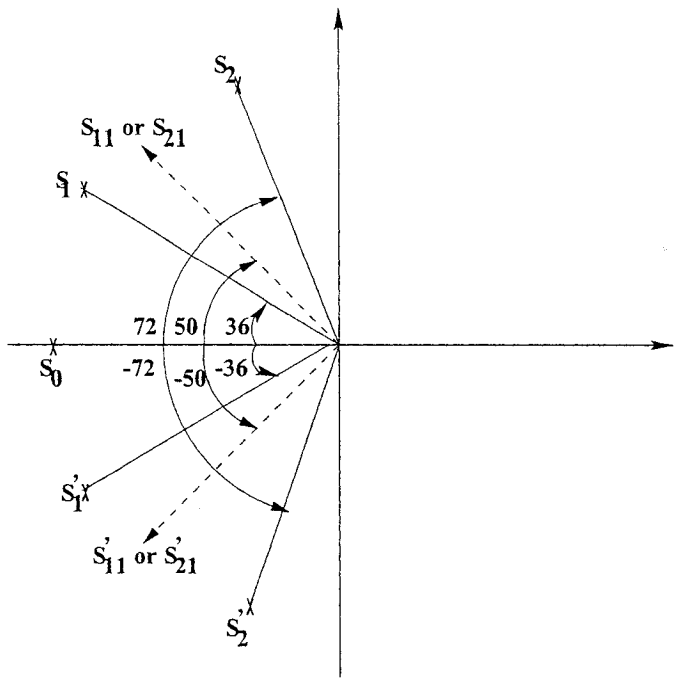

Figure 2.23: Fifth order Complementary Pole Pair Filter

Here the poles s_1 and $s_1^{'}$ are mirror image(complex conjugate pair) with each other and are located at angles $\pi/5$ and $-\pi/5$ respectively where as the poles s_2 and $s_2^{'}$ are located at angles $2\pi/5$ and $-2\pi/5$ respectively as shown in the Fig.(2.23).

The pole s_0 is located at the zero axis and is a negative real pole.

The poles s_1 and $s_1^{'}$ can be shifted by any angle ϕ_1 and similarly the poles s_2 and $s_2^{'}$ can also be shifted by an angle ϕ_2 provided which the filter should be stable in all means. i.e the pole s_1 should lie with in the 2^{nd} quadrant in the range between 0 and s_2, while s_2 should lie with in second quadrant in the range between s_1 and $\pi/2$. Also the pole s_0 remains stable on the negative real axis.

The simplified transfer function of the above Eqn.(2.47). when $\phi_1 = \phi_2 = 0$(when no poles are shifted) is given as below

$$T_5(s) = \frac{1}{s^5 + 3.236s^4 + 5.235s^3 + 5.235s^2 + 3.236s + 1} \tag{2.48}$$

Modifying further the above transfer function [24] gives

$$T_5(s) = \frac{1}{g(s) + f(s)}$$

where $g(s) = s^5 + 3.236s^4 + 5.235s^3 + 5.235s^2 + 3.236s + 1$ is a fifth order Butterworth polynomial and $f(s) = k$ (a constant).

For our case when there none of the poles s_1, s_1', s_2 *and* s_2' are shifted, i.e when $\phi_1 = \phi_2 = 0$, we have the range of k to be $-1 \leq k \leq 1.0900$.

Like wise the stability conditions for any shift in ϕ_1 and ϕ_2 can be determined by the Program A1 till the shift where the filter is stable.

The results tabulated below in Table{2.5} show the stability conditions (range of) k for different shifts in angles ϕ_1 *and* ϕ_2 (in degrees).

Shift in angle ϕ_1	*Shift in angle* ϕ_2	*Stability Condition*
0°	0°	$-1 \leq k \leq 1.0900$
5°	5°	$-1 \leq k \leq 1.2061$
5°	10°	$-1 \leq k \leq 1.7313$
10°	−5°	$-1 \leq k \leq 0.7539$
10°	−10°	$-1 \leq k \leq 0.5287$
15°	20°	$-1 \leq k \leq 1.4471$
15°	25°	*UNSTABLE*
20°	−10°	$-1 \leq k \leq 0.4255$
20°	−15°	$-1 \leq k \leq 0.1930$
25°	10°	$-1 \leq k \leq 0.9535$
30°	10°	$-1 \leq k \leq 0.3100$
35°	−5°	$-1 \leq k \leq 0.3760$
35°	−10°	$-1 \leq k \leq 0.2491$
−5°	40°	$-1 \leq k \leq 2.3056$
−5°	45°	*UNSTABLE*
−10°	−10°	$-1 \leq k \leq 0.6850$
−10°	−15°	$-1 \leq k \leq 0.3156$
−15°	15°	$-1 \leq k \leq 1.8156$
−15°	20°	$-1 \leq k \leq 1.9710$
−20°	50°	$-1 \leq k \leq 2.6637$
−30°	60°	$-1 \leq k \leq 2.8309$
−35°	45°	$-1 \leq k \leq 2.6656$

Table 2.5: Stability conditions for fifth order Butterworth LPF when the poles s_1 and s_2 are shifted by angles ϕ_1 & ϕ_2

(d) Sixth order Complementary Pole Pair Filter

For a sixth order Butterworth filter, the transfer function obtained is given by

$$T_6(s) = \frac{1}{(s^2 + 2\cos(\frac{\pi}{12} + \phi_1)s + 1)(s^2 + 2\cos(\frac{3\pi}{12} - \phi_2)s + 1)(s^2 + 2\cos(\frac{5\pi}{12} + \phi_3)s + 1)} \tag{2.49}$$

The above transfer function for order n=6(even) has its poles having an angle $\theta_1 = \left(\frac{(2k-1)\times\pi}{2n}\right) = \left(\frac{(2\times1-1)\times\pi}{2\times6}\right) = \frac{\pi}{12}(15°)$, $\theta_2 = \left(\frac{(2\times2-1)\times\pi}{2\times6}\right) = \frac{3\pi}{12}(45°)$ and $\theta_3 = \left(\frac{(2\times3-1)\times\pi}{2\times6}\right) = \frac{5\pi}{12}(75°)$.

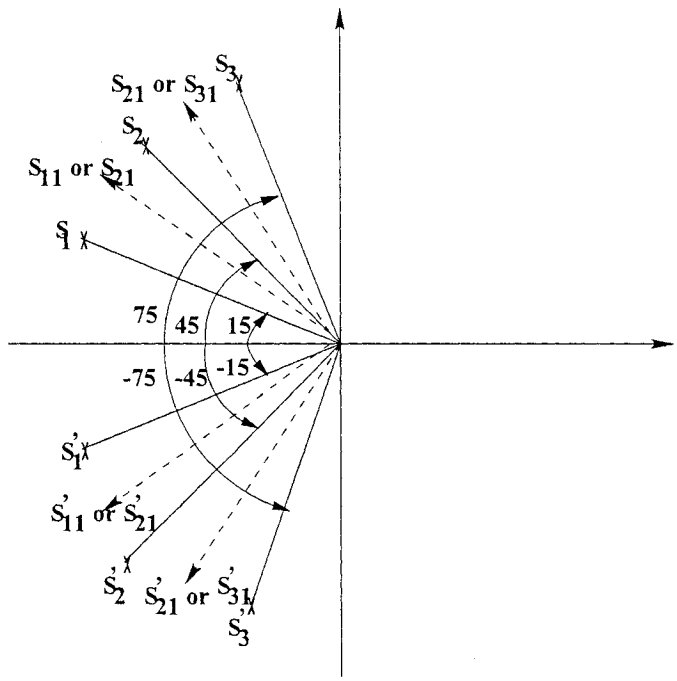

Figure 2.24: Sixth order Butterworth(CPP's) Filter

The pole pairs s_1 and s_3 are Complementary Pole Pairs(CPP's) as their corresponding angles $\theta_1$and θ_3 add upto $\pi/2$ when there is no shift in ϕ_1 and ϕ_3.

$$i.e.\ \theta_1 + \theta_3 = \pi/12 + 5\pi/12 = \pi/2. \tag{2.50}$$

Here the poles s_1 and $s_1^{'}$ are mirror image with each other(complex conjugate pair) and are located at angles $\pi/12$ and $-\pi/12$. Similarly the poles s_2 and $s_2^{'}$ are mirror image with each other and are located at angles $3\pi/12$ and $-3\pi/12$ and also the poles s_3 and$s_3^{'}$ are mirror images with each other and are located at angles $5\pi/12$ and $-5\pi/12$ from the origin as shown in the Fig.(2.24).

The poles s_1 and $s_1^{'}$ can be shifted by any angle ϕ_1 , similarly the poles s_2, $s_2^{'}$ and s_3, $s_3^{'}$ can also be shifted by an angle ϕ_2 and ϕ_3 respectively, provided which the filter should remain stable in all means, i.e the pole s_1 should lie with in the second quadrant in the range between 0 and s_2, while the pole s_2 should lie with in

the second quadrant in the range between s_1 and s_3 and the pole s_3 should lie in the range between s_2 and $\pi/2$ in the second quadrant.

The simplified transfer function of the above Eqn.(2.49). when $\phi_1 = \phi_2 = \phi_3 = 0$ is given as below

$$T_6(s) = \frac{1}{s^6 + 3.8636s^5 + 7.4637s^4 + 9.1410s^3 + 7.4637s^2 + 3.8636s + 1} \tag{2.51}$$

Modifying further the above transfer function [24] gives

$$T_6(s) = \frac{1}{g(s) + f(s)}$$

where $g(s) = s^6 + 3.8636s^5 + 7.4637s^4 + 9.1410s^3 + 7.4637s^2 + 3.8636s + 1$ is a sixth order Butterworth polynomial and $f(s) = k$ (a constant).

For our case when there none of the poles s_1, $s_1^{'}$, $s_2, s_2^{'}, s_3 \, and \, s_3^{'}$ are shifted, i.e when $\phi_1 = \phi_2 = \phi_3 = 0$, we have the range of k to be $-1 \leq k \leq 1.014$.

Like wise the stability conditions for any shift in ϕ_1, ϕ_2 and ϕ_3 can be determined by the Program A1 till the shift where the filter is stable.

The results tabulated below in Table{2.6} show the stability conditions (range of) k for different shifts in angles ϕ_1, ϕ_2 and ϕ_3 (in degrees).

$Shift\ in\ angle\ \phi_1$	$Shift\ in\ angle\ \phi_2$	$Shift\ in\ angle\ \phi_3$	$Stability\ Condition$
0°	0°	0°	$-1 \leq k \leq 1.0319$
0°	0°	−30°	$-1 \leq k \leq 1.6181$
0°	10°	−40°	$-1 \leq k \leq 1.8943$
0°	−5°	−25°	$-1 \leq k \leq 1.4570$
0°	−20°	−10°	$-1 \leq k \leq 0.8927$
0°	−30°	5°	$-1 \leq k \leq 0.3596$
5°	5°	5°	$-1 \leq k \leq 0.9113$
5°	15°	0°	$-1 \leq k \leq 1.7939$
5°	20°	−55°	$UNSTABLE$
5°	25°	−40°	$-1 \leq k \leq 2.0090$
5°	−10°	10°	$-1 \leq k \leq 0.5272$
5°	−20°	−10°	$-1 \leq k \leq 0.8712$
5°	−25°	0°	$-1 \leq k \leq 0.5581$
5°	−20°	15°	$UNSTABLE$

Table 2.6: Stability conditions for sixth order Butterworth LPF when the poles s_1, s_2 and s_3 are shifted by angles ϕ_1, ϕ_2 & ϕ_3

(e) Seventh order Complementary Pole Pair Filter

For a seventh order Butterworth filter, the transfer function obtained is given by

$$T_7(s) = \frac{1}{(s+1)(s^2+2\cos(\frac{\pi}{7}+\phi_1)s+1)(s^2+2\cos(\frac{2\pi}{7}-\phi_2)s+1)(s^2+2\cos(\frac{3\pi}{7}+\phi_3)s+1)} \tag{2.52}$$

The above transfer function for order n= 4(even) has its poles having an angle $\theta_1 = \left(\frac{k\times\pi}{n}\right) = \left(\frac{1\times\pi}{7}\right) = \frac{\pi}{7}(25.714°)$, $\theta_2 = \left(\frac{2\times\pi}{7}\right) = \frac{2\pi}{7}(51.428°)$ and $\theta_3 = \left(\frac{(2\times3-1)\times\pi}{2\times6}\right) = \frac{3\pi}{7}(77.142°)$

Here the poles s_1 and $s_1^{'}$ are mirror image with each and are located at angles $\pi/7$ and $-\pi/7$ respectively. Similarly the poles s_2 and $s_2^{'}$ mirror image with each other and are located at angles $2\pi/7$ and $-2\pi/7$ respectively. Also the poles s_3 and$s_3^{'}$ are mirror image with each other and are located at angles $3\pi/7$ and$-3\pi/7$ respectively from the origin as shown in Fig.(2.25)

The pole s_0 is located at the zero axis and is a negative real pole.

The poles s_1 and $s_1^{'}$ can be shifted by any angle ϕ_1 , similarly poles s_2, $s_2^{'}$ and

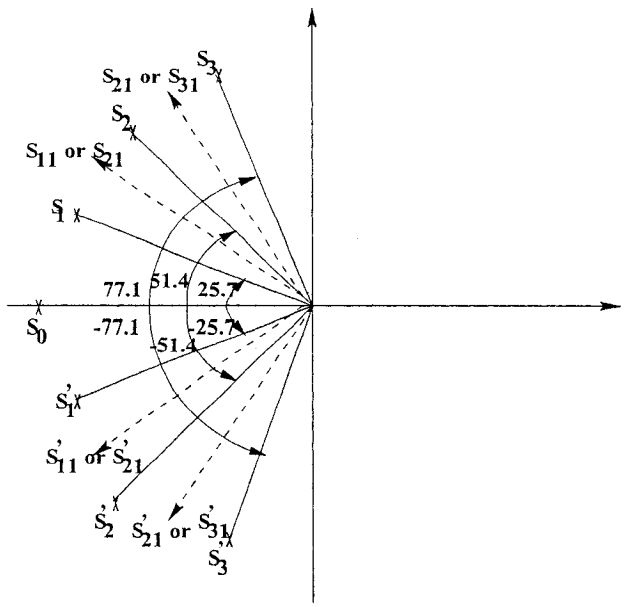

Figure 2.25: Seventh order Butterworth Filter

s_3, $s_3^{'}$ can also be shifted by an angle ϕ_2 and ϕ_3 respectively, provided which the filter should remain stable in all means, i.e the pole s_1 should lie with in the second quadrant in the range between 0 and s_2, while the pole s_2 should lie with in the second quadrant in the range between s_1 and s_3 and the pole s_3 should lie in the range between s_2 and $\pi/2$ in the second quadrant. Also the pole s_0 remains stable on the negative real axis.

The simplified transfer function of the above Eqn.(2.52). when $\phi_1 = \phi_2 = \phi_3 = 0$ is given as below

$$T_7(s) = \frac{1}{s^7 + 4.4939s^6 + 10.0977s^5 + 14.5916s^4 + 14.5916s^3 + 10.0977s^2 + 4.4939s + 1} \tag{2.53}$$

Modifying further the above transfer function [24] gives

$$T_7(s) = \frac{1}{g(s) + f(s)}$$

where $g(s) = s^7+4.4939s^6+10.0977s^5+14.5916s^4+14.5917s^3+10.0977s^2+4.4939s+1$ is a seventh order Butterworth polynomial and $f(s) = k$ (a constant).

For our case when none of the poles s_1, $s_1^{'}$, s_2, $s_2^{'}$, s_3 *and* $s_3^{'}$ are shifted, i.e when $\phi_1 = \phi_2 = \phi_3 = 0$, we have the range of k to be $-1 > k < 1.0014$.

Like wise the stability conditions for any shift in ϕ_1, ϕ_2 and ϕ_3 can be determined by the Program A1 till the shift where the filter is stable.

The results tabulated below in Table{2.7} show the stability conditions (range) of k for different shifts in angles ϕ_1, ϕ_2, *and* ϕ_3 (in degrees).

Shift in angle ϕ_1	*Shift in angle* ϕ_2	*Shift in angle* ϕ_3	*Stability Condition*
0°	0°	0°	$-1 \leq k \leq 1.0014$
0°	0°	10°	$-1 \leq k \leq 0.9194$
0°	5°	−30°	$-1 \leq k \leq 1.4715$
0°	10°	5°	$-1 \leq k \leq 1.0624$
0°	25°	−25°	$-1 \leq k \leq 1.5981$
0°	−5°	−15°	$-1 \leq k \leq 1.1562$
5°	5°	0°	$-1 \leq k \leq 0.9642$
5°	5°	5°	$-1 \leq k \leq 0.9551$
5°	10°	−10°	$-1 \leq k \leq 1.2385$
5°	10°	−40°	*UNSTABLE*
5°	15°	−35°	$-1 \leq k \leq 1.5878$
−25°	−10°	−15°	$-1 \leq k \leq 1.1701$
−10°	30°	−45°	$-1 \leq k \leq 1.8684$
20°	5°	−20°	$-1 \leq k \leq 1.2913$

Table 2.7: Stability conditions for seventh order Butterworth LPF when the poles s_1, s_2 and s_3 are shifted by angles ϕ_1, ϕ_2 & ϕ_3

(f) Eighth order Complementary Pole Pair Filter

For an eighth order Butterworth filter, the transfer function obtained is given by

$$T_8(s) = \left\{ \frac{1}{(s^2 + 2\cos(\frac{\pi}{16} + \phi_1)s + 1)(s^2 + 2\cos(\frac{3\pi}{16} - \phi_2)s + 1)} \right\} \bullet$$

$$\left\{ \frac{1}{(s^2 + 2\cos(\frac{5\pi}{16} + \phi_3)s + 1)(s^2 + 2\cos(\frac{7\pi}{16} - \phi_4)s + 1)} \right\} \tag{2.54}$$

The above transfer function for order n=4(even) has its poles having angles $\theta_1 = \left(\frac{(2k-1)\times\pi}{2n}\right) = \left(\frac{(2\times1-1)\times\pi}{2\times8}\right) = \frac{\pi}{16}(11.25°)$, $\theta_2 = \left(\frac{(2\times2-1)\times\pi}{2\times8}\right) = \frac{3\pi}{16}(33.75°)$, $\theta_3 = \left(\frac{(2\times3-1)\times\pi}{2\times8}\right) = \frac{5\pi}{16}(56.25°)$ and $\theta_4 = \left(\frac{(2\times4-1)\times\pi}{2\times8}\right) = \frac{7\pi}{16}(78.75°)$.

The pole pairs (s_1, s_4) and (s_2, s_3) are Complementary Pole Pairs(CPP's) as their corresponding angles (θ_1, θ_4) and (θ_2, θ_3) add upto $\pi/2$ when there is no shift in ϕ_1, ϕ_2, ϕ_3 and ϕ_4.

$$i.e.\ \theta_1 + \theta_4 = \pi/16 + 7\pi/12 = \pi/2. \tag{2.55}$$

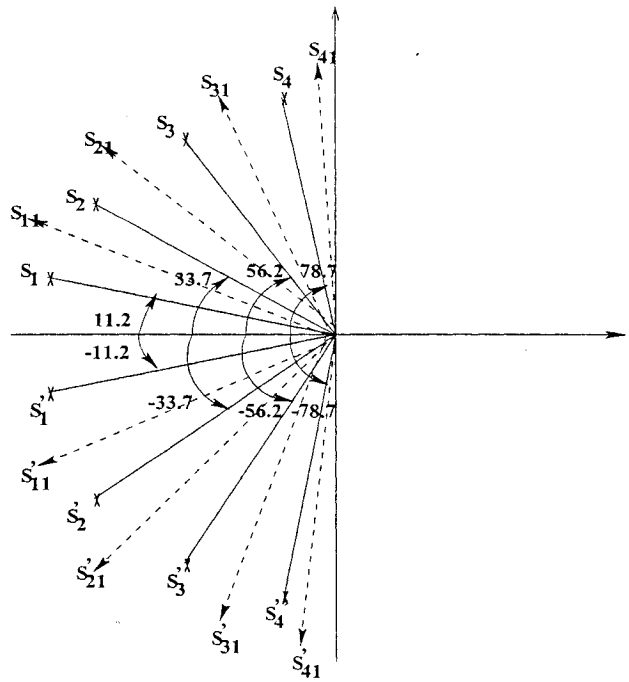

Figure 2.26: Eighth order Butterworth(CPP's) Filter

and

$$\theta_2 + \theta_3 = 3\pi/16 + 5\pi/16 = \pi/12. \tag{2.56}$$

Here the poles s_1 and $s_1^{'}$ are mirror image(complex conjugate pairs) with each other and are located at angles $\pi/16$ and $-\pi/16$ respectively, likewise the poles s_2 and $s_2^{'}$ are mirror image and are located at angles $3\pi/16$ and $-\pi/16$ respectively. Also the poles s_3 and$s_3^{'}$ are mirror image with each other which are located at angles $5\pi/16$ and $-5\pi/16$ respectively, and the poles s_4 and $s_4^{'}$ are mirror image and are located at an angle $7\pi/16$ and $-7\pi/16$ respectively from the origin as shown in the Fig.(2.26).

The poles s_1 and $s_1^{'}$ can be shifted by any angle ϕ_1 , similarly poles s_2, $s_2^{'}$, s_3, $s_3^{'}$, s_4 and $s_4^{'}$ can also be shifted by an angle ϕ_2 , ϕ_3 and ϕ_4 respectively, provided which the filter should remain stable in all means.

i.e.the pole s_1 should lie with in the second quadrant in the range between

$Shift\,in\,angle\,\phi_1$	$Shift\,in\,angle\,\phi_2$	$Shift\,in\,angle\,\phi_3$	$Shift\,in\,angle\,\phi_4$	$Stability\,Condition$
0°	0°	0°	0°	$-1 \leq k \leq 1.0001$
0°	0°	−20°	5°	$-1 \leq k \leq 1.2542$
0°	0°	−15°	15°	$-1 \leq k \leq 1.2940$
0°	0°	−20°	40°	$-1 \leq k \leq 1.5303$
0°	0°	5°	0°	$-1 \leq k \leq 0.9333$
0°	5°	−15°	−10°	$-1 \leq k \leq 1.1709$
0°	5°	−5°	−5°	$-1 \leq k \leq 1.0633$
0°	5°	0°	25°	$UNSTABLE$
0°	5°	10°	10°	$-1 \leq k \leq 1.0177$
−5°	−5°	−5°	−5°	$-1 \leq k \leq 0.9886$
5°	5°	5°	5°	$-1 \leq k \leq 1.0076$
10°	5°	10°	5°	$-1 \leq k \leq 0.9217$
−10°	15°	−10°	15°	$-1 \leq k \leq 1.3504$

Table 2.8: Stability conditions for eighth order Butterworth LPF when the poles s_1, s_2, s_3 and s_4 are shifted by angles ϕ_1, ϕ_2 ,ϕ_3 & ϕ_4

0 and s_2, while the pole s_2 should lie with in the second quadrant in the range between s_1 and s_3 and the pole s_3 should lie in the range between s_2 and s_4 in the 2^{nd} quadrant, the pole s_4 should lie in the range between s_3 and $\pi/2$ in the second quadrant.

The simplified transfer function of the above Eqn.(2.54) when $\phi_1 = \phi_2 = \phi_3 = \phi_4 = 0$ is as given below

$$T_8(s) = \frac{1}{(s^8 + 5.1256s^7 + 13.1360s^6 + 21.8440s^5 + 25.6857s^4 + 21.8440s^3 + 13.1360s^2 + 5.1256s + 1)} \quad (2.57)$$

Modifying further the above transfer function [24] gives

$$T_8(s) = \frac{1}{g(s) + f(s)}$$

where $g(s) = s^8 + 5.1256s^7 + 13.1360s^6 + 21.8440s^5 + 25.6857s^4 + 21.8440s^3 + 13.1360s^2 + 5.1256s + 1$ is an eighth order Butterworth polynomial and $f(s) = k$ (a constant).

For our case when none of the poles s_1, $s_1^{'}$, $s_2, s_2^{'}, s_3$, $s_3^{'}$, $s_4\,and\,s_4^{'}$ are shifted, i.e when $\phi_1 = \phi_2 = \phi_3 = \phi_4 = 0$, we have the range of k to be $-1 > k < 1.0001$.

Like wise the stability conditions for any shift in ϕ_1, ϕ_2, ϕ_3 and ϕ_4 can be determined by the Program A1 till the shift where the filter is stable.

The results tabulated in Table{2.8} show the stability conditions(range of) 'k' for different shifts in angles ϕ_1, ϕ_2, ϕ_3 and ϕ_4(in degrees).

2.10.6 Two -dimensional CPPF

With the above results in 1-D, we shall extend the same to the construction of complementary pole-pair filters to the 2-D case also. In this case, the 2-D CPPF is simply obtained as a product of two cascaded 1-D filters as an independent product. This means that variation of pole parameters in each dimension is independent too.

The concept of 2-D CPPF has been studied using the same transfer function that was used earlier in this chapter. The transfer function used in this case and the roots are determined as follows.

Let

$$T_1(s_1) = \frac{1}{g_1(s_1) + f_1(s_1)}$$

where $g_1(s_1) = s_1^3 + 2s_1^2 + 2s_1 + 1$ is a third order Butterworth polynomial and $f_1(s_1) = k_1$ (a constant).

Similarly for $g_2(s_2)$ and $f_2(s_2)$ in the second dimension, we have

$$T_2(s_2) = \frac{1}{g_2(s_2) + f_2(s_2)}$$

where $g_2(s_2) = s_2^3 + 2s_2^2 + 2s_2 + 1$ and $f_2(s_2) = k_2$.

The above transfer function gives two complex poles on the 2nd and 3rd quadrants respectively forming angles of $+60°$ and $-60°$ respectively with the X-axis in the negative direction. The values of k_1 and k_2 are chosen as the optimum values for elliptical symmetry as was derived from Program A3. The values are chosen to be $k_1 = -0.45$ and $k_2 = -0.20$ and the poles(S_1 and S'_{11}) are determined based on the transfer function.

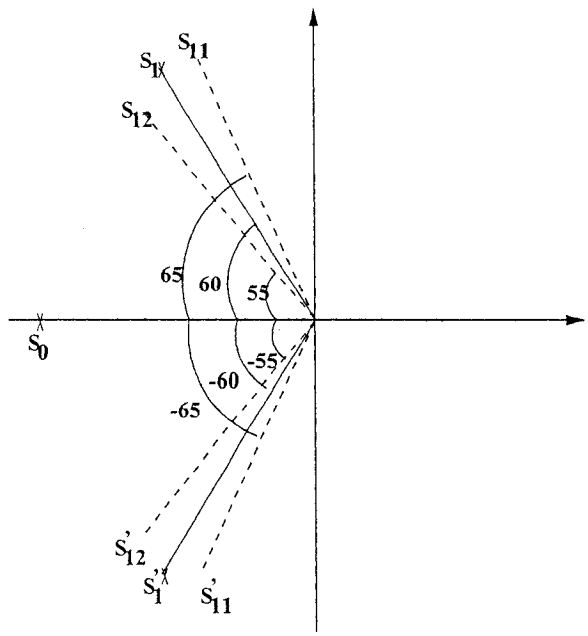

Figure 2.27: Shift of poles by angle of $\pm 5^{deg}$ for two independent transfer functions.

The poles are then shifted by an angle $\pm 5°$ as shown in Fig.(2.27), giving rise to two different pole-pairs (S_{11}, S'_{11}) and (S_{12}, S'_{12}) making angles of $\pm 65°$ and $\pm 55°$ respectively with the negative real axis.

The poles for these angles are then calculated and the transfer function is determined. The optimum range of k for stability, for these transfer functions is found to be

(a) For positive shift in pole of 5°(away from each other) : $-1 < k < 2.4049$

(b) For negative shift in pole of 5°(towards from each other) : $-1 < k < 3.61$

When the poles are shifted by 5° , then the filter exhibits elliptical symmetry at the values of $k_1 = -0.47$ & $k_2 = -0.23$. And, when the poles are shifted by -5° , the filter exhibits elliptical symmetry at the values of $k_1 = -0.42$ & $k_2 = -0.18$.

The Program for the 2-D case follows the same pattern as the 1-D case and therefore has not been shown. Figs.(2.28(a) and (b)) show the 2-D filter response before any pole parameter transformation has been applied to it.

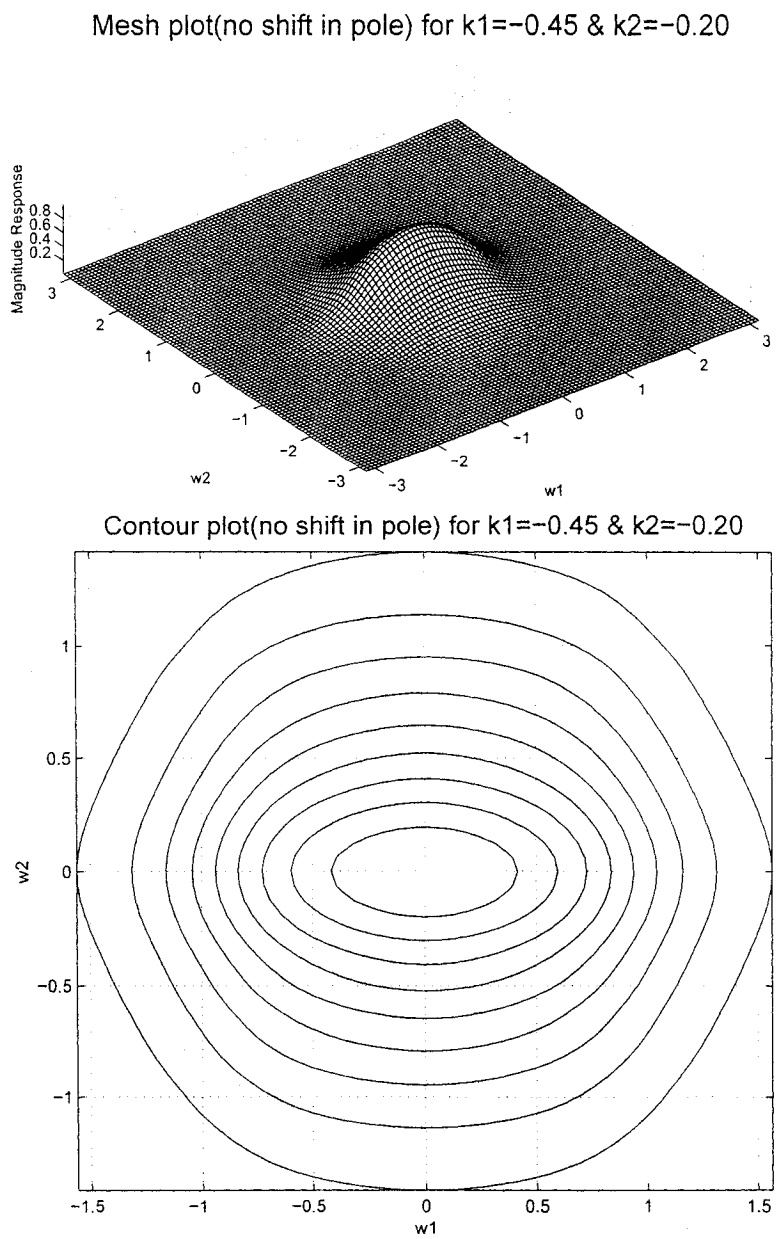

Figure 2.28: 2-D CPPF showing near elliptical symmetry at k1=-0.45 and k2=-0.20.

Figs.((2.29) and (2.30)) show the 2-D filter response after a pole shift of $+5°$ has been applied to it. Applying Program A3 to these responses(Figs.(2.31) and (2.32)), it has been found that at $k_1 = -0.47$ & $k_2 = -0.23$, it exhibits near elliptical symmetry for the magnitude range $0.49 < Mag < 0.51$. This has been shown only for this case (as in Fig(2.31(c)), as an illustration. The same procedure has however been used in determining the value of k_1 and k_2 for all the cases of pole shifts discussed in this section.

Figs.(2.33) and (2.34) show the 2-D filter response after a pole of -5° has been applied to it. From Figs.(2.35) and (2.36), it is seen that near elliptical symmetry has been obtained at a value of $k_1 = -0.42$ & $k_2 = -0.18$.

For both positive negative pole-parameter shifting, it has been found that elliptical symmetry can still be achieved within the optimum stability range of k_1 and k_2. The same can be achieved for different values of θ_0, i.e., for different values in the angle and therefore different values of k_1 and k_2 . The plots that follow show the above simulation for values of $\theta_0 = \pm 10°, \pm 25°$.

Figs.(2.37) and (2.38) show the 2-D filter response after a pole shift of $+10°$ has been applied to it. Here it is seen that near elliptical symmetry has been obtained at values $k_1 = -0.53$ & $k_2 = -0.33$.

Figs.(2.39) and (2.40) show the 2-D filter response after a pole shift of $-10°$ has been applied to it. Here it is seen that near elliptical symmetry has been obtained at values $k_1 = -0.40$ & $k_2 = -0.15$.

Figs.(2.41) and (2.42) show the 2-D filter response after a pole shift of $+25°$ has been applied to it. Here it is seen that near elliptical symmetry has been obtained at values $k_1 = -0.82$ & $k_2 = -0.69$.

Figs.(2.43) and (2.44) show the 2-D filter response after a pole shift of $-25°$ has been applied to it. Here it is seen that near elliptical symmetry has been obtained at values $k_1 = -0.36$ & $k_2 = -0.08$.

Table{2.9} summarizes the results for the six cases that has been discussed.

Angular Shift(in degrees)	Stability range of k	Values of k_1 & k_2 for elliptical symmetry
$\theta_0 = -25$	$-1 \leq k \leq 5.9606$	$k_1 = -0.36$ & $k_2 = -0.08$
$\theta_0 = -10$	$-1 \leq k \leq 4.239$	$k_1 = -0.40$ & $k_2 = -0.15$
$\theta_0 = -5$	$-1 \leq k \leq 3.61$	$k_1 = -0.42$ & $k_2 = -0.18$
$\theta_0 = +5$	$-1 \leq k \leq 2.4049$	$k_1 = -0.47$ & $k_2 = -0.23$
$\theta_0 = +10$	$-1 \leq k \leq 1.836$	$k_1 = -0.53$ & $k_2 = -0.33$
$\theta_0 = +25$	$-1 \leq k \leq 0.3790$	$k_1 = -0.82$ & $k_2 = -0.69$

Table 2.9: Summary of the results achieved due to different values of angular shift in the complex poles and their corresponding values of k_1 & k_2 for elliptical symmetry. The range of magnitude chosen for all the above cases is 0.49<Mag<0.51.

As it can be seen, for different values of angular shift in the complex poles in each of the cases, the values of k_1 & k_2 also shift correspondingly for near elliptical symmetry. However with greater increase in the value of positive angular shift, it can be seen that the filter does not precisely holds the elliptic symmetry principle within the stable region of k. Comparing the elliptical symmetric characteristic for $\theta_0 = \pm 5°, \pm 10°$ *and* $\pm\ 25°$, it can be easily deduced that for $+25°$ the elliptical symmetric property reduces considerably.

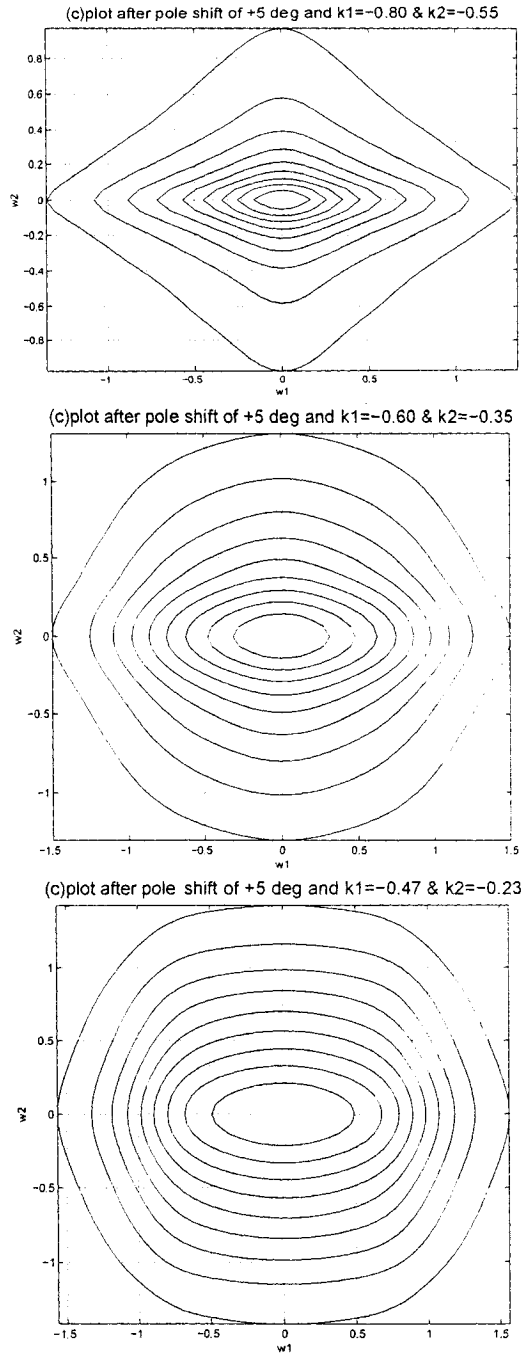

Figure 2.29: 2-D CPPF after pole parameter transformation of $\theta_0 = +5^{\text{deg}}$ for (a) k1=-0.80 and k2=-0.55 (b) k1=-0.60 and k2=-0.35 (c) k1=-0.47 and k2=-0.23 (showing near elliptical symmetry).

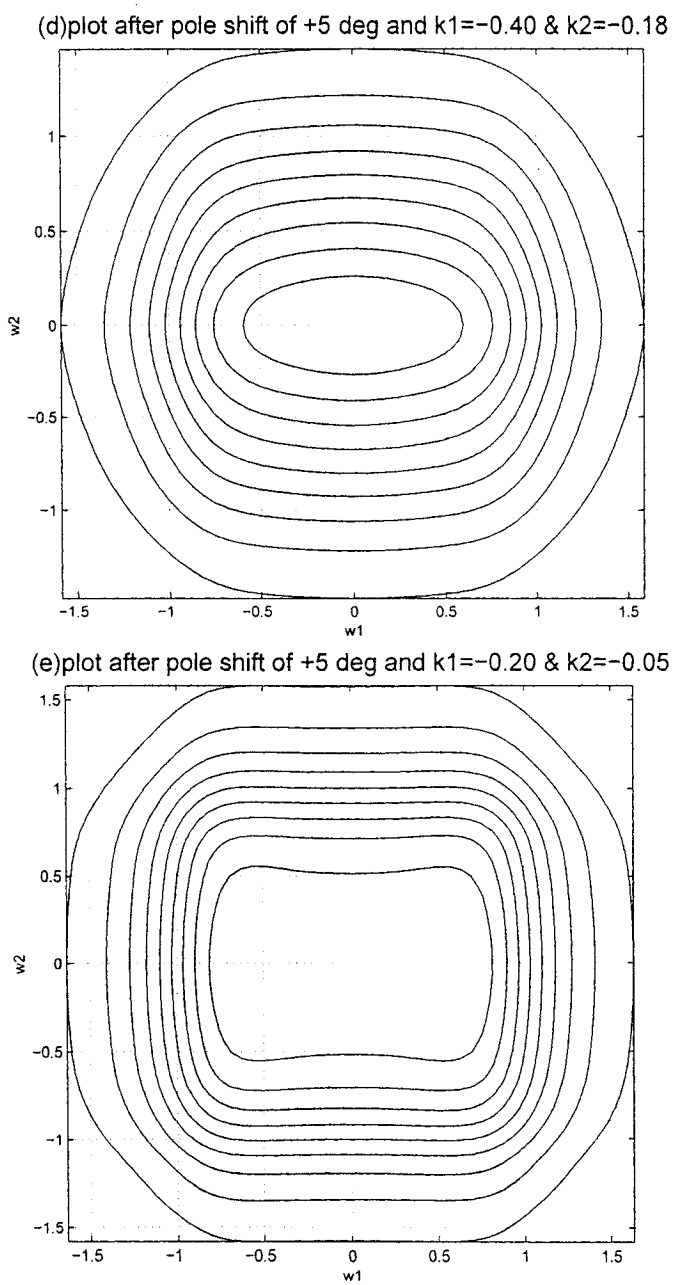

Figure 2.30: 2-D CPPF after pole parameter transformation of $\theta_0 = +5°$ for (a) k1=-0.40 and k2=-0.18 (b) k1=-0.20 and k2=-0.05.

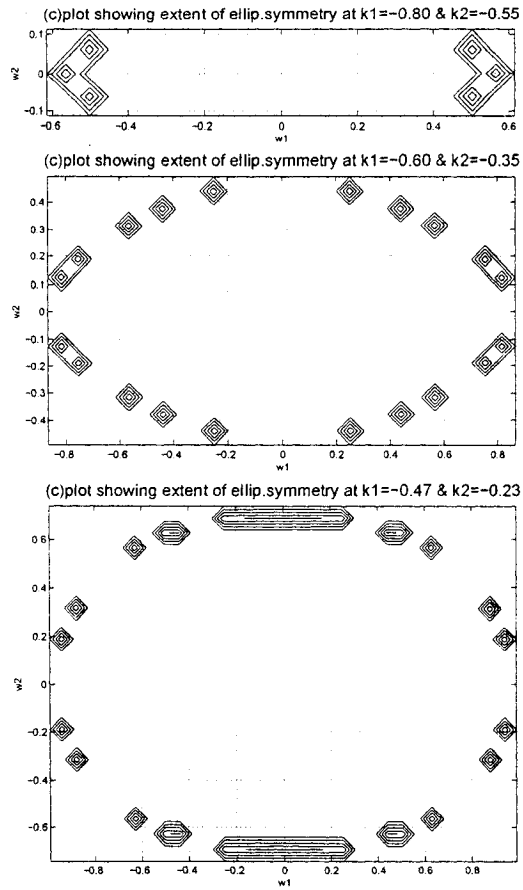

Figure 2.31: Plots to illustrate the extent of elliptical symmetry obtained after shifting the poles of the original transfer functions by $+5°$ for Figs.(2.29(a), (b) & (c)).

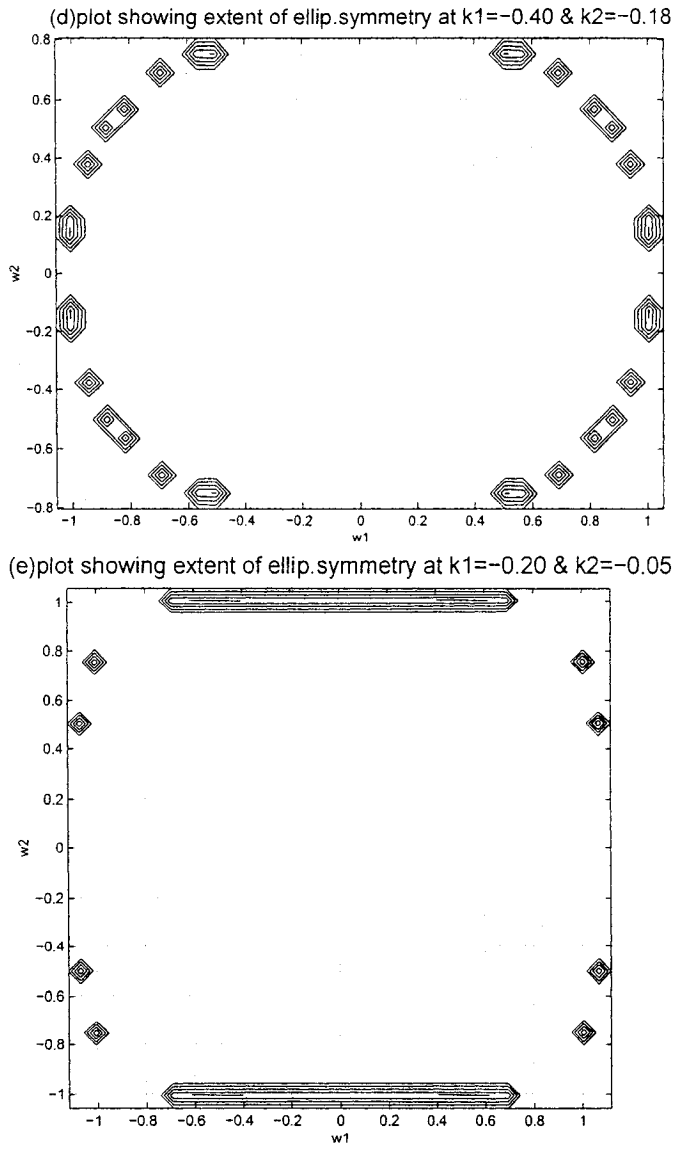

Figure 2.32: Plots to illustrate the extent of elliptical symmetry obtained after shifting the poles of the original transfer functions by $+5°$ for Figs.(2.30(a) & (b)).

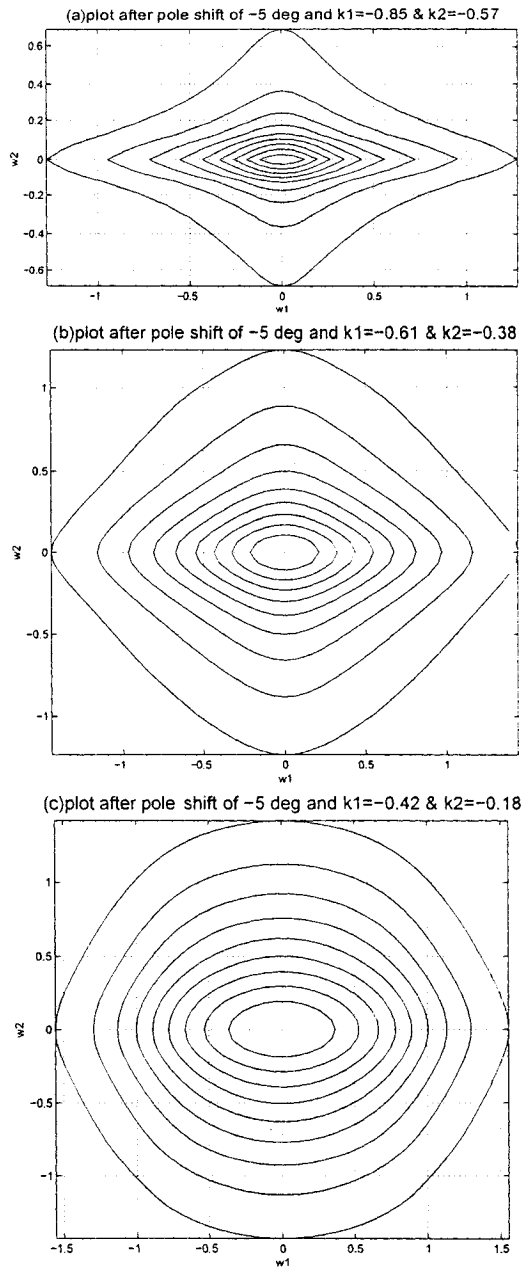

Figure 2.33: 2-D CPPF after pole parameter transformation of $\theta_0 = -5°$ for (a) k1=-0.85 and k2=-0.57 (b) k1=-0.61 and k2=-0.38 (c) k1=-0.42 and k2=-0.18(showing near elliptical symmetry)

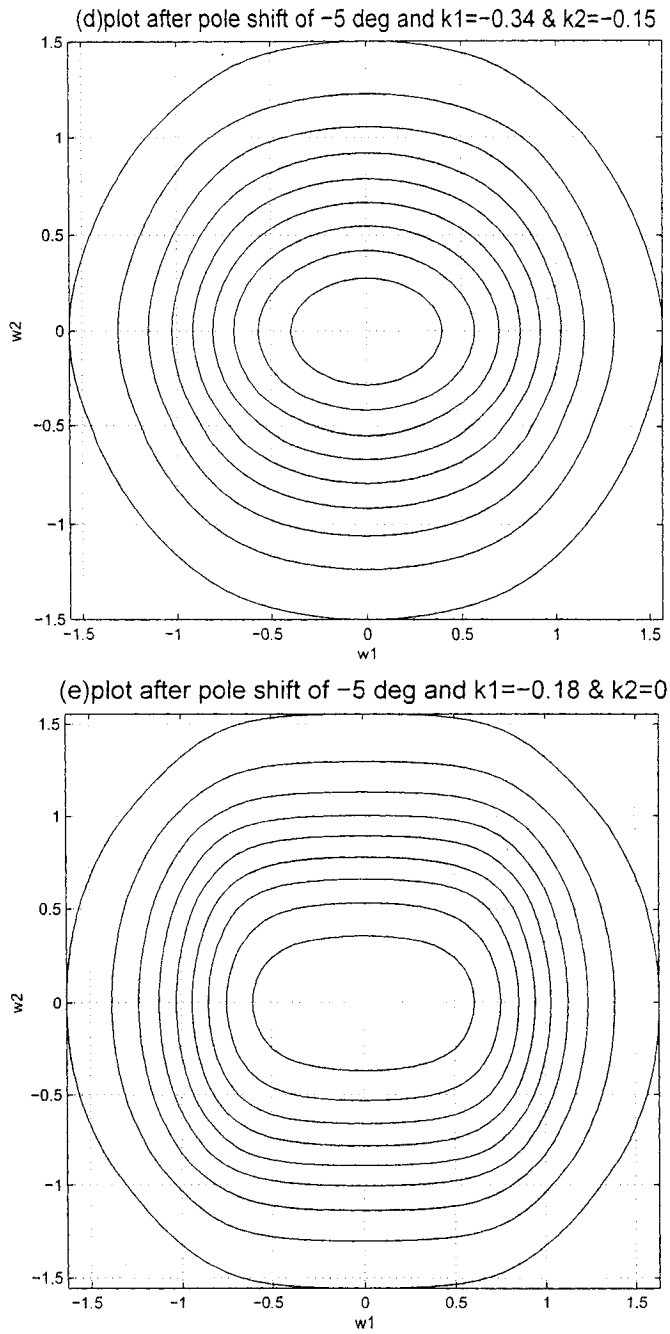

Figure 2.34: 2-D CPPF after pole parameter transformation of $\theta_0 = -5°$ for (a) k1=-0.34 and k2=-0.15 (b) k1=-0.18 and k2=0

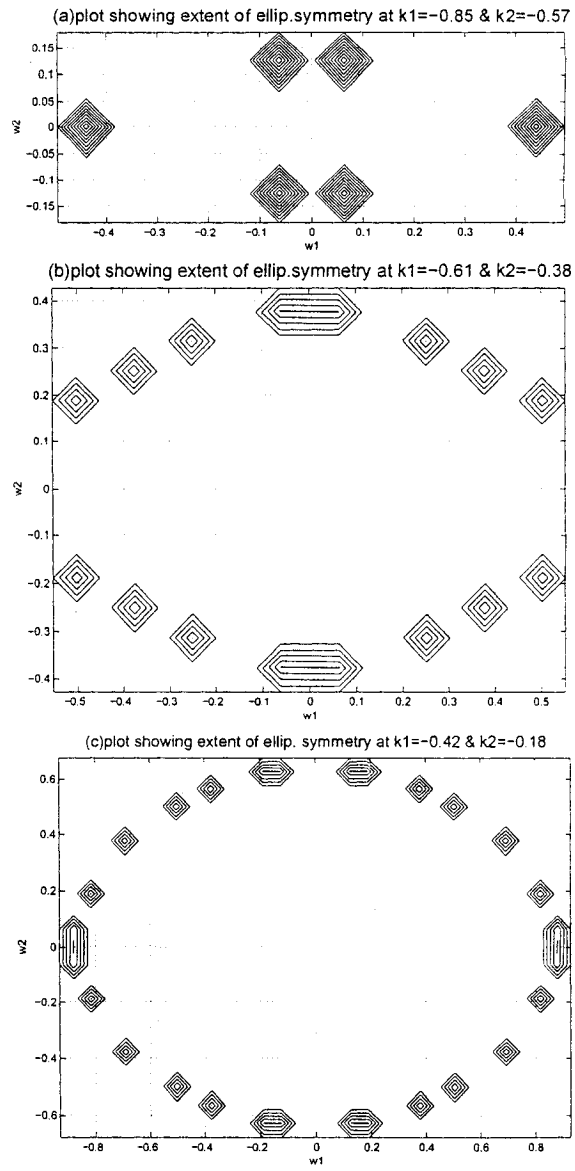

Figure 2.35: Plots to illustrate the extent of elliptical symmetry obtained after shifting the poles of the original transfer functions by $-5°$ for Figs.(2.33(a), (b) & (c)).

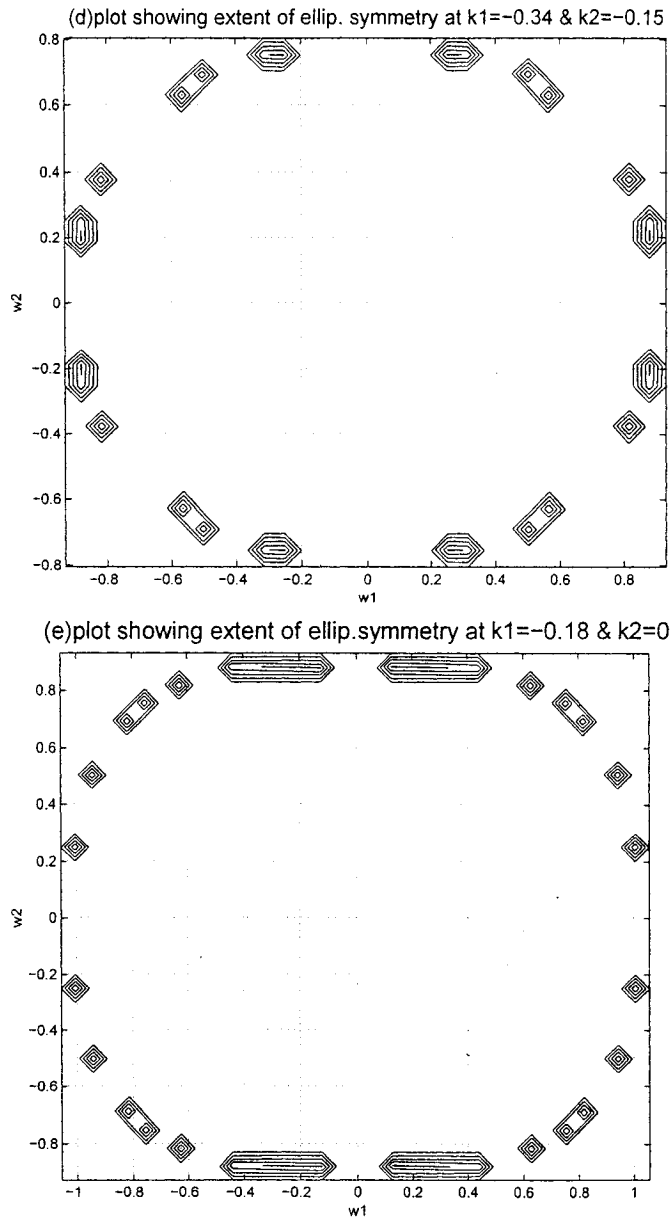

Figure 2.36: Plots to illustrate the extent of elliptical symmetry obtained after shifting the poles of the original transfer functions by -5° for Figs.(2.34(a) & (b)).

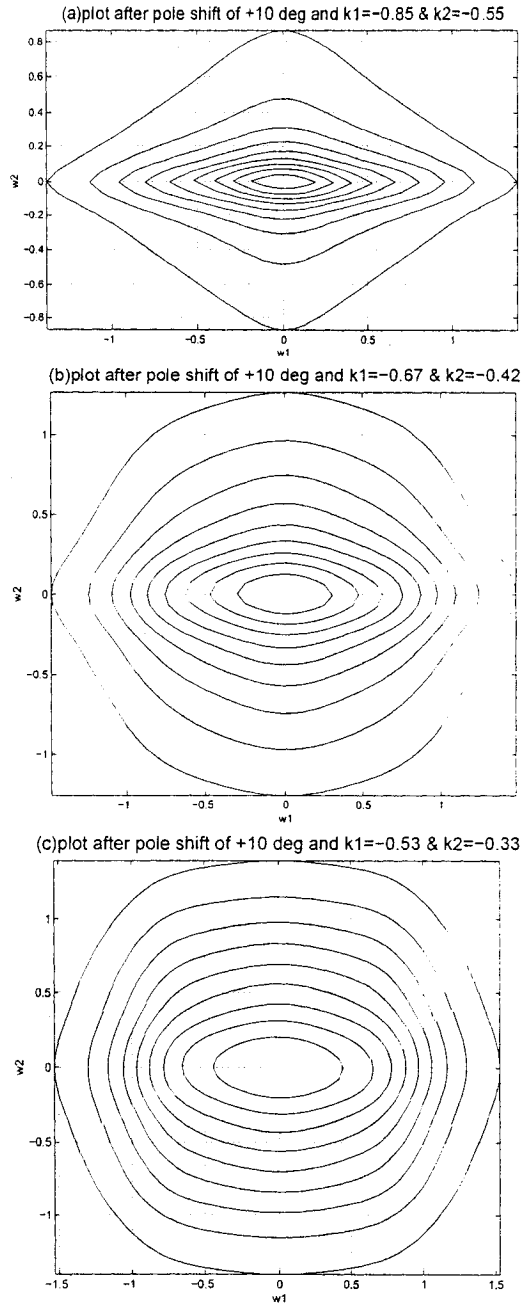

Figure 2.37: 2-D CPPF after pole parameter transformation of $\theta_0 = +10°$ for (a) k1=-0.85 and k2=-0.55 (b) k1=-0.67 and k2=-0.42 (c) k1=-0.53 and k2=-0.33(showing near elliptical symmetry).

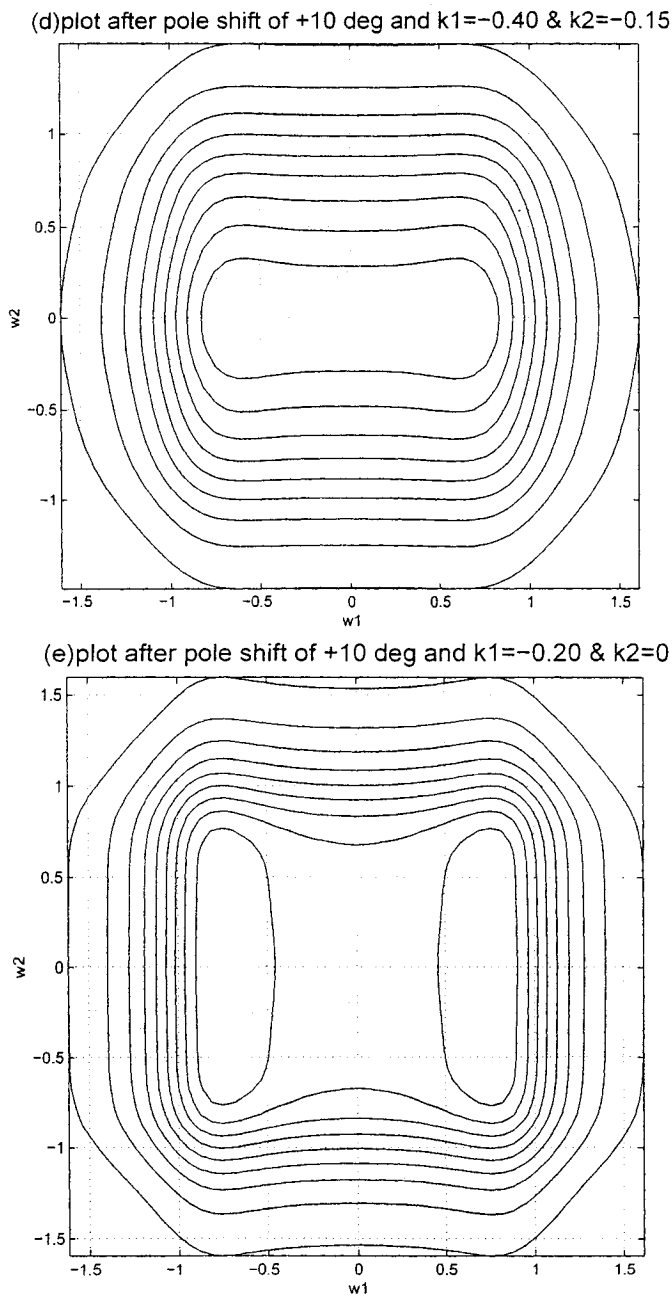

Figure 2.38: 2-D CPPF after pole parameter transformation of $\theta_0 = +10°$ for (a) k1=-0.40 and k2=-0.15 (b) k1=-0.20 and k2=0.

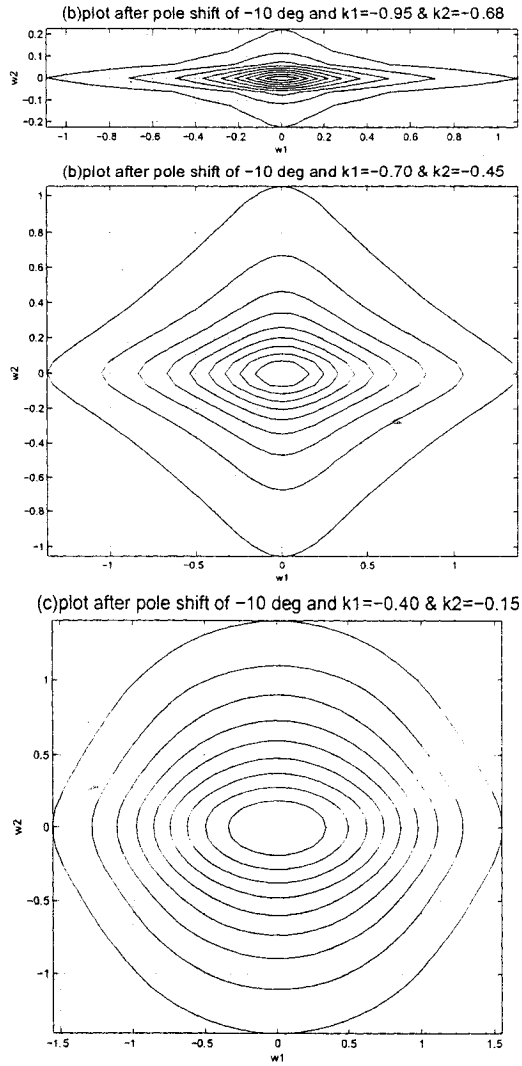

Figure 2.39: 2-D CPPF after pole parameter transformation of $\theta_0 = -10°$ for (a) k1=-0.95 and k2=-0.68 (b) k1=-0.70 and k2=-0.45 (c) k1=-0.40 and k2=-0.15(showing near elliptical symmetry).

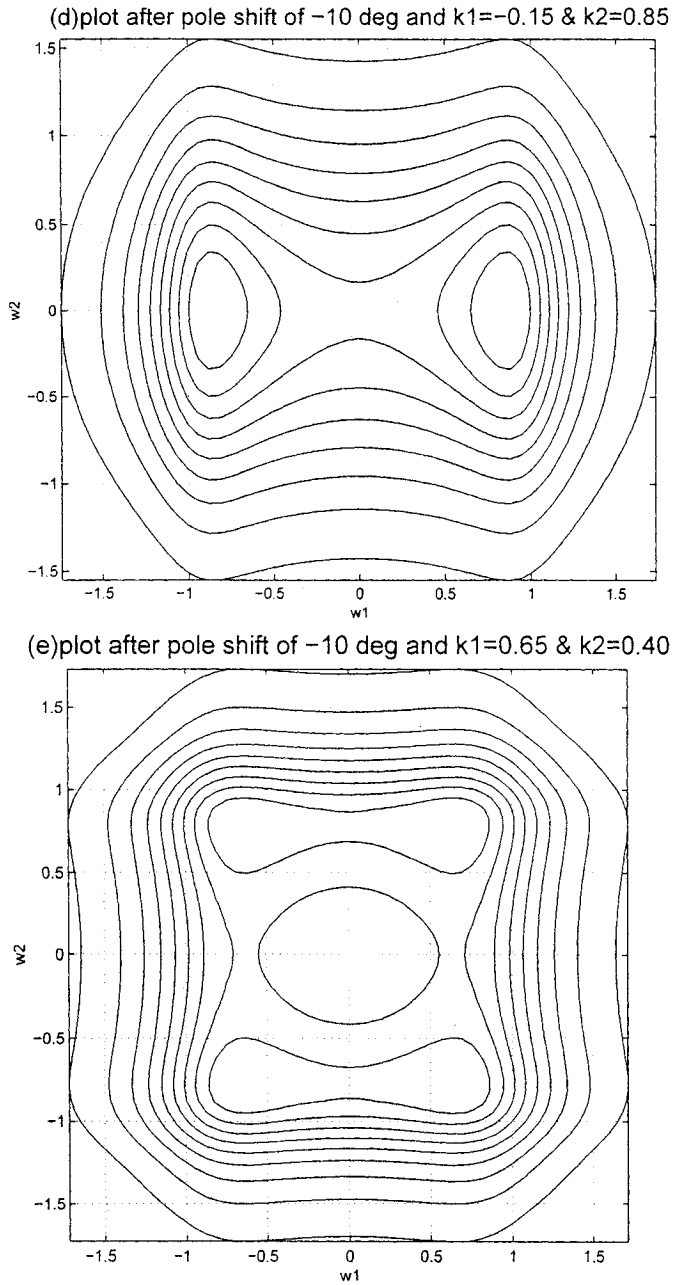

Figure 2.40: 2-D CPPF after pole parameter transformation of $\theta_0 = -10°$ for (a) k1=-0.15 and k2=0.85 (b) k1=0.65 and k2=0.40.

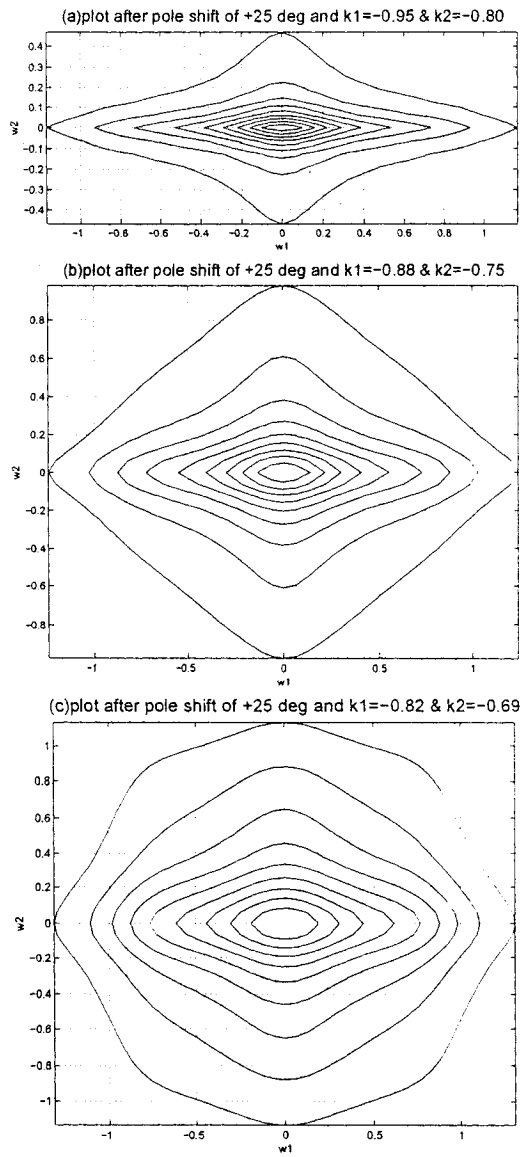

Figure 2.41: 2-D CPPF after pole parameter transformation of $\theta_0 = +25°$ for (a) k1=-0.95 and k2=-0.80 (b) k1=-0.88 and k2=-0.75 (c) k1=-0.82 and k2=-0.69(showing near elliptical symmetry).

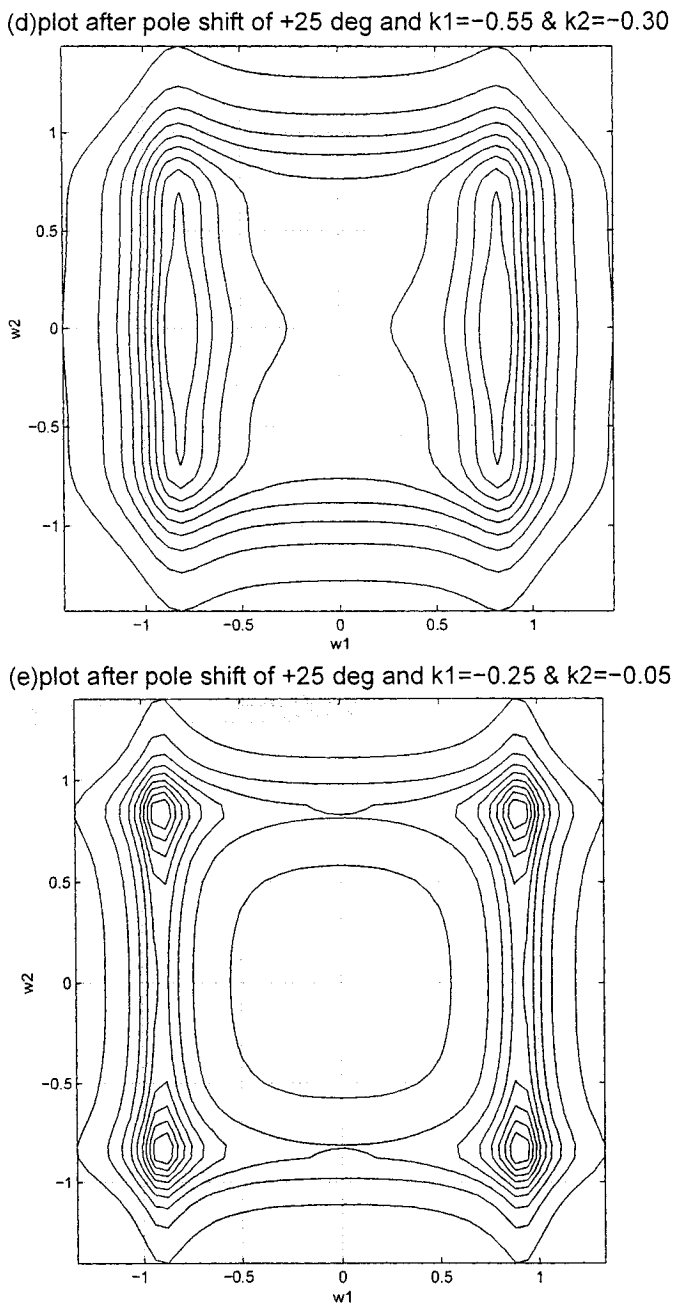

Figure 2.42: 2-D CPPF after pole parameter transformation of $\theta_0 = +25°$ for (a) k1=-0.55 and k2=-0.30 and (b) k1=-0.25 and k2=-0.05.

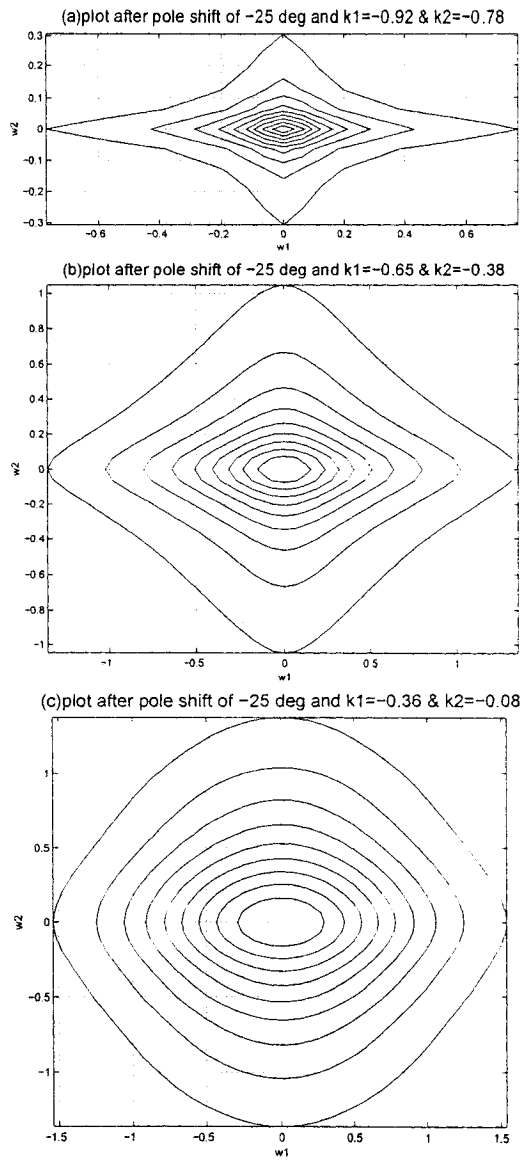

Figure 2.43: 2-D CPPF after pole parameter transformation of $\theta_0 = -25°$ for (a) k1=-0.92 and k2=-0.78 (b) k1=-0.65 and k2=-0.38 (c) k1=-0.36 and k2=-0.08(showing near elliptical symmetry)

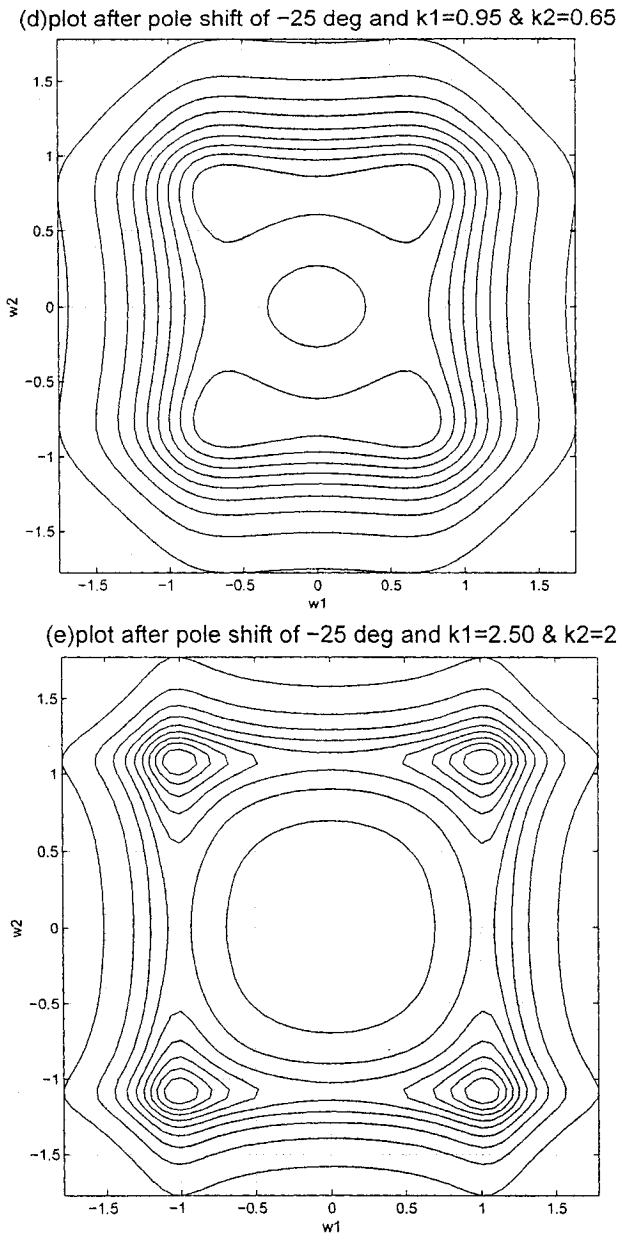

Figure 2.44: 2-D CPPF after pole parameter transformation of $\theta_0 = -25°$ for (a) k1=0.95 and k2=0.65 (b) k1=2.50 and k2=2.0.

2.10.7 Summary and Discussion

In summary, this chapter has shown in detail the approximation to elliptical symmetry that can be achieved in stable, 2-D lowpass transfer functions, starting from, two 1-D transfer functions. The study has been done using both Butterworth and Chebyshev transfer functions. Another interesting aspect of filter design namely the effect of pole parameter transformation on elliptical symmetry has been studied in the 2-D case and the results have been shown.

In the study of Butterworth filters, extensive simulations have been done for the third order filter and results have been plotted. An algorithm to determine the extent of elliptical symmetry in specific magnitude ranges has been written and this has been used in all the above cases, as a tool to determine the range and value of the feedback factors k_1 & k_2 for elliptical symmetry for each of the above cases. It has been found from the results obtained, elliptical symmetry varies with the values of k_1 & k_2 with in the stability limits of k. Specific magnitude ranges has been chosen for all the cases, so as to be consistent with the comparative study.

In the Chebyshev study, it has been proved that the values of k_1 & k_2 for elliptical symmetry, varies as a function of ripple width ϵ. For the same order and different value of ripple width, results have been plotted and tabulated.

The effect of pole-parameter transformation on elliptical symmetry has been studied with six different cases of pole-parameter transformation and the results have been tabulated. It has been proved from the results that, the greater the deviation form the original poles of the transfer functions, the smaller the value of k for stability and thus elliptical symmetry.

Thus, in this Thesis, this chapter is an important work towards the study of 2-D near elliptical symmetric filters possessing denominator transfer functions.

Chapter 3

Generation of Stable 2-D Bandpass, Bandstop and Highpass Filters and their Approximation to Elliptical Symmetry

The previous chapter dealt with the implementation of 2-D lowpass Filter design only. In this chapter, the implementation of other types of filters namely highpass filter, bandpass filter and bandstop filter and their approximation to Elliptical symmetry will be discussed. We will restrict our discussion, in this chapter, to the Butterworth filter design only.

3.1 Bandpass Filter

Bandpass filters have a specific band or range of frequencies above and below which they attenuate signals. Thus, very low and very high frequency components are attenuated and the signals within the specified pass-band range possess a high gain.

The design of 2-D IIR Butterworth bandpass filter is carried out in the same

manner as the lowpass design, in principle, by first designing the 1-D Butterworth filter and then combining two similar 1-D transfer functions as a product. The code has been written in MATLAB(Program B1) using the different built-in subroutines to achieve the filter specifications. The following procedure has been adopted to design the filter.

(1) The required specifications namely the order of the filter(N) and the upper and lower pass-band edges(W_n), as a 1×2 matrix, are first defined. The filter chosen in this case has an analog cut-off frequency of [0.4, 1] and is of the fourth order.

(2) The numerator and denominator polynomials of the analog transfer function are determined using the MATLAB function "*butter*" for the Bandpass filter design.

In this case, the fourth order Bandpass transfer function(1D) is given by

$$H_{BP}(s) = \frac{0.1296s^4}{(s^8 + 1.5679s^7 + 2.8291s^6 + 2.4459s^5 + (2.0405 + 0.1296k)\,s^4 + 0.9784s^3 + 0.4527s^2 + 0.1003s + 0.0256)} \tag{3.1}$$

Now in order for Eqn.(3.1) to be stable, the range of 'k' needs to be determined. Following the same method suggested in Chapter-2 and from Eqn.(2.14) we have

$$\frac{m(s) + m_1(s)}{n(s)} = \frac{s^8 + 2.8291s^6 + (2.0405 + 0.1296k)s^4 + 0.4527s^2 + 0.0256}{1.5679s^7 + 2.4459s^5 + 0.9784s^3 + 0.1003s} \tag{3.2}$$

Now Eqn.(3.2) can be split into partial fractions as follows:

$$k_\infty s + \sum_i \frac{k_i s}{s^2 + \beta_i^2} + \frac{k_0}{s} = \frac{s^8 + 2.8291s^6 + (2.0405 + 0.1296k)s^4 + 0.4527s^2 + 0.0256}{1.5679s(s^2 + 0.9999)(s^2 + 0.4003)(s^2 + 0.1598)} \tag{3.3}$$

where $\beta_1 = 0.9999$, $\beta_2 = 0.4003$, $\beta_3 = 0.1598$ are the roots of the denominator of Eqn.(3.2).

For Eqn.(3.3). to be a strictly Hurwitz polynomial, $k_i > 0$.

Therefore, we find the values of k_i such that $k_i > 0$, and from the equations obtained, we find the range of k for stability.

Solving Eqn.(3.3), we have the following ranges of k, for which Eqn.(3.1) is stable.

$$k < 1.6632,\ k > -0.7487,\ k < 1.6509 \tag{3.4}$$

Thus, the resultant range of k for which Eqn.(3.1). is stable is given by

$$-0.7487 < k < 1.6509 \tag{3.5}$$

(3) Bilinear transformation is then applied to determine the digital counter part. This is done using the MATLAB function "*bilinear*". Refer to Program B2.

(4) Now we have the digital transfer function of the 1-D filter. The same procedure as above, is extended to the second dimension and the transfer function for the second dimension is obtained independently.

(5) The product of the two 1-D polynomials is then determined.

(6) A general subroutine suitable for any order of the filter has been written to determine the frequency response of the 2-D filter. Refer Program B2. The corresponding contour plots are plotted using the MATLAB function "*contour*".

The MATLAB program namely, Program B1 and B2 have been written for the Bandpass filter specifications given by

$W_n1 = W_n2$	$N1 = N2$
[0.4 1]	4

All frequencies are in radians. The scripts 1 and 2 refer to the first and second dimensions, respectively.

Program B1

```
%%2D BAND PASS BUTTERWORTH IIR FILTER
    clear all
    close all;
    N1=4;
    Wn1=[0.4,1];
    N2=N1;
```

```
Wn2=Wn1;
[B1,A1]=butter(N1,Wn1,'s');
[B2,A2]=butter(N2,Wn2,'s');
for k1=-1.0:0.1:1.65
for k2=-1.0:0.1:1.65
zz=ker_progb2_mag(B1,A1,k1);
lim=pi;
interval=pi/50;
w1=0:interval:lim;
w2=0:interval:lim;
[ww1,ww2]=meshgrid(w1,w2);
figure;
contour(ww1,ww2,zz);
axis('image');
xlabel('w1');
ylabel('w2');
zlabel('Magnitude Response');
title('2-D Butterworth BPF','FontSize',16);
grid on;
end
end
```

Program B2

```
%% Function to determine the transfer function of the filter for a given k1,k2
    function[zz]=ker_progb2_mag(B1,A1,k1);
    B2=B1;
    [R C]=size(A1);
    A1((C+1)/2)=A1((C+1)/2)+k1*B1((C+1)/2);
    A2((C+1)/2)=A2((C+1)/2)+k2*B2((C+1)/2);
    %%%Bilinear transformation of the transfer function
    [N1,D1]=bilinear(B1,A1,1);
    [N2,D2]=bilinear(B2,A2,1);
    %%to determine the 2-D transfer function
    for m=1:1:size(N1,2)
    for n=1:1:size(N2,2)
    N(m,n)=N1(m)*N2(n);
    end
    end
    for m=1:1:size(D1,2)
    for n=1:1:size(D2,2)
    D(m,n)=D1(m)*D2(n);
```

```
end
end
lim=pi;
interval=pi/50;
c1=0;
for w1=0:interval:lim
c2=0;
c1=c1+1;
for w2=0:interval:lim
c2=c2+1;
for col=1:1:size(N2,2)
NRow(1,col)=(cos(w2)+j*sin(w2))^(size(N2,2)-col);
end
for row=1:1:size(N2,2)
NCol(row,1)=(cos(w1)+j*sin(w1))^(size(N1,2)-row);
end
NR=NRow*N'*NCol;
a=real(NR);
b=imag(NR);
for col=1:1:size(D2,2)
DRow(1,col)=(cos(w2)+j*sin(w2))^(size(D2,2)-col);
end
for row=1:1:size(D2,2)
DCol(row,1)=(cos(w1)+j*sin(w1))^(size(D1,2)-row);
end
DR=DRow*D'*DCol;
c=real(DR);
d=imag(DR);
MOD(c1,c2)=(sqrt((a*c+b*d)^2+(b*c-a*d)^2))/(c^2+d^2);
end
end
[ww1,ww2]=meshgrid(w1,w2);
zz=MOD/(max(max(MOD)));
%%End of Program
```

The results of the algorithm namely the contour plots for the first quadrant are as shown in Figs.(3.1) and (3.2). A large number of plots for all possible values of k within the stability ranges were plotted. Only the plots of interest have been shown. As it can be seen from the Figs.(3.1) and(3.2), there is a certain range of k for which elliptical symmetry is exhibited in the frequency response for specific magnitude

ranges. From Section 2.8 using Program A3, the extent of elliptical symmetry is determined for the above responses and the optimum values of k_1 and k_2 for which we have the closest proximity to elliptical symmetry is determined.

The plots in Figs.(3.3) and (3.4) show the extent of elliptical symmetry for the responses shown in Figs.(3.1) and (3.2). The plot for $k_1 = k_2 = 1.65$ is not shown since there are no points within this magnitude range which approximate to elliptical symmetry.

It is evident from the above plots that at $k_1 = -0.25$ *and* $k_2 = -0.08$, the response exhibits near elliptical symmetry and for other values of k_1 and k_2 apart from these, elliptical symmetry ceases to exist.

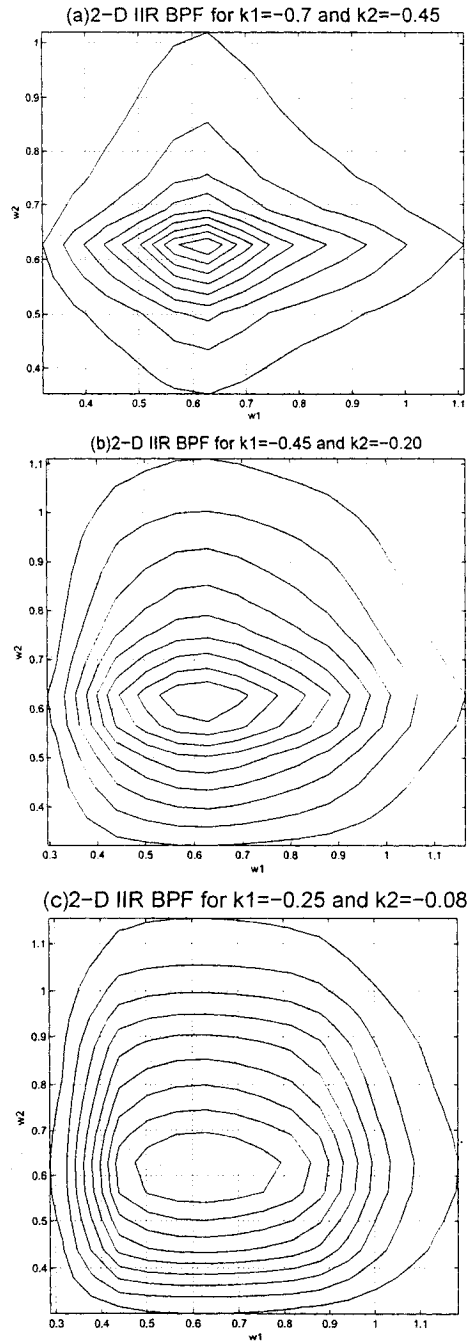

Figure 3.1: Contour plots of Fourth order 2-D IIR Butterworth Bandpass filter (a) k1=-0.75 and k2=-0.45 (b) k1=-0.45 and k2=-0.20 (c) k1=-0.25 and k2=-0.08

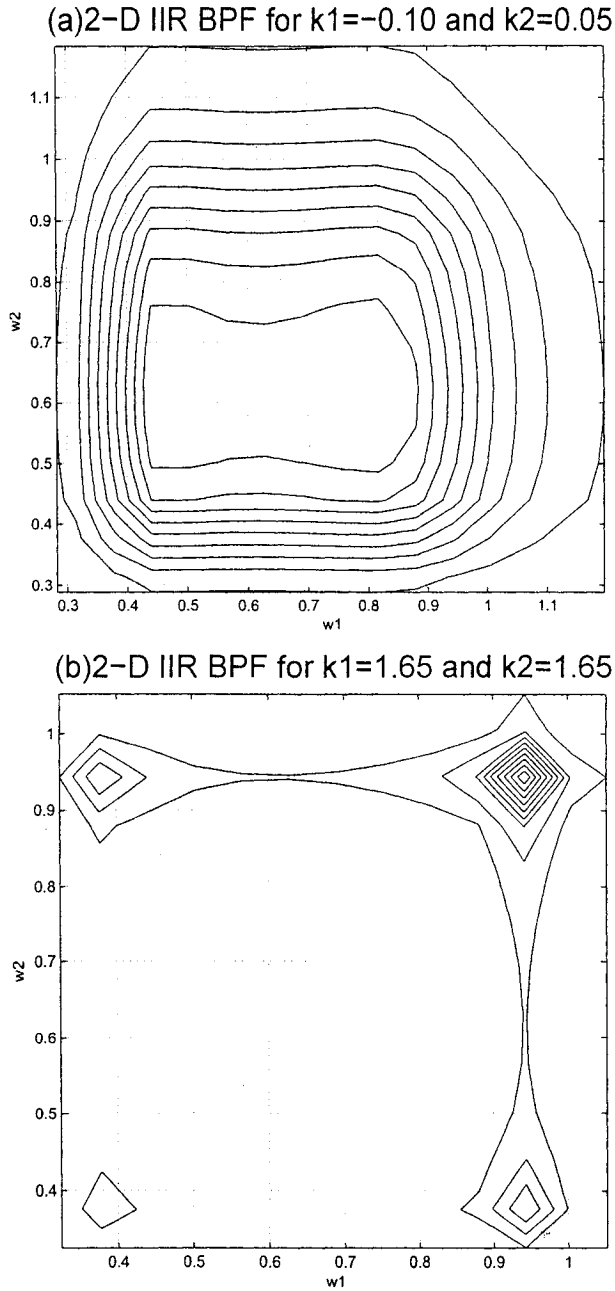

Figure 3.2: Contour plots of 2-D IIR Butterworth Bandpass filter (a) k1=-0.10 and k2=0.05 (b) k1=1.65 and k2=1.65

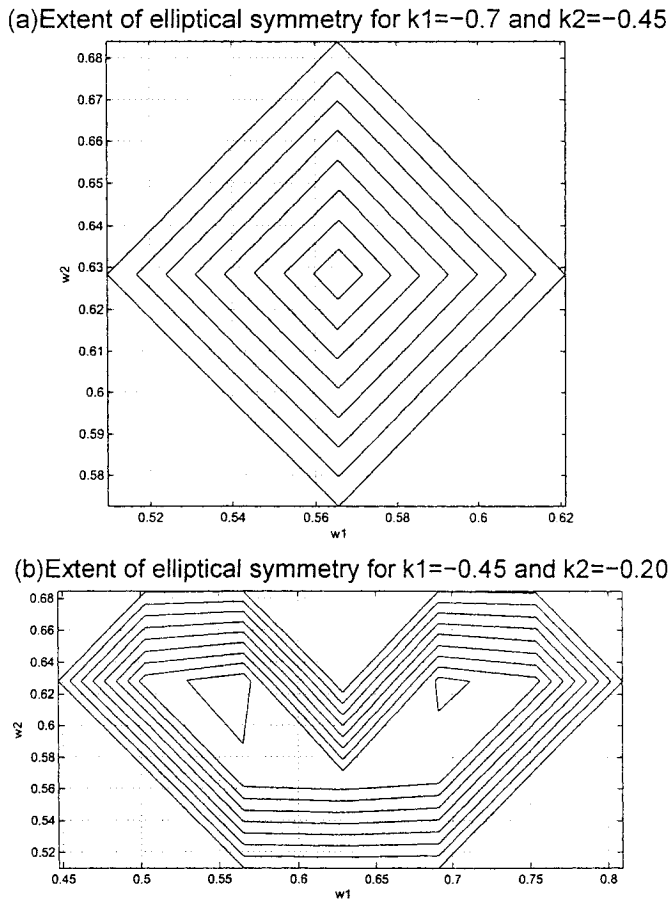

Figure 3.3: Plots showing the extent of elliptical symmetry for (a) k1=-0.75 and k2=-0.45 (b) k1=-0.45 and k2=-0.20. The magnitude range under consideration is 0.8<Mag<1.

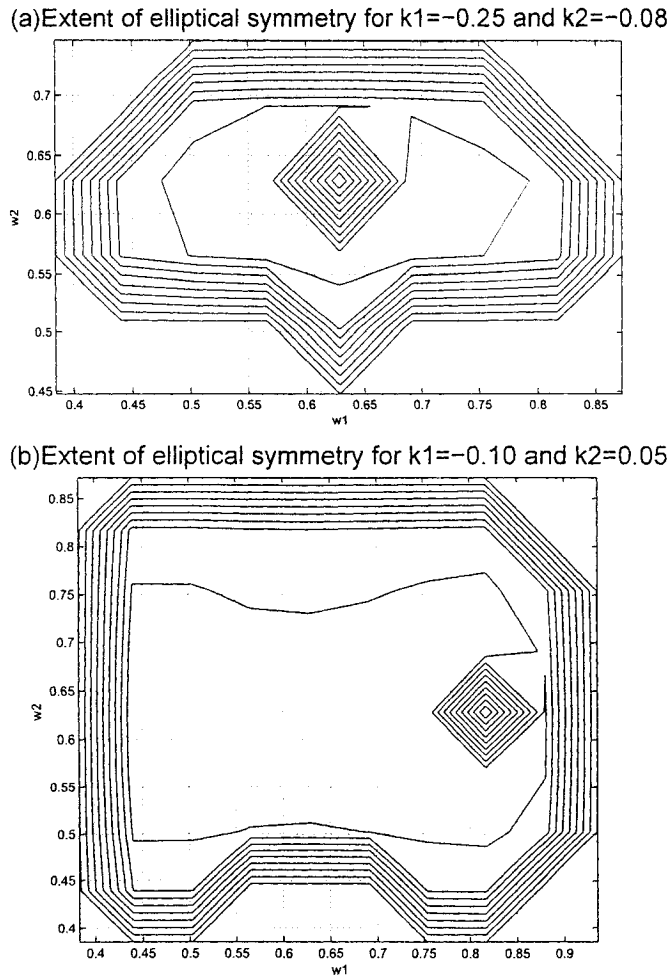

Figure 3.4: Plots showing the extent of elliptical symmetry for (a) k1=-0.25 and k2=-0.08 (b) k1=-0.10 & k2=0.05. The magnitude range under consideration is 0.8<Mag<1.

3.2 Bandstop Filter

Bandstop filters have a specific band or range of frequencies within which they attenuate signals. Thus, very low and very high frequency components of signals have a high gain and the signals within the specified attenuation range have very low gain.

The design of 2-D IIR Butterworth Bandstop filter is carried out in the same manner as the bandpass design, in principle, by first designing the 1-D Butterworth filter and then combining two similar 1-D transfer functions as a product. The code has been written using MATALAB(Program B3) using the different built-in subroutines to achieve the filter specifications. The following procedure has been adopted to design the filter:

(1)In this case, the required specifications namely the order of the filter(N) and the upper and lower pass-band edges(W_n), as a 1×2 matrix, are first defined. The filter chosen in this case has an analog cut-off frequency of [0.4, 1] and is of the fourth order.

(2)The numerator and denominator polynomials of the analog transfer function are determined using the MATLAB function "*butter*" for the Bandstop filter design.

In this case, the fourth order Bandstop transfer function(1D) is given by

$$H_{BS}(s) = \frac{s^8 + 1.6s^6 + 0.96s^4 + 0.256s^2 + 0.0256}{(s^8 + 1.5679s^7 + 2.8291s^6 + 2.4459s^5 + 2.0405s^4 + 0.9784s^3 + 0.4527s^2 + 0.1003s + 0.0256)} \tag{3.6}$$

Having determined the numerator and denominator polynomials for the analog transfer function, the filter transfer function(1D) is then determined, as from Eqn.(2.13). This is given by

$$H_{BSo}(s) = \frac{s^8 + 1.6s^6 + 0.96s^4 + 0.256s^2 + 0.0256}{(s^8 + 1.5679s^7 + 2.8291s^6 + 2.4459s^5 + 2.0405s^4 + 0.9784s^3 + 0.9784s^3 + 0.4527s^2 + 0.1003s + 0.0256 + k(s^8 + 1.6s^6 + 0.96s^4 + 0.256s^4 + 0.0256)} \quad (3.7)$$

Now for Eqn.(3.7) to be stable, the range of k needs to be determined. Following the same suggested in Chapter-2 and from Eqn.(2.14) we have

$$\frac{m(s) + m_1(s)}{n(s)} = \frac{k(s^8 + 1.6s^6 + 0.96s^4 + 0.256s^4 + 0.0256))}{(s^8 + 2.8291s^6 + 2.0405s^4 + 0.4527s^2 + 0.0256 + 1.5679s^7 + 2.4459s^5 + 0.9784s^3 + 0.1003s} \quad (3.8)$$

Now Eqn.(3.8) can be split into partial fractions as follows:

$$k_\infty s + \sum_i \frac{k_i s}{s^2 + \beta_i^2} + \frac{k_0}{s} = \frac{k(s^8 + 1.6s^6 + 0.96s^4 + 0.256s^4 + 0.0256))}{(s^8 + 2.8291s^6 + 2.0405s^4 + 0.4527s^2 + 0.0256 + 1.5679s(s^2 + 0.9999)(s^2 + 0.4003)(s^2 + 0.1598)} \quad (3.9)$$

where $\beta_1 = 0.9999$, $\beta_2 = 0.4003$, $\beta_3 = 0.1598$ are the roots of the denominator of Eqn.(3.8).

For Eqn.(3.9) to be a strictly Hurwitz polynomial, $k_i > 0$.

Therefore, we find the values of k_i such that $k_i > 0$ and from the equations obtained, we find the range of k for stability.

Solving Eqn.(3.9), we have the following ranges of k respectively, for which Eqn.(3.7) is stable.

$$-1 < k < \infty, \; no\, range, \; k < 1.6628, \; k < 1.6456 \quad (3.10)$$

Thus, the resultant range of k for which Eqn.(3.7) is stable is given by

$$-1 < k < 1.6456 \quad (3.11)$$

(3)Bilinear transformation is then performed to determine the digital counter part. This is done using the MATLAB function "*bilinear*". Refer to Program B4.

(4)Now we have the digital transfer function of the 1-D filter. The same procedure as above, is extended to the second dimension and the transfer function for the second dimension is obtained independently.

(5)The product of the two 1-D polynomials is then determined.

(6)A general subroutine suitable for any order of the filter has been written to determine the frequency response of the 2-D filter. Refer Program B4. The corresponding contour plots are plotted using the MATLAB function "*contour*".

The MATLAB program namely, Program B3 and B4 have been written for the Bandstop filter specifications given by

$W_n1 = W_n2$	$N1 = N2$
[0.4 1]	4

All frequencies are in radians. The scripts 1 and 2 refer to the first and second dimensions, respectively.

Program B3

```
%%2D-BAND-STOP BUTTERWORTH FILTER
    clear all;
    close all;
    N1=4;
    Wn1=[0.4 1];
    N2=N1;
    Wn2=Wn1;
    [B1,A1]=butter(N1,Wn1,'stop','s');
    [B2,A2]=butter(N2,Wn2,'stop','s');
    for k1=-1.0:0.1:1.65
    for k2=-1.0:0.1:1.65
    zz=ker_progb4_mag(B1,A1,k1);
    lim=pi;
    interval=pi/50;
    w1=0:interval:lim;
    w2=0:interval:lim;
    [ww1,ww2]=meshgrid(w1,w2);
    figure;
    contour(ww1,ww2,zz);
```

```
axis('image');
xlabel('w1');
ylabel('w2');
zlabel('Magnitude Response');
title('2-D IIR Butterworth BSF','FontSize',16);
grid on;
end
end
```

Program B4

```
%%Function to determine the transfer function of the filter for a given k1,k2
function [zz]=ker_progb4_mag(B1,A1,k1);
B2=B1;
[R C]=size(A1);
for t=0:2:C-1
A1(C-t)=A1(C-t)+k1*B1(C-t);
A2(C-t)=A2(C-t)+k2*B2(C-t);
end
%%%Bilinear transformation of the transfer function
[N1,D1]=bilinear(B1,A1,1);
[N2,D2]=bilinear(B2,A2,1);
%%to determine the 2-D transfer function
for m=1:1:size(N1,2)
for n=1:1:size(N2,2)
N(m,n)=N1(m)*N2(n);
end
end
for m=1:1:size(D1,2)
for n=1:1:size(D2,2)
D(m,n)=D1(m)*D2(n);
end
end
lim=pi;
interval=pi/50;
c1=0;
for w1=0:interval:lim
c2=0;
c1=c1+1;
for w2=0:interval:lim
c2=c2+1;
for col=1:1:size(N2,2)
```

```
NRow(1,col)=(cos(w2)+j*sin(w2))^(size(N2,2)-col);
end
for row=1:1:size(N2,2)
NCol(row,1)=(cos(w1)+j*sin(w1))^(size(N1,2)-row);
end
NR=NRow*N'*NCol;
a=real(NR);
b=imag(NR);
for col=1:1:size(D2,2)
DRow(1,col)=(cos(w2)+j*sin(w2))^(size(D2,2)-col);
end
for row=1:1:size(D2,2)
DCol(row,1)=(cos(w1)+j*sin(w1))^(size(D1,2)-row);
end
DR=DRow*D'*DCol;
c=real(DR);
d=imag(DR);
MOD(c1,c2)=(sqrt((a*c+b*d)^2+(b*c-a*d)^2))/(c^2+d^2);
end
end
w1=0:interval:lim;
w2=0:interval:lim;
[ww1,ww2]=meshgrid(w1,w2);
zz=MOD/(max(max(MOD)));
%%End of Program
```

The results of the algorithm namely the contour plots for the first quadrant are as shown in Figs.(3.5) and (3.6). A large number of plots for all possible values of k within the stability ranges were plotted. Only the plots of interest have been shown. As it can be seen from the Figs.(3.5) and (3.6), there is a certain range of k for which elliptical symmetry is exhibited in the frequency response for specific magnitude ranges. From Section 2.8 using Program A3, the extent of elliptical symmetry is determined for the above responses and the optimum value of k for which we have the closest proximity to elliptical symmetry is determined.

The plots in Figs.(3.7) and (3.8) show the extent of elliptical symmetry for the responses shown in Figs.(3.5) and (3.6). The plot for $k_1 = k_2 = 1.64$ is not shown since there are no points within this magnitude range which approximate to

elliptical symmetry.

It is evident from the above plots that at $k_1 = -0.55$ and $k_2 = -0.30$, the response exhibits near elliptical symmetry and for other values of k_1 and k_2, the elliptical symmetry gradually ceases to exist. For the above study of Bandstop filter, near elliptcial-symmetry has been considered for both the lower and upper pass-band in order to evaluate the optimum value of k_1 and k_2.

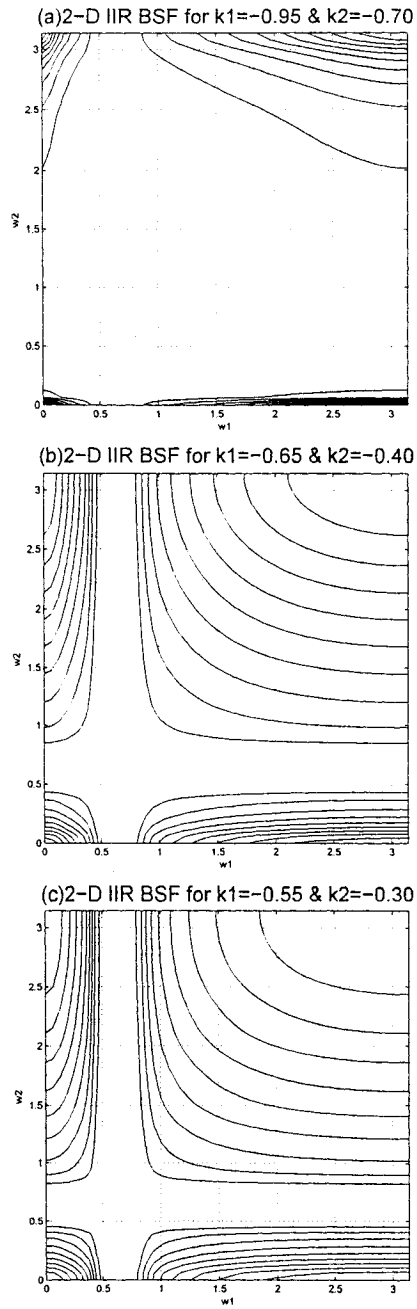

Figure 3.5: Contour plots of Fourth order 2-D IIR Butterworth Bandpass filter (a) k1=-0.95 and k2=-0.70 (b) k1=-0.65 and k2=-0.40 (c) k1=-0.55 and k2=-0.30.

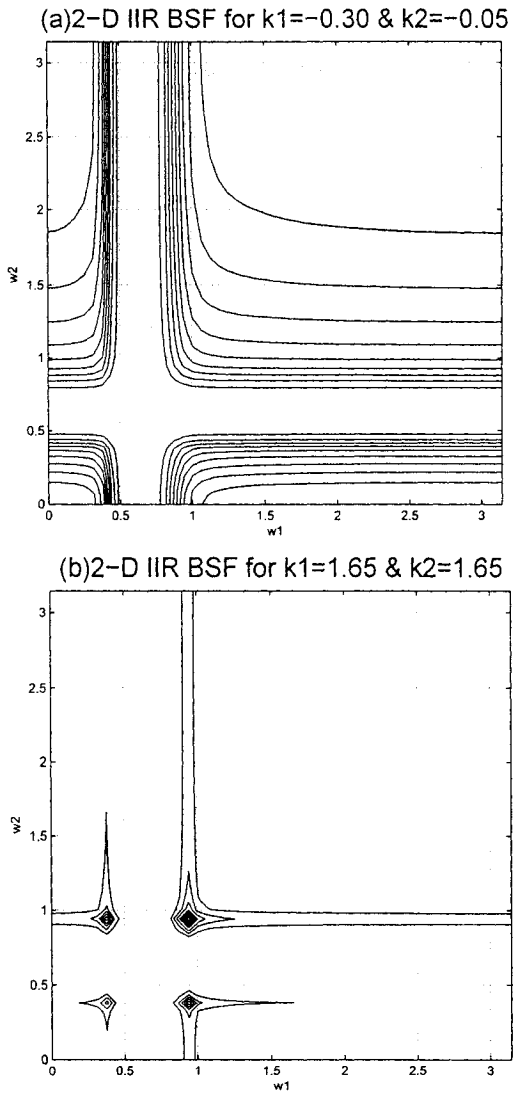

Figure 3.6: Contour plots of Fourth order 2-D IIR Butterworth Bandpass filter (a) k1=-0.30 and k2=-0.05 (b) k1=1.65 and k2=1.65.

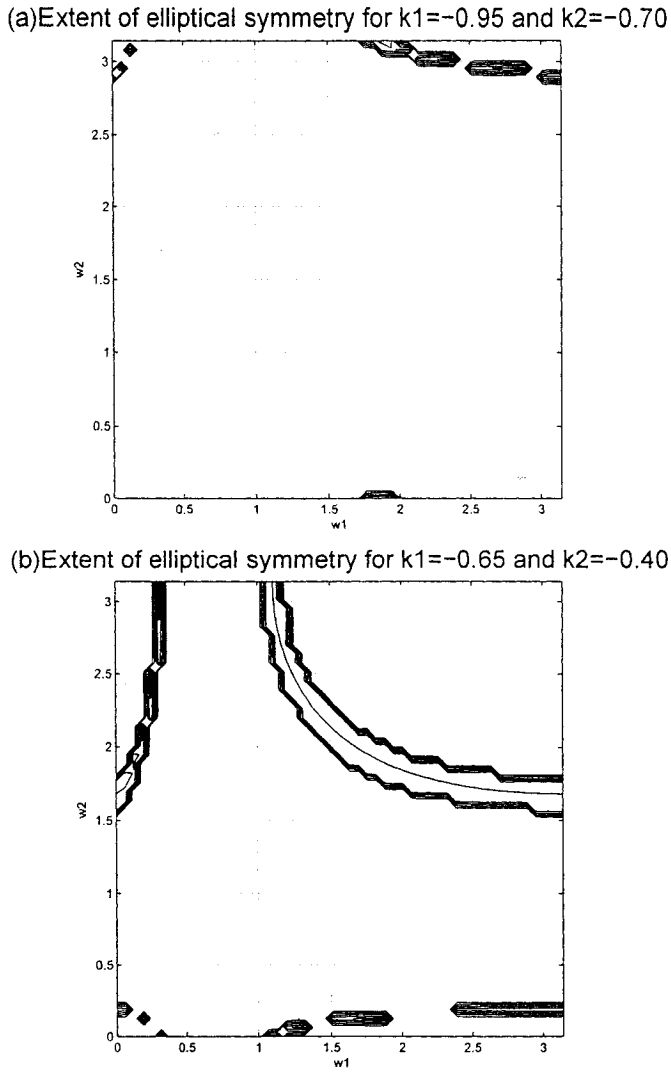

Figure 3.7: Plots showing the extent of elliptical symmetry for (a) k1=-0.95 and k2=-0.70 (b) k1=-0.65 and k2=-0.40. The magnitude range under consideration is 0.45<Mag<0.55.

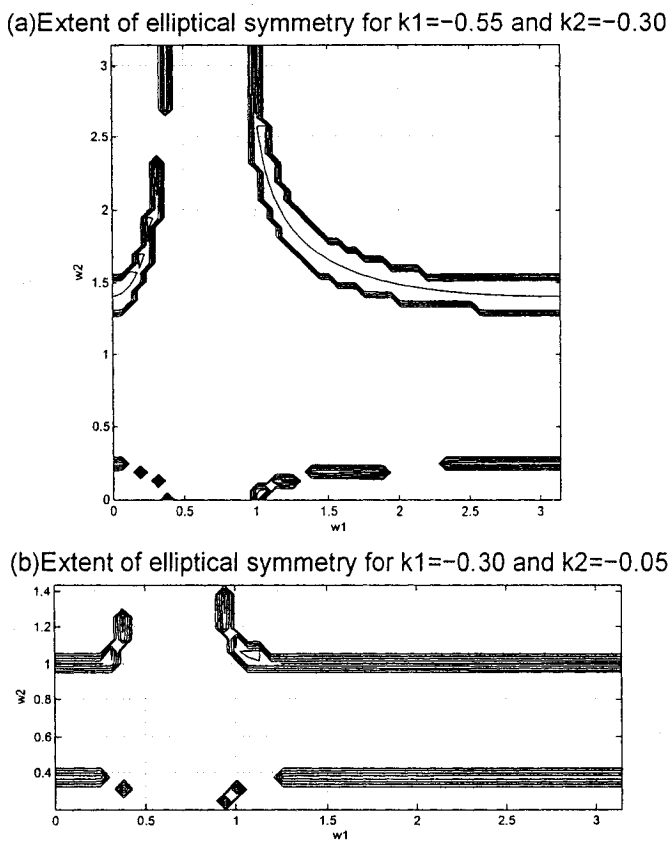

Figure 3.8: Plots showing the extent of elliptical symmetry for (a) k1=-0.55 and k2=-0.30 (b) k1=-0.30 and k2=-0.05. The magnitude range under consideration is 0.45<Mag<0.55.

3.3 Highpass Filter

Highpass filters have a specific value of frequency above which they allow signals. Thus, low frequency components of signal are attenuated and the signals above the specified range have a high gain.

The design of 2-D IIR Butterworth highpass filter is carried out in the same manner as the lowpass design, in principle, by first designing the 1-D Butterworth filter and then combining two similar 1-D transfer functions as a product. The code has been written using MATALAB(Program B5) using the various built-in subroutines, to achieve the filter specifications. The following procedure has been adopted to design the filter:

(1)In this case, the required specifications namely the pass-band edge (W_1) and the order of the filter (N) are first defined. The filter chosen in this case has an analog cut-off frequency of [0.4] and it has been chosen to be of the fourth order.

(2)The numerator and denominator polynomials of the analog transfer function are determined using the MATLAB function "*butter*" for the highpass filter design.

In this case, the fourth order Highpass transfer function(1D) is given by

$$H_{HP} = \frac{s^4}{s^4 + 1.0453s^3 + 0.5463s^2 + 0.167s^2 + 0.0256} \tag{3.12}$$

Having determined the numerator and denominator polynomials for the analog transfer function, the filter transfer function(1D) is then determined, as from Eqn.(2.13). This is given by

$$H_{HPo} = \frac{s^4}{s^4(1+k) + 1.0453s^3 + 0.5463s^2 + 0.167s^2 + 0.0256} \tag{3.13}$$

Now for Eqn.(3.13) to be stable, the range of k needs to be determined. Following the same method suggested in Chapter-2 and from Eqn.(2.14) we have

$$\frac{m(s) + m_1(s)}{n(s)} = \frac{s^4(1+k) + 0.5463s^2 + 0.0256}{1.0453s^3 + 0.167s^2} \tag{3.14}$$

Now Eqn.(3.14) can be split into partial fractions as follows:

$$k_\infty s + \sum_i \frac{k_i s}{s^2 + \beta_i^2} + \frac{k_0}{s} = \frac{s^4(1+k) + 0.5463s^2 + 0.0256}{1.0453s(s^2 + 0.16)} \tag{3.15}$$

where $\beta_1 = 0.16$, is the root of the denominator polynomial of Eqn.(3.14).

For Eqn.(3.15) to be a strictly Hurwitz polynomial, $k_i > 0$.

Therefore, we find the values of k_i such that $k_i > 0$and from the equations obtained, we find the range of k for stability.

Solving Eqn.(3.15), we have the following ranges of k respectively, for which Eqn.(3.13) is stable.

$$-1 < k < \infty,\ k < 1.4140 \tag{3.16}$$

Thus, the resultant range of k for which Eqn.(3.13) is stable is given by

$$-1 < k < 1.4140 \tag{3.17}$$

(3) Bilinear transformation is then performed to determine the digital counter part. This is done using the MATLAB function "*bilinear*". Refer to Program B6.

(4) Now we have the digital transfer function of the 1-D filter. The same procedure as above, is extended to the second dimension and the transfer function for the second dimension is obtained independently.

(5) The product of the two 1-D polynomials is then determined.

(6) A general subroutine suitable for any order of the filter has been written to determine the frequency response of the 2-D filter. Refer Program B6. The corresponding contour plots are plotted using the MATLAB function "*contour*".

The MATLAB program namely, Program B5 and B6 have been written for the Highpass filter specifications given by

$W_n1 = W_n2$	$N1 = N2$
[0.4]	4

All frequencies are in radians. The scripts 1 and 2 refer to the first and second dimensions, respectively.

Program B5

```
%2D-HIGHPASS BUTTERWORTH IIR FILTER
        clear all;
        close all;
        N1=4;
        Wn1=[0.4];
        N2=N1;
        Wn2=Wn1;
        [B1,A1]=butter(N1,Wn1,'high','s');
        [B2,A2]=butter(N2,Wn2,'high','s');
        for k1=-1.0:0.1:1.4
        for k2=-1.0:0.1:1.4
        zz=ker_progb6_mag(B1,A1,k1);
        lim=pi;
        interval=pi/50;
        w1=0:interval:lim;
        w2=0:interval:lim;
        [ww1,ww2]=meshgrid(w1,w2);
        figure;
        contour(ww1,ww2,zz);
        axis('image');
        xlabel('w1');
        ylabel('w2');
        zlabel('Magnitude Response');
        title('2-D IIR Butterworth HPF','FontSize',16);
        grid on;
        end
        end
```

Program B6

```
%%Function to determine the transfer function of the filter for a given k1,k2
        function [zz]=ker_progb6_mag(B1,A1,k1);
        B2=B1;
        [R C]=size(A1);
        A1(1)=A1(1)+k1*B1(1);
        A2(1)=A2(1)+k2*B2(1);
        %%%Bilinear transformation of the transfer function
        [N1,D1]=bilinear(B1,A1,1);
        [N2,D2]=bilinear(B2,A2,1);
        %%To determine the 2-D transfer function of the IIR filter
        for m=1:1:size(N1,2)
```

```
for n=1:1:size(N2,2)
N(m,n)=N1(m)*N2(n);
end
end
for m=1:1:size(D1,2)
for n=1:1:size(D2,2)
D(m,n)=D1(m)*D2(n);
end
end
lim=pi;
interval=pi/50;
c1=0;
for w1=0:interval:lim
c2=0;
c1=c1+1;
for w2=0:interval:lim
c2=c2+1;
for col=1:1:size(N2,2)
NRow(1,col)=(cos(w2)+j*sin(w2))^(size(N2,2)-col);
end
for row=1:1:size(N2,2)
NCol(row,1)=(cos(w1)+j*sin(w1))^(size(N1,2)-row);
end
NR=NRow*N'*NCol;
a=real(NR);
b=imag(NR);
for col=1:1:size(D2,2)
DRow(1,col)=(cos(w2)+j*sin(w2))^(size(D2,2)-col);
end
for row=1:1:size(D2,2)
DCol(row,1)=(cos(w1)+j*sin(w1))^(size(D1,2)-row);
end
DR=DRow*D'*DCol;
c=real(DR);
d=imag(DR);
MOD(c1,c2)=(sqrt((a*c+b*d)^2+(b*c-a*d)^2))/(c^2+d^2);
end
end
w1=0:interval:lim;
w2=0:interval:lim;
[ww1,ww2]=meshgrid(w1,w2);
zz=MOD/(max(max(MOD)));
%%End of Program
```

The results of the algorithm namely the contour plots for the first quadrant are as shown in Figs.(3.9) and (3.10). A large number of plots for all possible values of k within the stability ranges were plotted. Only the plots of interest have been shown. As it can be seen from the plots, there is a certain range of k for which elliptical symmetry is exhibited in the frequency response for specific magnitude ranges. From Section 2.7 using Program A3, the extent of elliptical symmetry is determined for the above responses and the optimum value of k for which we have the closest proximity to elliptical symmetry is determined.

The plots in Figs.(3.11) and (3.12) show the extent of elliptical symmetry for the responses shown in Figs.(3.9) and (3.10). The plot for $k_1 = k_2 = 1.4$ is not shown since there are no points within this magnitude range which approximate to elliptical symmetry.

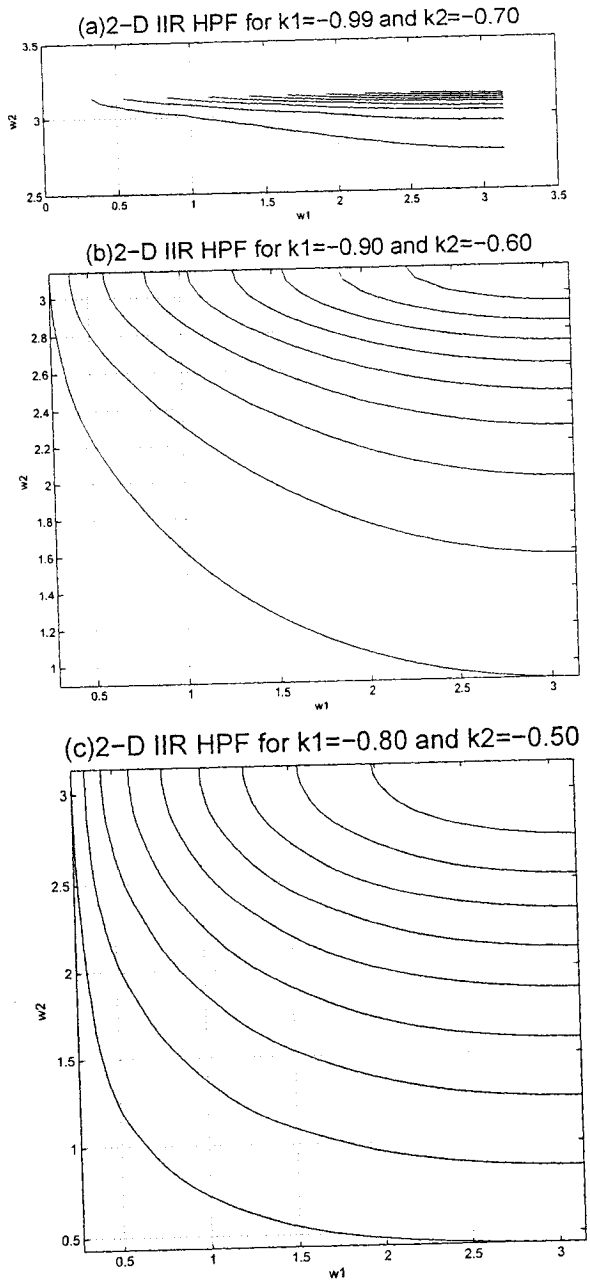

Figure 3.9: Contour plots of Fourth order 2-D IIR Butterworth highpass filter (a) k1=-0.99 and k2=-0.70 (b) k1=-0.90 and k2=-0.60 (c) k1=-0.8 and k2=-0.50.

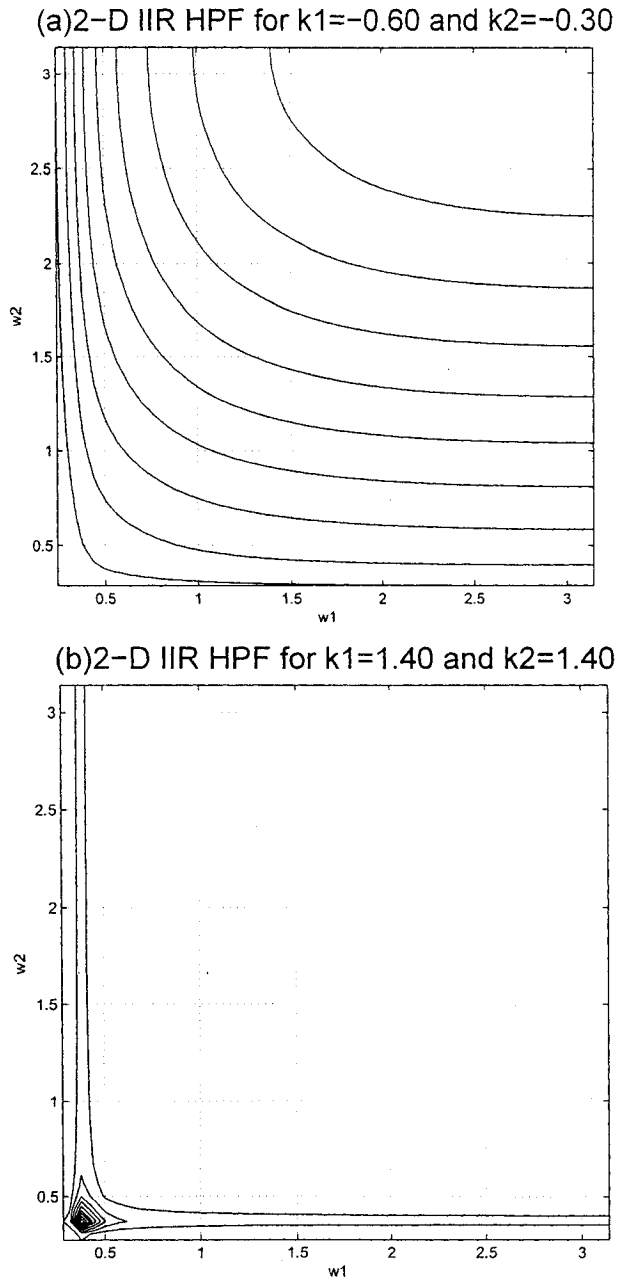

Figure 3.10: Contour plots of Fourth order 2-D IIR Butterworth Bandpass filter (a) k1=-0.60 and k2=-0.30 (b) k1=1.40 and k2=1.40.

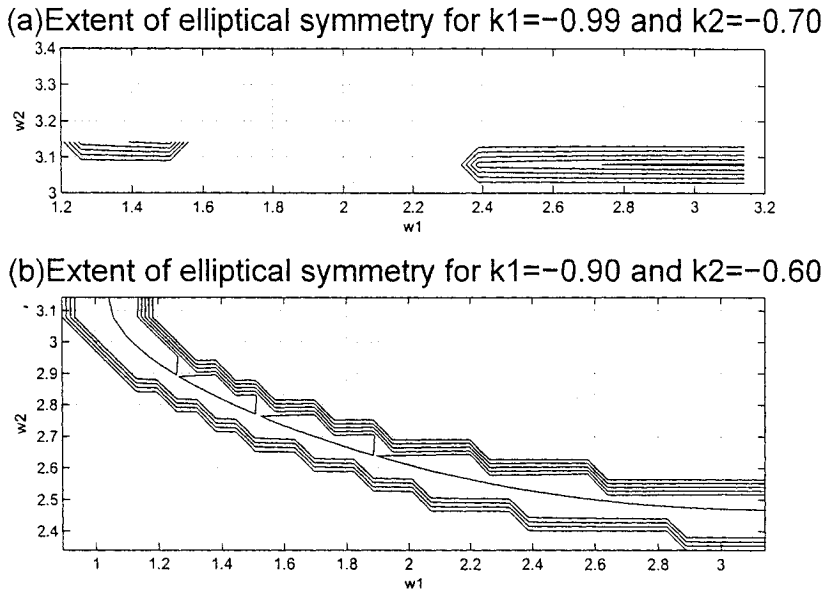

Figure 3.11: Plots showing the extent of elliptical symmetry for (a) k1=-0.99 and k2=-0.70 (b) k1=-0.90 and k2=-0.60. The magnitude range under consideration is 0.45<Mag<0.55.

It is evident from the plots that at $k_1 = -0.80$ & $k_2 = -0.50$, the response exhibits near elliptical symmetry and for other values of k_1 & k_2, the elliptical symmetry gradually ceases to exist. However, it is noted that, specifically for a Highpass filter, since the pass-band range extends to infinity, it is really not possible to define a elliptical symmetric response all over the pass-band. In this section, strictly, near-elliptical symmetry has been demonstrated in the transition band.

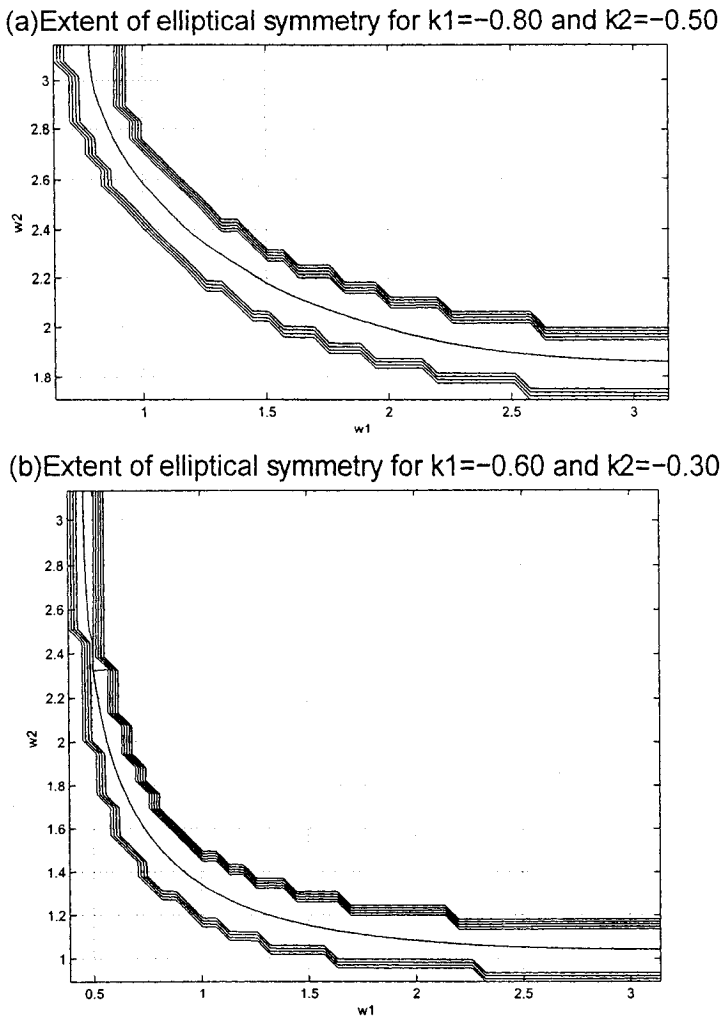

Figure 3.12: Plots showing the extent of elliptical symmetry for (a) k1=-0.80 and k2=-0.50 (b) k1=-0.60 and k2=-0.30. The magnitude range under consideration is 0.45<Mag<0.55.

3.4 Summary and Discussion

This chapter has dealt with the design of 2-D bandpass, bandstop and highpass IIR Butterworth filters and their approximation to elliptical symmetry within stability limits.

For the bandpass filter, near elliptical symmetry has been obtained corresponding to a single quadrant for the filter response. This is because the bandpass response is obviously a closed response within a quadrant, and elliptical symmetry in one quadrant means corresponding symmetry in all the four quadrants.

For the bandstop filter, near elliptical symmetry can be seen in the two transition regions(lower and upper) and depending on the requirement, the study can be extended to a more specific region. Here also, the example shown takes into account the elliptical symmetry for both these regions of interest. In the lower transition region and below, elliptical symmetry study can be extended due to the response from all the four quadrants. The upper transition band and higher, however extend to infinity and therefore, this study can only be restricted to the lower part of the upper transition region.

For the highpass filter, however, as has been mentioned before, the elliptical symmetry study can only be studied in the lower transition region due to the infinite bound of the pass-band region.

In general, from the results obtained above, it can be seen that near elliptical symmetry has been obtained in certain frequency ranges for a particular value of a magnitude range. Depending on the required application, it is possible to change the specification in such a manner that elliptical symmetry for a different magnitude range can be studied and analyzed.

Chapter 4

Combination Filters

Certain applications require specific types of symmetric response which may be uniquely obtained by combination of two or more filters of the same kind or of different kinds. This has been carried out before in different ways in 1-D analysis. This chapter deals with such types of combination filters, extended to the second dimension. In this chapter, it will be shown that transfer functions of one or more filters can be arithmetically added and/or subtracted to achieve a specific type of response. It is also intended here to study the extent of elliptical symmetry that can be achieved by such types of combination filters in each dimension.

In this chapter we will deal with three different types of combination filters, namely:

1. lowpass and bandpass combination
2. bandpass filter obtained as a result of the subtraction of two lowpass filters.
3. bandstop filter obtained as a result of adding a lowpass and a highpass filter.

The above filters are obtained by combining the transfer functions of the two different types of filters.

4.1 Lowpass and Bandpass Combination Filter

First we will consider one of the most elementary types of combination namely, the combination of a lowpass and a bandpass filter to form a specific type of response, in which the pass-band of the eventual combination filter will have variable gain depending upon how the transition regions of the lowpass and the bandpass filter add up. Fig.(4.1) shows the one-dimensional interpretation of the lowpass and bandpass combination filter. The design procedure is simple.

Firstly the individual filters, namely the lowpass and the bandpass filter have been designed separately based on the design parameters shown in Table {4.1}. The individual filters are designed and analyzed separately for their respective responses.

Another important aspect of this study, has been to analyze the extent of elliptical symmetry of the combination filter when the individual filters are themselves approximated to elliptical symmetry.

In this case, the lowpass and bandpass filters have been separately analyzed for elliptical symmetry following the same procedure in Chapter-3. Following that analysis, we have the results as follows.

Lowpass Transfer function in the first dimension= $\frac{0.0625}{s_1^4+1.3066s_1^3+0.8536s_1^2+0.3266s_1+0.0625}$

Range of k for stability= $-1 < k < 1.4143$

Values of k_1 and k_2 for near elliptical symmetry= -0.42 & -0.22.

The plots in Fig.(4.2) show the response for the lowpass filter corrected for near elliptical symmetry.

The bandpass filter considered here in the second dimension(s_2), has the same response as the one shown in Section 3.1. (Refer Section 3.1 for transfer function and figures).

The effective response of the combination filter which is obtained as a result of adding the lowpass and the bandpass transfer functions is shown in Fig.(4.3(a)).

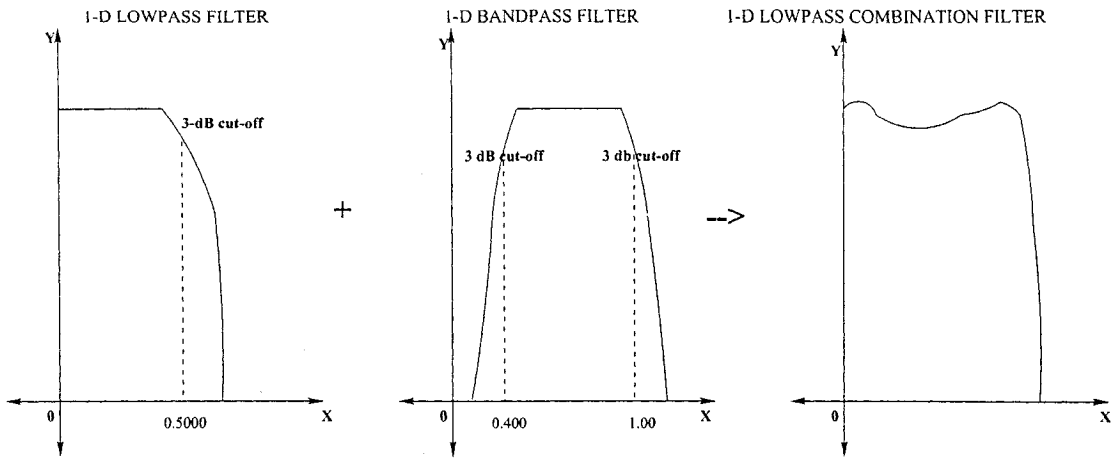

Figure 4.1: A one-dimensional interpretation of the Lowpass + Bandpass combination

	Lowpass Filter	Bandpass Filter
Order	4	4
Cut-off(rad)	0.5	[0.4 1]

Table 4.1: Combination filter parameters: Lowpass+Bandpass Filter.

The response of the combination filter as shown in Fig.(4.3(a)), has then been studied to test its closeness to elliptical symmetry using Program A3(Chapter-2). This study reveals the plot of Fig(4.3(b)).

From Fig.(4.3(b)), it is evident that, near elliptical symmetry cannot be obtained in the transition region, although the individual filters are near-elliptical symmetric in their respective transition regions. Elliptical symmetry is however, found to be possible in the pass-band regions of the combination filter within which the individual lowpass and bandpass pass-band regions are not effected by the magnitude response of each other. It is seen that the bandpass region of the combination filter exhibits near elliptical symmetry to an extent.

The Program to obtain these results has been written in MATLAB and is shown below in Program C1.

Program C1

```
%%2D LOW PASS + BAND PASS COMBINATION BUTTERWORTH IIR FILTER
    clear all; close all;
    %%2-D LOW PASS BUTTERWORTH FILTER
    Lk1=-0.42; LN1=4; LWn1=0.5; LN2=LN1; LWn2=LWn1;
    Lk2=-0.22
    [LB1, LA1]=butter(LN1,LWn1,'low','s');
    [LB2, LA2]=butter(LN2,LWn2,'low', 's');
    LPTF=kerthproga2(LB1,LA1,Lk1);
    %%2-D BAND PASS BUTTERWORTH FILTER
    Bk1=-0.25;BN1=4; BWn1=[0.4 1]; BN2=BN1; BWn2=BWn1;
    Bk2=-0.08;
    [BB1, BA1]=butter(BN1,BWn1,'s');
    [BB2, BA2]=butter(BN2,BWn2,'s');
    LPTF=ker_progb2_mag(BB1,BA1,Bk1);
    TTF=LPTF+BPTF;
    TTF=TTF/(max(max(TTF)));
    lim=pi; interval=pi/50;
    w1=0:interval:lim; w2=0:interval:lim;
    [ww1,ww2]=meshgrid(w1,w2);
    figure;
    contour(ww1,ww2,TTF);
    axis('image'); xlabel('w1'); ylabel('w2'); zlabel('Magnitude Response');
    title('(a) 2-D Lowpass + Bandpass Combination Filter','FontSize',16);
    grid on;
```

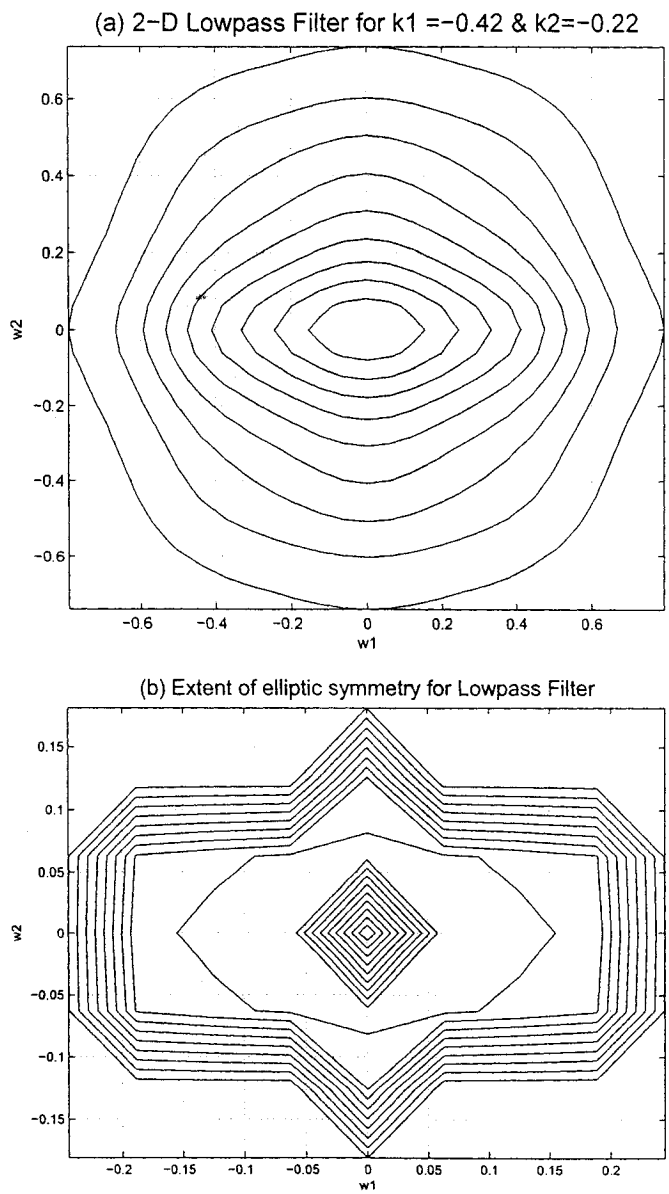

Figure 4.2: Plots showing (a) the response of the Lowpass filter (b) approximation to elliptical symmetry between magnitude range [0.8 1] (normalized) derived from Program A3.

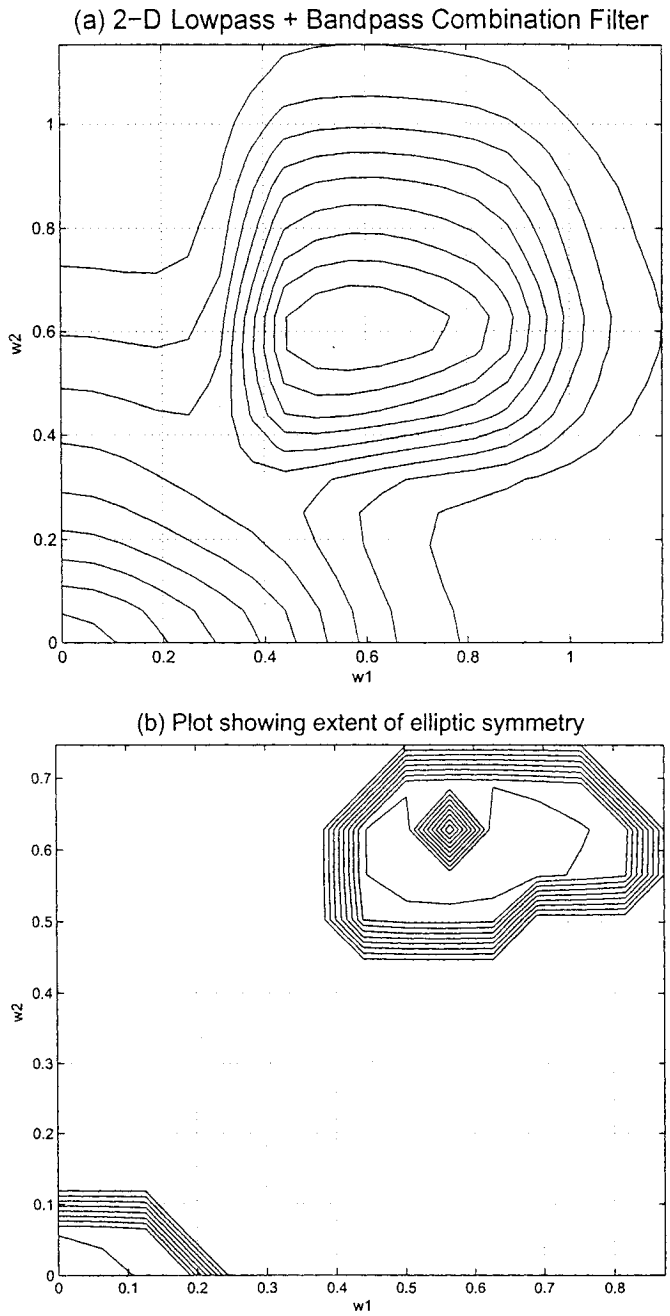

Figure 4.3: Plots showing (a) the response of the combination filter (b) the extent of elliptical symmetry in the combination of a Lowpass and a Bandpass filter. Magnitude range under study=[0.8 1](normalized) derived from Program A3.

4.2 Lowpass and Lowpass Combination Filter

Here we consider an interesting combination namely, the combination of two lowpass filters to form an eventual bandpass response. Fig.(4.4) shows the one-dimensional interpretation of the two lowpass combination filter. It shows that when two lowpass filters of different cut-off frequencies (the first one higher than the second one) are subtracted from each other, we get an eventual bandpass response.

The design procedure is simple. First, the individual lowpass filters are designed separately based on the design parameters shown in Table {4.2}. The important aspect of this study has been to analyze the extent of elliptical symmetry of the combination filter when the individual filters are themselves approximated to elliptical symmetry.

In our case, both the lowpass filters have been separately analyzed for elliptical symmetry following the same procedure as in Chapter-3. Note that the first lowpass filter has been considered here for illustration follows the same design as the one that was chosen in Section 4.1.

The analysis of the Lowpass filters are as follows:

Lowpass Transfer function(1)=$\frac{0.0625}{s_1^4+1.3066s_1^3+0.8536s_1^2+0.3266s_1+0.0625}$

Range of k for stability=$-1 < k < 1.4143$

Values of k_1 and k_2 for near elliptical symmetry for Filter 1= -0.42 & -0.22.

Lowpass Transfer function(2)=$\frac{0.0016}{s_2^4+0.5226s_2^3+0.1366s_2^2+0.0209s_2+0.0016}$

Range of k for stability=$-1 < k < 1.4360$

Values of k_1 and k_2 for near elliptical symmetry for Filter 2= -0.35 & -0.16.

The plots in Figs.(4.5) and (4.6) show the response for the Lowpass filters corrected for near elliptical symmetry for a specific magnitude range. It is seen that the individual filters exhibit near elliptical symmetry within the specific magnitude range.

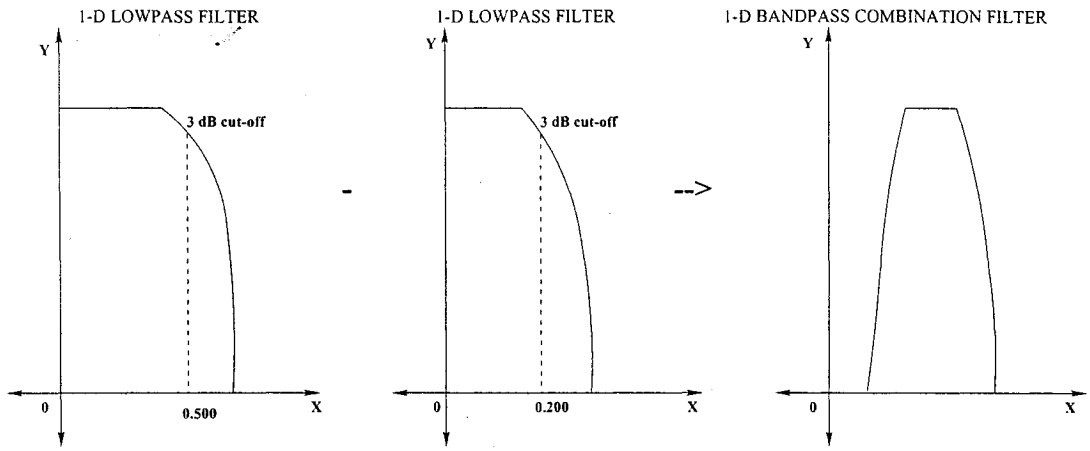

Figure 4.4: A one-dimensional interpretation of the Lowpass filter combination.

	Lowpass Filter1	Lowpass Filter2
Order	4	4
Cut-off(rad)	0.5	0.2

Table 4.2: Combination filter parameters: Lowpass-Lowpass filter.

The effective response of the combination filter which is obtained as a result of subtracting the lowpass filter(2) and from lowpass Filter(1) is shown in Fig.(4.7). This figure shows both the magnitude and contour plots of the combination filter which approximates to a Bandpass response. The extent of elliptical symmetry has been tested for this combination filter and it has been seen that the combination filter exhibits near elliptical symmetry in the outer range of subtraction. Theoretically, the subtraction of two lowpass filters should result in a bandpass filter. From the combination filter plots, it is seen that a bandpass filter with a short pass-band region has been obtained. Near elliptical symmetry is possible in the outer boundary of this pass-band region. Elliptical symmetry exists for certain magnitudes in the pass-band regions of the individual filters which are not affected by the magnitude response of each other.

The program to obtain these results has been written in MATLAB and is shown below in Program C2.

Program C2

```
%%2D LOWPASS - LOWPASS COMBINATION BUTTERWORTH IIR FILTER
    clear all; close all;
    %%2-D LOW PASS BUTTERWORTH FILTER-1
    Lk1=-0.42; LN1=4; LWn1=0.5; LN2=LN1; LWn2=LWn1;
    Lk2=-0.22
    [LB1, LA1]=butter(LN1,LWn1,'low','s');
    [LB2, LA2]=butter(LN2,LWn2,'low', 's');
    LPTF=kerthproga2(LB1,LA1,Lk1);
    LPTF=LPTF/max(max(LPTF));
    %%2-D LOW PASS BUTTERWORTH FILTER-2
    lk1=-0.35; lN1=4; lWn1=0.2; lN2=lN1; lWn2=lWn1;
    lk2=-0.16;
    [lB1, lA1]=butter(lN1,lWn1,'s');
    [lB2, lA2]=butter(lN2,lWn2,'s');
    lPTF=kerthproga2(lB1,lA1,lk1);
    lPTF=lPTF/max(max(lPTF));
    TTF=LPTF-lPTF;
    TTF=TTF/(max(max(TTF)));
    lim=pi; interval=pi/50;
    w1=-lim:interval:lim; w2=-lim:interval:lim;
    [ww1,ww2]=meshgrid(w1,w2);
    mesh(ww1,ww2,TTF);
    figure;
    contour(ww1,ww2,TTF);
    axis('image'); xlabel('w1'); ylabel('w2'); zlabel('Magnitude Response');
    title(' 2-D Butterworth Lowpass - Lowpass Combination Filter','FontSize',16);
    grid on;
```

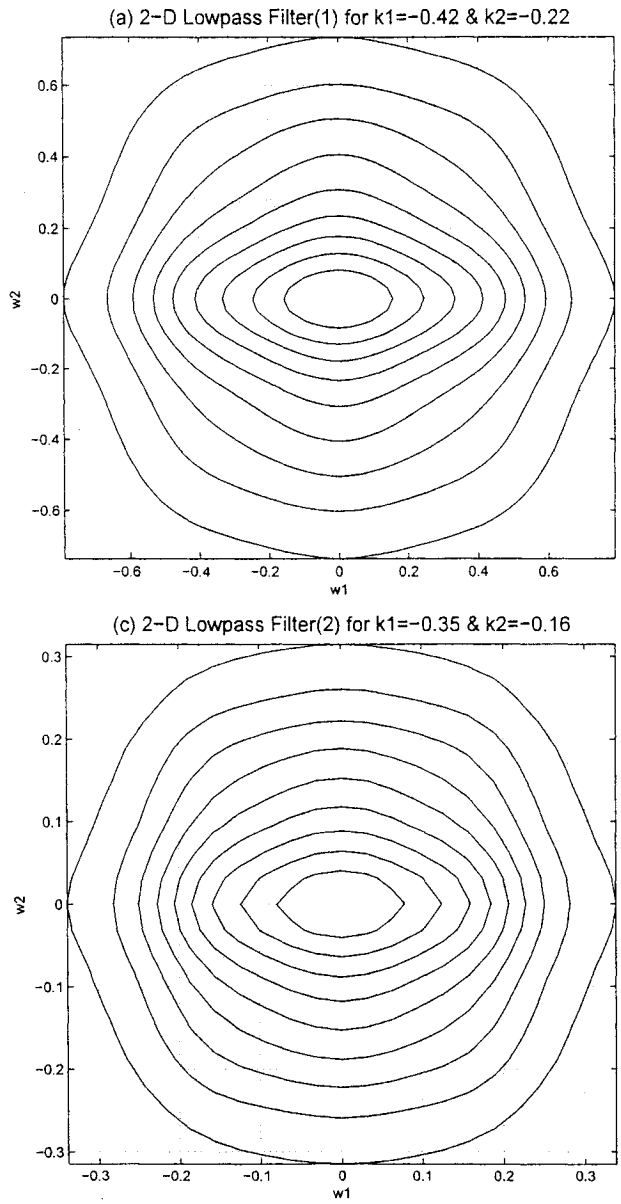

Figure 4.5: Contour Plots showing the response of the Lowpass filters (a) Filter (1) for k1=-0.42 and k2=-0.22 and (b) Filter (2) for k1=-0.35 and k2=-0.16

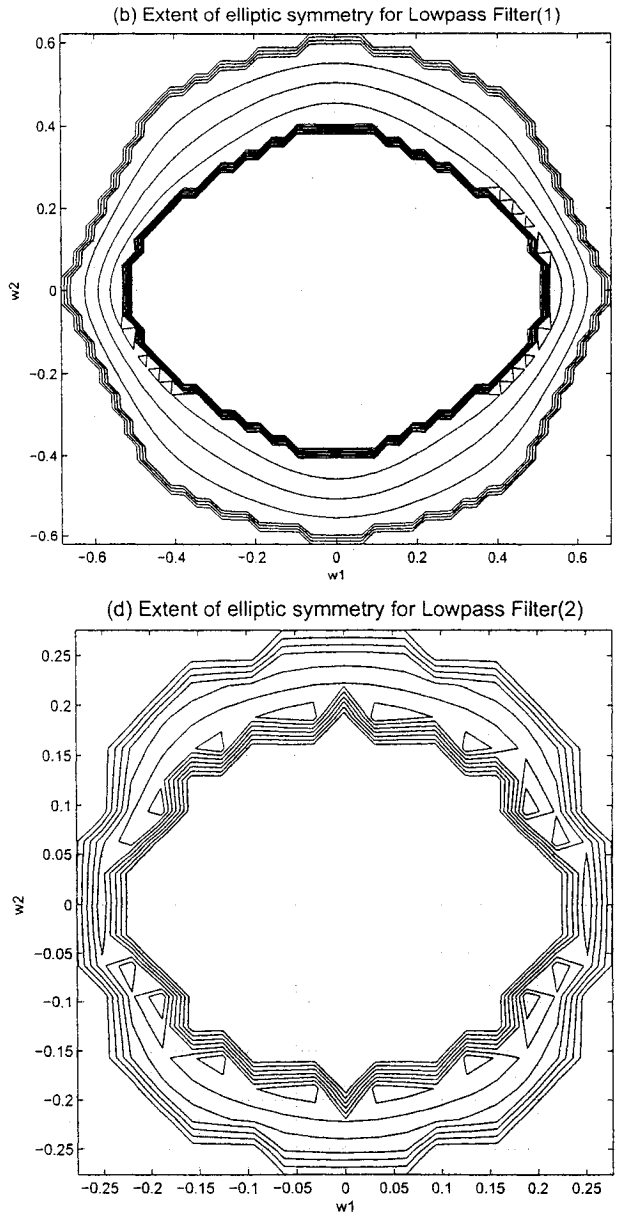

Figure 4.6: Plots (a) and (b) showing their approximation for Figs.(4.5(a) and (b)) respectively to elliptical symmetry for specific magnitude range [0.2, 0.4] (normalized) derived from Program A3.

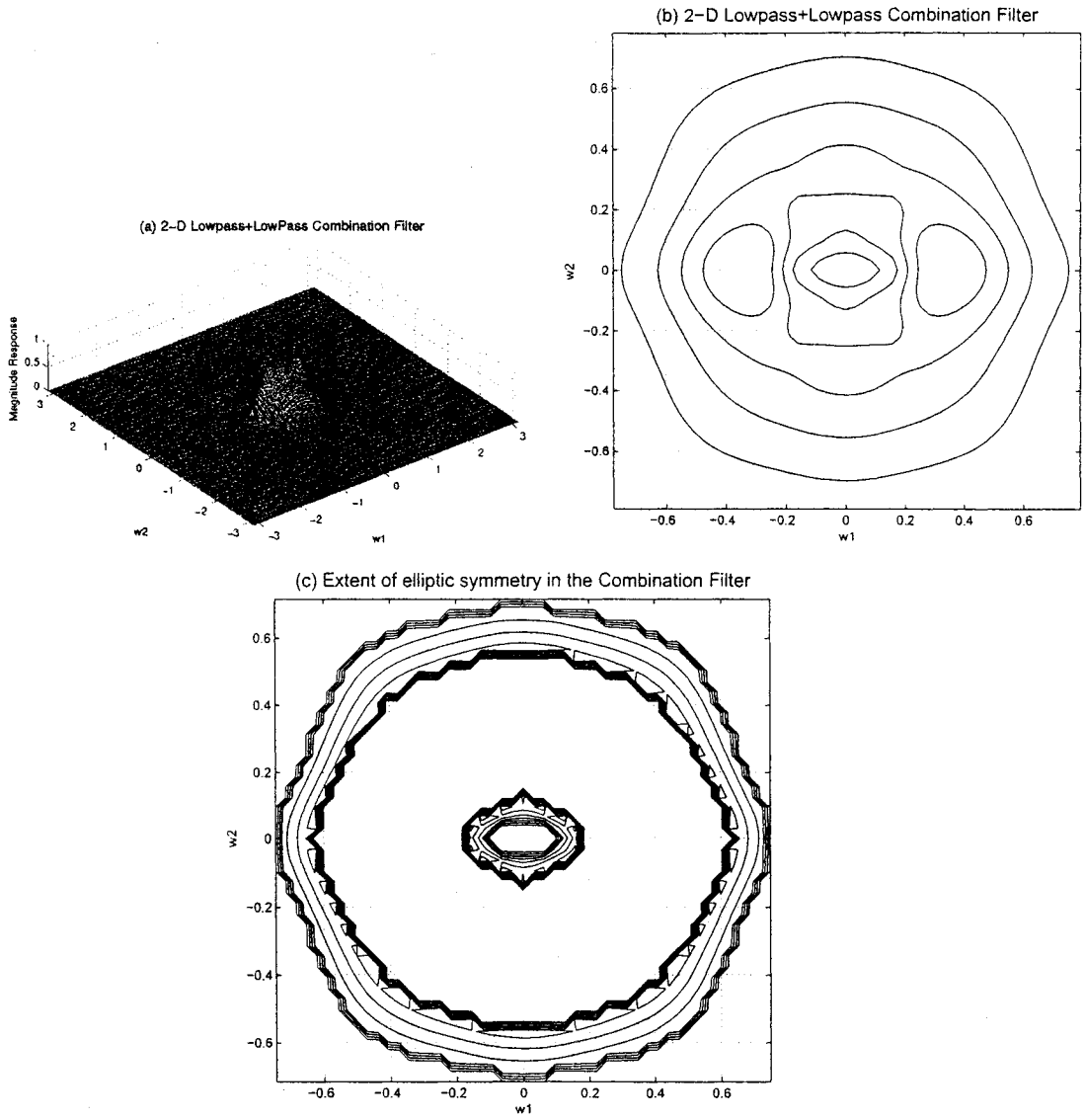

Figure 4.7: Plots (a) and (b) showing the response of the combination filter(magnitude and contour plots respectively) and plot (c) showing the extent of elliptical symmetry in this response between the magnitude range [0.2, 0.4] (normalized) derived from Program A3.

4.3 Lowpass and Highpass combination Filter

We will now consider another type of combination filter which effectively yields a bandstop filter by combining arithmetically, the responses of a lowpass and highpass filters. We will consider the lowpass and highpass filters with near elliptical symmetric responses on their outer limits so that the bandstop filter can also be studied for its extent of elliptical symmetry by the combination of the above filters. Fig.(4.8) shows the one-dimensional interpretation of the lowpass and highpass combination filter. The design procedure, here again, is very simple in its sense. Firstly the individual filters, namely the Lowpass and the Highpass filter have been designed separately based on the design parameters shown in Table {4.3}. The individual filters are designed and analyzed separately for their respective responses.

Another important aspect of this study has been to analyze the extent of elliptical symmetry of the combination filter when the individual filters are themselves approximated to elliptical symmetry.

In our case, the lowpass and the highpass filters have been separately analyzed for elliptical symmetry following the same procedure as in Chapter-3. Following that analysis, we have the following results:

Lowpass Transfer function=$\frac{0.0625}{s_1^4+1.3066s_1^3+0.8536s_1^2+0.3266s_1+0.0625}$

Range of k for stability=$-1 < k < 1.4143$

Values of k_1 and k_2 for near elliptical symmetry= -0.42 & -0.22.

Note that the lowpass filter considered here, follows the same design as that considered in Section(4.1).

The plots in Fig.(4.9) show the response for the lowpass filter corrected for near elliptical symmetry.

The highpass filter considered here, has a cutoff frequency of [0.7] leaving a stop-band range for the combination filter between [0.5, 0.7]. The highpass filter is first studied independently, for elliptical symmetry following the same method as suggested in Section 3.3. Following that analysis we have the following results:

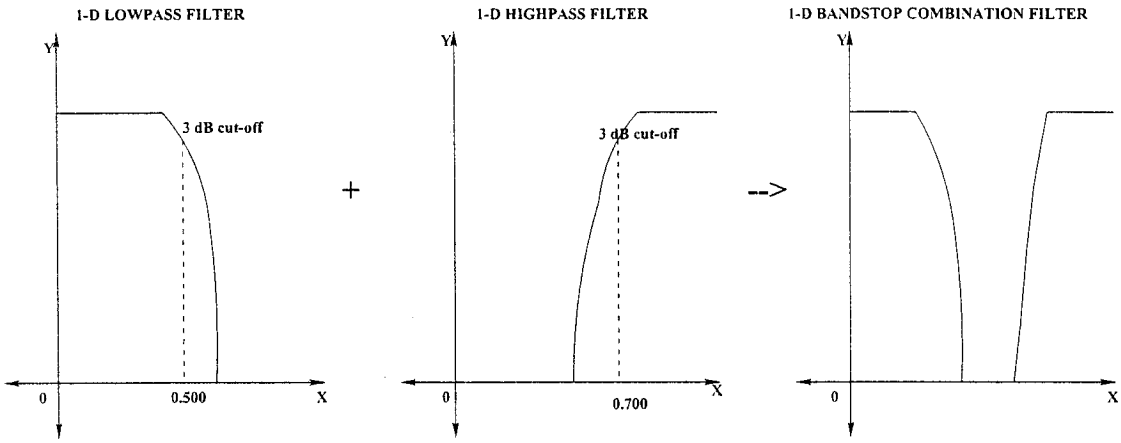

Figure 4.8: A one-dimensional interpretation of the Lowpass+Highpass combination.

	Lowpass Filter	Highpass Filter
Order	4	4
Cut-off(rad)	0.5	0.7

Table 4.3: Combination filter parameters: Lowpass+Highpass filter

Highpass Transfer function=$\frac{s^4}{s_2^4+1.8292s_2^3+1.6730s_2^2+0.8963s_2+0.2401}$

Range of k for stability=$-1 < k < 1.4167$

Values of k_1 and k_2 for near elliptical symmetry = -0.85 & -0.55.

The response of the highpass filter after its test for stability due to variation in parameters k_1 and k_2 is as shown in Fig.(4.10). The response of the combination filter is as shown in Figs.(4.11(a), (b) & (c)) has then been tested for its extent of elliptical symmetry using Program A3(Chapter-2).

This study reveals the following plots. The reason why the magnitude range of [0.2, 0.4] is chosen for study of elliptical symmetry is that, the transition regions of the individual filters lie around this value of magnitude range.

It is evident from Fig.(4.11(c)) that near elliptical symmetry can still be obtained in the transition region of the combination filter. Elliptical symmetry is also not affected by the responses of the filters in their respective pass-bands due to the effect of their combined magnitudes.

The Program to obtain these results were written in MATLAB and is shown below in Program C3

Program C3

```
%%2D LOWPASS + HIGHPASS COMBINATION BUTTERWORTH IIR FILTER
    clear all; close all;
    %%2-D LOW PASS BUTTERWORTH FILTER
    Lk1=-0.42; LN1=4; LWn1=0.5; LN2=LN1; LWn2=LWn1;
    Lk2=-0.22
    [LB1, LA1]=butter(LN1,LWn1,'low','s');
    [LB2, LA2]=butter(LN2,LWn2,'low', 's');
    LPTF=kerthproga2(LB1,LA1,Lk1);
    %%2-D HIGH PASS BUTTERWORTH FILTER
    Hk1=-0.85; HN1=4; HWn1=0.7 ; HN2=HN1; HWn2=HWn1;
    Hk2=-0.55;
    [HB1, HA1]=butter(HN1,HWn1,'high','s');
    [HB2, HA2]=butter(HN2,HWn2,'high','s');
    HPTF=kerthproga2(HB1,HA1,Hk1);
    TTF=LPTF+HPTF;
    TTF=TTF/(max(max(TTF)));
    lim=pi; interval=pi/50;
    w1=0:interval:lim; w2=0:interval:lim;
    [ww1,ww2]=meshgrid(w1,w2);
    figure;
    mesh(ww1,ww2,TTF);
    axis('image'); xlabel('w1'); ylabel('w2'); zlabel('Magnitude Response');
    title(' 2-D Butterworth Lowpass + Highpass Combination Filter','FontSize',16);
    grid on;
    figure;
    contour(ww1,ww2,TTF);
    axis('image'); xlabel('w1'); ylabel('w2'); zlabel('Magnitude Response');
    title(' 2-D Butterworth Lowpass + Highpass Combination Filter','FontSize',16);
    grid on;
```

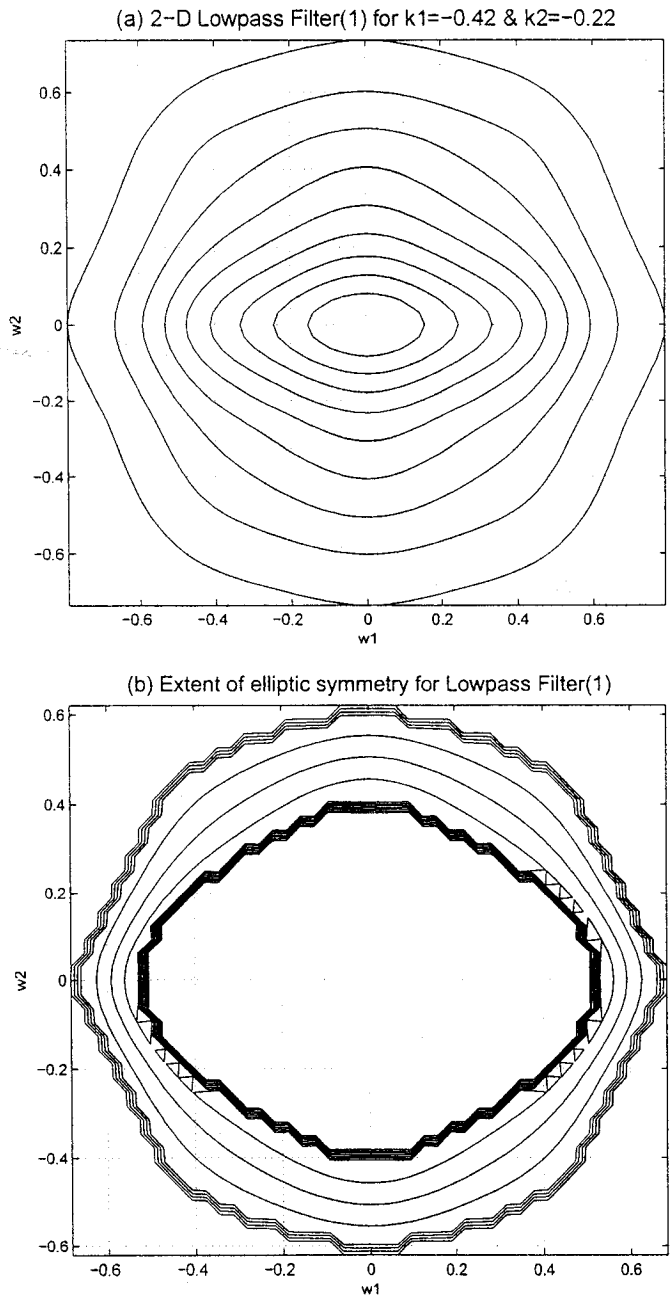

Figure 4.9: Plot (a) showing the response of the Lowpass filter and plot (b) showing its approximation to elliptical symmetry between magnitude range [0.2, 0.4](normalized) derived from Program A3.

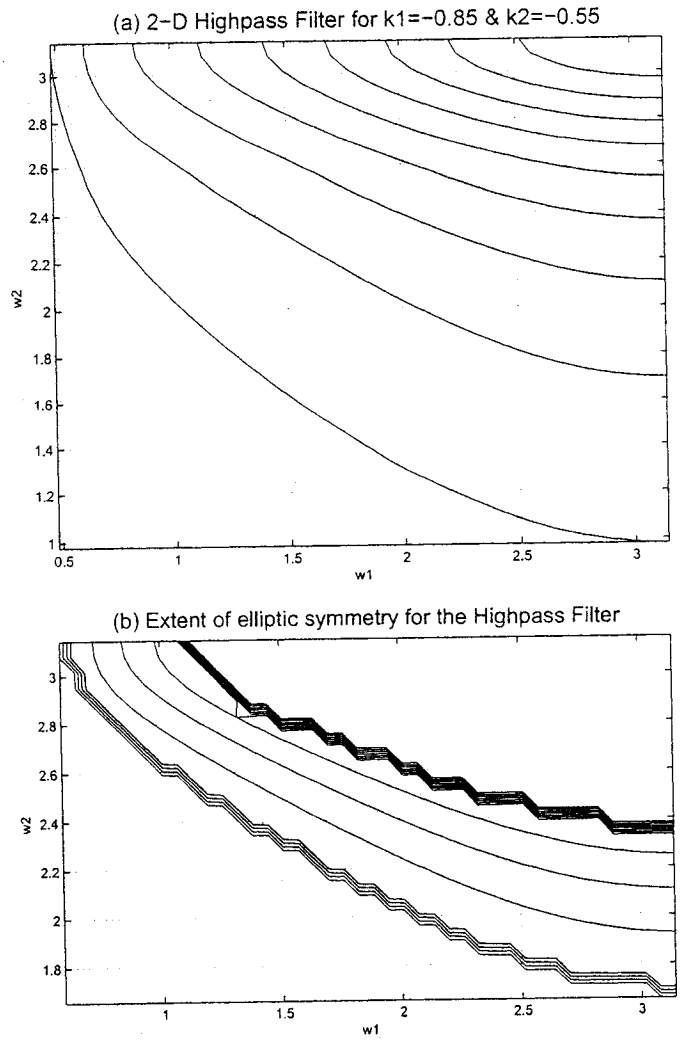

Figure 4.10: Plot (a) showing the response of the Highpass filter and plot (b) showing its extent of elliptical symmetry for k1= -0.85 and k2=-0.55 in the magnitude range [0.2, 0.4](normalized) derived from Program A3.

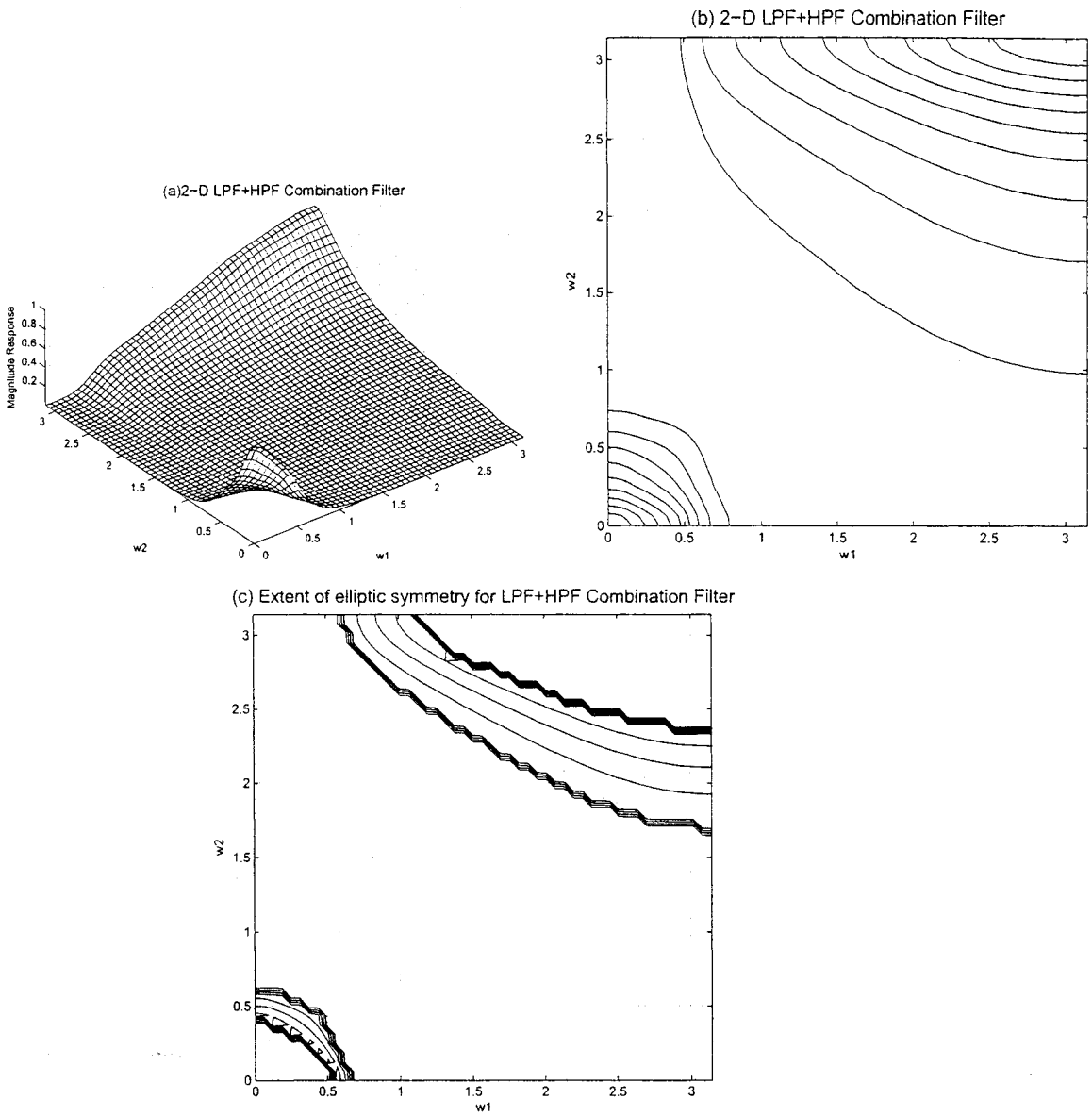

Figure 4.11: Plots (a) and (b) showing the response of the combination filter(magnitude and contour plots respectively) and plot (c) showing the extent of elliptical symmetry in this response between the magnitude range [0.2, 0.4] (normalized) derived from Program A3.

4.4 Summary and Discussion

In this Chapter, we have dealt with three different types of combination filters. The purpose of this chapter has been to study the effect of combining individual filters which have near elliptical symmetry in their transition regions. The effective combination filter has been studied and analyzed to see if the elliptical symmetry still exists in its response.

The first combination filter in each dimension to be studied is the effect of a lowpass and a bandpass filter to form a lowpass filter of larger pass-band. This study reveals that near elliptical symmetry in the combination filter can only be obtained in the individual pass-band regions of the two filters and the transition region does not exhibit elliptical symmetry.

The second combination filter in each dimension to be studied is the effect of combining (subtracting) two lowpass filters of different pass-widths, to obtain a bandpass filter. Here it has been shown that elliptical symmetry exists to an extent in the transition regions of the bandpass combination filter. Elliptical symmetry also exists in the individual filter's pass-band regions where-in the responses of the individual filter do not effect each other.

The third combination in each dimension to be studied is the effect of combining a lowpass and a highpass filter to form a bandstop combination filter. Here again, it has been proved that elliptical symmetry exists in the transition region of the bandstop combination filter response.

This chapter is just the first step towards the study of combining filter responses to obtain unique and user specific responses. Modern image processing softwares use this feature to obtain specific responses towards enhancing image quality.

Chapter 5

Conclusions

Multi-dimensional system and analysis is a topic that is developing in great pace and specifically 2-D systems are used widely in modern image processing software and analysis. 2-D filters are one of the main uses that 2-D system finds itself in. Modern image processing softwares [27] require sufficient amount of pre-processing steps of the raw image data that is being used for analysis. These pre-processing stage largely uses Butterworth filters of a given order to correct the image and mould it for efficient image analysis. Image processing itself, in its true sense, uses different kinds of filters for various image manipulation purposes such as sharpening, smoothening, edge detection and other arithmetic operations. In all these cases we deal with image data which is truly two-dimensional in its sense. Thus it becomes necessary that we deal with 2-D filters which do not have any preferential orientation towards data manipulation because the image signal itself, does not have any preferential spatial direction. This fact has been the main motivation behind this thesis work. This study, in all its chapters, focuses mainly on the extent of elliptical symmetry of 2-D filters obtained as a result of simplistic design procedures. Other interesting aspects such as Complementary pole pair filters and their effect on elliptical symmetry and the effect of combining different types of 2-D filter functions have also been studied and analyzed.

5.1 Elliptical Symmetry of 2-D Filters

A simple method for designing 2-D IIR filters, namely using the product of two 1-D IIR transfer function has been implemented. The important factor to be considered for filter design is the stability of the filters. It is necessary to test stability for any filter design, in order that the filter does not become unstable for a bounded input frequency. However there is more flexibility with IIR filters in terms of parameter modifications to obtain a required set of filters. The main problem, however, affecting the design of IIR filters is the stability of the filters. Bringing the filter into second dimension also increases the complexity to test stability. This again is one of the main reasons why 2-D filters obtained as the product of two, 1-D filters have been used in this thesis. Methods have already been proposed [24] to perform a stability check on such types of separable denominator transfer functions in two dimensions. In this thesis, these have been used, to test the designed filter for stability, before further analysis is carried out. This ensures that the filter is stable and can withstand the various parameter modifications that it undergoes for approximation to elliptical symmetry. It has also been shown in [24], that it is possible to have variable magnitude characteristics for 2-D filters by changing feedback factor k (in our case k_1 and k_2 in both dimensions) in the IIR filter transfer function, within stability limits, and obtain responses close to different kinds of (in our case elliptical) symmetries. This is the important factor used in this thesis to study the different possibilities of elliptical symmetry. The elliptical symmetry study in this thesis can be divided into four different groups based on the nature and type of filters that have been used, namely lowpass filter study, study of filters due to complementary pole-pair effects, study of the other common types of filters namely highpass, bandpass and bandstop filters and the study of combination of these common types of filters. All the filter transfer function considered in the above study have an infinite impulse response. Following is a summary of the various conclusions we have obtained as a result of this study.

5.1.1 Study of Elliptical Symmetry in Lowpass Filters

In Chapter-2, we have concentrated on the two most commonly used filter transfer functions, namely, the Butterworth and the Chebyshev transfer functions. These are used to approximate 2-D elliptical symmetry.

Butterworth Filters

The transfer function that has been used in this thesis for this type of filter is of third order. The point here is to adhere to the lowest order possible that an easily illustrate the effect of elliptical symmetry. Higher order filters can be used for the same kind of analysis but will involve more complexity in terms of design, computer programming and time of execution. Thus, it is sufficient to consider a third order transfer function to illustrate the approximation to elliptical symmetry.

2-D filters have been plotted first, simply as a product of two 1-D filters in it and with out any further effort, elliptical symmetry is not possible. The feedback factor k is then tested for stability limits($-1 < k < 3$) and for this specific third order transfer function (Eqn.(2.13)) various filters are plotted between these limits and the transfer function is analyzed. A program has been written in MATLAB to find the stability conditions of k of a Butterworth filter for different orders of $'n'$(from 3 to 8) when none of the poles in that particular filter are shifted. Table{2.1} shows the stability conditions of k for different order of n. It has been found that elliptical symmetry exists(Fig.(2.4)) at a value of $k_1 = -0.45$ and $k_2 = -0.20$. A separate program has been written using MATLAB to study the magnitude characteristic of each of these filters obtained as a function of k_1 and k_2 and elliptical symmetry has been studied between the normalized magnitude range of $0.49 < Mag < 0.51$. It is from this program that the accurate values of k_1 and k_2(Fig.(2.8) are determined for closest proximity to elliptical symmetry. It is possible to study a different magnitude range of interest and for each of these range, there will exist different values of k_1 and k_2 for near elliptical symmetry.

Chebyshev Filters

There are two transfer functions that have been used to study the case of Chebyshev filters. These two transfer functions are different from each other based on the single most important factor of distinction between filters of this type namely, the ripple width. The transfer function of the filters that have been used to study these cases is of third order. The ripple widths that have been considered are $\epsilon = 0.1526$ and $\epsilon = 0.3493$.

For the first case, where the ripple width is $\epsilon = 0.1526$, it has been found that elliptical symmetry exists for values of $k_1 = -0.80$ and $k_2 = -0.45$, if the magnitude range under study is $0.49 < Mag < 0.51$.

For the second case, where the ripple width is $\epsilon = 0.3493$, it has been found that elliptical symmetry exists for values of $k_1 = -0.30$ and $k_2 = -0.10$, if the magnitude range under study is $0.49 < Mag < 0.51$.

In effect, for the parameters chosen in their respective cases, the first case (Fig.(2.13)) exhibits better elliptical symmetry than the second case (Fig.(2.17c)). Hence, for a given ripple width and order of a Chebyshev filter, it is possible to determine the values of k_1 and k_2(within stability limits) and the range of magnitude response over which elliptical symmetry is possible.

5.1.2 Study of Elliptical symmetry in Complementary Pole-Pair Filter

Complementary pole-pair filters are a unique set of filters obtained as a result of change in the pole-parameters. In this case the pole-parameter that has been chosen for study of different kinds of filters is the polar angle of the poles of these filters. The stability conditions of k for different orders(from3 to 8) of the Butterworth filter when the poles are shifted are found and tabulated in Tables {2.3}, {2.4}, {2.5}, {2.6}, {2.7} and {2.8} respectively. This study has been illustrated in one dimension

to explain the nature of these types of filters [13] and it has then been extended to the second dimension for the purpose of meeting the objective of this thesis.

Elliptical symmetry study here has been carried out for different cases based on the change in the polar angles of $\pm 5°$, $\pm 10°$ and $\pm 25°$. It is seen from Fig.(2.29c), Fig.(2.33c), Fig.(2.37c), Fig(2.39c), Fig(2.41c) and Fig(2.43c) that the best possible elliptical symmetries can be obtained within the magnitude range $0.49 < Mag < 0.51$, are for the respective values of k_1 and k_2 as shown in each plot. It can also be observed that elliptical symmetry ceases to exist, as the angle of the pole parameter variation increases. The same can also be proved for a different magnitude range under study. In this case we will have different values of k_1 and k_2 for elliptical symmetry for each of the angle variation but the effective disintegration in elliptical symmetry will still be experienced for greater increase in the polar angle.

5.1.3 Study of Elliptical Symmetry in 2-D Highpass, Bandpass and Bandstop Filters

Common types of filters that are used in practice, apart from the lowpass filters, are the highpass, bandpass and bandstop filters. In Chapter-3, the extent of elliptical symmetry on 2-D filters of the above types have been studied.

Bandpass Filters

The bandpass filter that has been studied in this case has an analog cut-off frequency between [0.4, 1.0] and has been chosen to be fourth order. The IIR transfer function of such a filter is then determined(Eqn.(3.1)) and the values of k for which the filter is stable is found to be in the range $-0.7487 < k < 1.6509$. Within these limits, it has been found that the filter exhibits near elliptical symmetry only in high magnitude ranges $0.8 < Mag < 1.0$ and for the values of $k_1 = -0.25$ and $k_2 = -0.08$(Fig.(3.1c)), near elliptical symmetry has been obtained within the specified

magnitude range. Here, it is noted that the study of elliptical symmetry for bandpass filter has been shown only for one quadrant. This is due to the fact that, 2-D filters with separable denominator polynomials exhibit symmetry about the X and Y axis and elliptical symmetry is a possibility within only one of the quadrants. It is also seen that for higher values of k_1 and k_2, elliptical symmetry completely ceases to exist.

Bandstop Filters

The bandstop filter that has been studied in this case has an analog cut-off frequency between [0.4, 1.0] and has been chosen to be fourth order. The IIR transfer function of such a filter is then determined(Eqn.(3.6)) and the values of k for which the filter is stable is found to be in the range $-1 < k < 1.6456$. Within these limits, it has been found that the filter exhibits near elliptical symmetry only in magnitude ranges $0.45 < Mag < 0.55$ and for the values of $k_1 = -0.55$ and $k_2 = -0.30$(Fig.(3.5c)), near elliptical symmetry has been obtained within the specified magnitude range. Here too, the study of elliptical symmetry has been shown only for one quadrant. Although it is possible that for frequencies lower than the lower cut-off frequencies, elliptical symmetry can exist covering all four quadrants. It is noted that near elliptical symmetry can only be seen within the lower cut-off region in both dimensions, since for the higher cut-off region, there cannot be a closed response covering all four quadrants, as the response extends to infinity. For higher values of k_1 and k_2, even this extent of elliptical symmetry ceases to exist.

Highpass Filters

The highpass filter that has been used in this case is a fourth order filter with a cut-off beyond [0.4]. For a highpass filter, since the pass-band region exists from a certain cut-off frequency to infinity, it is entirely not possible to define elliptical symmetry in the passband. It can only be defined for a single quadrant(half a semi-ellipse)

and it has to be assumed that the symmetry exists upto infinity. Having defined the transfer function from the known parameters mentioned above(Eqn.(3.12)), the range of k for stability of the filter is given by $-1 < k < 1.4140$. It has been found that there exists a symmetry that can be approximated to an ellipse, at infinity for values of $k_1 = -0.80$ and $k_2 = -0.50$. Beyond this value this symmetry ceases to exist. Although elliptical symmetry cannot be clearly visualized for a highpass filter with separable denominator transfer function, it has been proved that there exists a symmetry that approximates an ellipse at infinity in the transition region of the filter.

5.1.4 Study of Elliptical Symmetry in 2-D Combination Filters

Another interesting aspect that has been considered in Chapter-4 of this work is to combine some common filters that have already been approximated for elliptical symmetry and study the extent of elliptical symmetry on the combination filters. There are three such combinations which have been considered.

Lowpass and Bandpass Combination Filter

In this case a lowpass and a bandpass filter which have been already considered in Chapters 2 and 3 respectively, have been used to form a combination response which resembles a lowpass response with non-uniform gain in its pass-band region. This has been obtained by adding the individual responses of the filters. It is seen here that elliptical symmetry does not exist in the combination filter in the transition region but still exists in certain parts of the response which are not an effect of the combination(Fig.(4.3)).

Lowpass and Lowpass Combination Filter

In this case, two lowpass filters of different cut-off frequencies, [0.5] and [0.2] respectively, have been used to form a combination response which resembles a bandpass response. This has been obtained by subtracting the two responses. It is seen here that elliptical symmetry is a distinct possibility in the region shown in Fig.(4.7). This study can also be extended to different magnitude regions to see how the subtraction of two near elliptical symmetric filters affect the symmetry.

Lowpass and Highpass Combination Filter

In this case a lowpass and a highpass filter which have analog cut-off frequencies of [0.5] and [0.7] respectively, have been used to form a combination response which resembles a Bandstop response. This has been obtained by adding the individual responses of the filters. It is seen here too that elliptical symmetry only exists in certain regions of the filters which are not entirely affected by the individual response of each other(Fig.(4.11)). In this case the lowpass response and the highpass response show their individual closeness to elliptical symmetry and we do not see the same in the transition band.

Thus, the overall purpose of this thesis has been to study the effect of elliptical symmetry on separable denominator 2-D transfer functions. Four of the most common types of filters have been chosen and studied. It has been seen largely that elliptical symmetry is possible in the lowpass and the bandpass responses and is not a distinct possibility in the highpass and bandstop responses due to the unlimited response range. The different filters and cases considered have been obtained after number of simulations. However it is possible to vary the values of k_1 and k_2 or the magnitude range under study to obtain innumerable instances of near elliptical symmetry in these cases. There is a lot of scope for future work in this respect.

From the foregoing, it is clear that it is possible to obtain 2-D elliptical symmetric filters, starting from 1-D filters. These could be lowpass, highpass, bandpass

or bandstop filters, obtained either directly or by a combination of other filters. Apart from the configuration considered, it appears possible that there may exist other configurations exhibiting elliptical symmetry and this is a suggestion for further work.

An interesting investigation would be to start from two all-pass filters which give rise to complementary filters. A method can be developed so as to analyze the stability for higher order($n > 8$) filters. It is possible that optimization tehnique can be used for the design of the type of filters discussed. A method can be developed so as to predict the magnitude range when the error is fixed regarding elliptical symmetry. Also a method can be developed to observe whether the elliptical symmetry is inclined or not when the numerator of the starting function is changed. These are some suggestions for future work.

Chapter 6

Appendix

6.1 Program-A1

```
%Matlab program to determine the range of k given the order n and the deviation of one or more angles
    %program code for  orders of 3,4,5,6,7,&8 butterworth filters
    %t1,t2,t3,t4 are the shift in angles
    %value of k is determined only when the filter is stable
    Ts=1;
    n=input('Input the order of the filter,n=')

    %%%%%%%%%%%%%3rd ORDER%%%%%%%%%%%%%%
    if n==3
    t1=input('Input the shift in t1=')
    T1=pi/3+t1;
    if T1<0
    fprintf('Unstability condition,the range of K cannot be determined')
    break
    elseif T1>=pi/2
    fprintf('Unstability condition,the range of K cannot be determined')
    break
    end
    a=cos(0);
    b=cos(T1);
    H1=tf(1,[1 a ],Ts);
    H2=tf(1,[1 2*b 1],Ts);
    H3=H1*H2;
    H4=1/H3;
```

```
[num den]=tfdata(H4,'v');
L=[num];
l=length(L);
j=1;
for i=1:l
if mod(i,2)==0
c(j)=L(i);
else
d(j)=L(i);
end
j=j+1;
end
%Separating the odd n even terms
c;
d;
H5=tf(1,[d 0],Ts);
H6=tf(1,c,Ts);
H7=(1/H6);
%Generating Hurwitz polynomial
H8=H7*H5;
[f g]=tfdata(H8,'v');
N=[f];
NL=length(N);
D=[g];
DL=length(D);
[m n]=tfdata(H8,'v');
r=roots([n]);
r2=r(2)*r(3);
k=m(2)*r2-1
fprintf('-1>K<%6d\n',k)
fprintf('The range of K is between -1 and %d',k)

%%%%%%%%%%%%4th ORDER%%%%%%%%%%%%%%
elseif n==4
t1=input('Input the shift in t1=')
t2=input('Input the shift in t2=')
T1=(pi/8+t1)
T2=(3*pi/8-t2)
if T1<0
fprintf('Unstability condition,the range of K cannot be determined')
break
elseif T1>T2
fprintf('Unstability condition,the range of K cannot be determined')
```

```
break
elseif T2<T1
fprintf('Unstability condition,the range of K cannot be determined')
break
elseif T2>=pi/2
fprintf('Unstability condition,the range of K cannot be determined')
break
end
a=cos(T1);
b=cos(T2);
H1=tf(1,[1 2*a 1],Ts);
H2=tf(1,[1 2*b 1],Ts);
H3=H1*H2;
H4=1/H3;
[num den]=tfdata(H4,'v');
L=[num];
l=length(L);
j=1;
for i=1:l
if mod(i,2)==0
c(j)=L(i);
else
d(j)=L(i);
end
j=j+1;
end
%Separating the odd n even terms
c;
d;
H5=tf(1,[c 0],Ts);
H6=tf(1,d,Ts);
H7=(1/H6);
%Generating Hurwitz polynomial
H8=H7*H5;
[f g]=tfdata(H8,'v');
N=[f];
NL=length(N);
D=[g];
DL=length(D);
H10=1/ tf(1,[N(3)-D(4)/D(2)  0 1],Ts);
H11=H10*H5;
H12=1/(tf(1,[1 0],Ts)*D(2));
[m n]=tfdata(H11,'v');
```

```
r=roots([n]);
r2=r(2)*r(3);
r1=1;
k=m(2)-1
fprintf('-1>K<%6d\n',k)
fprintf('The range of K is between -1 and %d',k)

%%%%%%%%%%%%5th ORDER%%%%%%%%%%%%%%
elseif n==5
t1=input('Input the shift in t1=')
t2=input('Input the shift in t2=')
T1=pi/5+t1;
T2=2*pi/5-t2;
if T1<0
fprintf('Unstability condition,the range of K cannot be determined')
break
elseif T1>T2
fprintf('Unstability condition,the range of K cannot be determined')
break
elseif T2<T1
fprintf('Unstability condition,the range of K cannot be determined')
break
elseif T2>pi/2
fprintf('Unstability condition,the range of K cannot be determined')
break
end
a=cos(0);
b=cos(T1);
e=cos(T2);
H0=tf(1,[1 a ],Ts);
H1=tf(1,[1 2*b 1],Ts);
H2=tf(1,[1 2*e 1],Ts);
H3=H0*H1*H2;
H4=1/H3;
[num den]=tfdata(H4,'v');
L=[num];
l=length(L);
j=1;
for i=1:l
if mod(i,2)==0
c(j)=L(i);
else
d(j)=L(i);
```

```
end
j=j+1;
end
%Separating the odd n even terms
c;
d;
H5=tf(1,[d 0],Ts);
H6=tf(1,c,Ts);
H7=(1/H6);
%Generating Hurwitz polynomial
H8=H7*H5;
[f g]=tfdata(H8,'v');
N=[f];
NL=length(N);
D=[g];
DL=length(D);
[m n]=tfdata(H8,'v');
r=roots([n]);
r2=r(2)*r(3);
r1=r(4)*r(5);
k=(((m(4)*r1*r2)-(r1+r2)*1)-(r1*(m(2)*(r1*r2)-1)))/r2
fprintf('-1>K<%6d\n',k)
fprintf('The range of K is between -1 and %d',k)

%%%%%%%%%%%%%6th ORDER%%%%%%%%%%%%%%
elseif n==6
t1=input('Input the shift in t1=')
t2=input('Input the shift in t2=')
t3=input('Input the shift in t3=')
T1=pi/12+t1;
T2=3*pi/12-t2;
T3=5*pi/12+t3;
if T1<0
fprintf('Unstability condition,the range of K cannot be determined')
break
elseif T1>T2
fprintf('Unstability condition,the range of K cannot be determined')
break
elseif T2<T1
fprintf('Unstability condition,the range of K cannot be determined')
break
elseif T2>T3
fprintf('Unstability condition,the range of K cannot be determined')
```

```
break
elseif T3<T2
fprintf('Unstability condition,the range of K cannot be determined')
break
elseif T3>=pi/2
fprintf('Unstability condition,the range of K cannot be determined')
break
end
a=cos(T1);
b=cos(T2);
e=cos(T3);
H1=tf(1,[1 2*a 1],Ts);
H2=tf(1,[1 2*b 1],Ts);
H9=tf(1,[1 2*e 1],Ts);
H3=H1*H2*H9;
H4=1/H3;
[num den]=tfdata(H4,'v');
L=[num];
l=length(L);
j=1;
for i=1:l
if mod(i,2)==0
c(j)=L(i)
else
d(j)=L(i)
end
j=j+1;
end
%Separating the odd n even terms
c;
d;
H5=tf(1,[c 0],Ts);
H6=tf(1,d,Ts);
H7=(1/H6);
%Generating Hurwitz polynomial
H8=H7*H5;
[f g]=tfdata(H8,'v');
N=[f];
NL=length(N);
D=[g];
DL=length(D);
H10=1/ tf(1,[N(3)-D(4)/D(2) 0 N(5)-D(6)/D(2) 0 1],Ts);
H11=H10*H5;
```

```
H12=1/(tf(1,[1 0],Ts)*D(2));
[m n]=tfdata(H11,'v');
r=roots([n]);
r2=r(2)*r(3);
r1=r(4)*r(5);
k=(((m(4)*r1*r2)-(r1+r2)*1)-(r1*(m(2)*(r1*r2)-1)))/r2
fprintf('-1>K<%6d\n',k)
fprintf('The range of K is between -1 and %d',k)

%%%%%%%%%%%%7th ORDER%%%%%%%%%%%%%
elseif n==7
t1=input('Input the shift in t1=')
t2=input('Input the shift in t2=')
t3=input('Input the shift in t3=')
T1=pi/7+t1;
T2=2*pi/7-t2;
T3=3*pi/7+t3;
if T1<0
fprintf('Unstability condition,the range of K cannot be determined')
break
elseif T1>T2
fprintf('Unstability condition,the range of K cannot be determined')
break
elseif T2<T1
fprintf('Unstability condition,the range of K cannot be determined')
break
elseif T2>T3
fprintf('Unstability condition,the range of K cannot be determined')
break
elseif T3<T2
fprintf('Unstability condition,the range of K cannot be determined')
break
elseif T3>=pi/2
fprintf('Unstability condition,the range of K cannot be determined')
break
end
a=cos(T1);
b=cos(T2);
e=cos(T3);
H0=tf(1,[1 1],Ts);
H1=tf(1,[1 2*a 1],Ts);
H2=tf(1,[1 2*b 1],Ts);
H9=tf(1,[1 2*e 1],Ts);
```

```
H3=H0*H1*H2*H9;
H4=1/H3;
[num den]=tfdata(H4,'v');
L=[num];
l=length(L);
j=1;
for i=1:l
if mod(i,2)==0
c(j)=L(i);
else
d(j)=L(i);
end
j=j+1;
end
%Seperating the odd n even terms
c;
d;
H5=tf(1,[d 0] ,Ts);
H6=tf(1,c,Ts);
H7=(1/H6);
%Generating Hurwitz polynomial
H8=H7*H5;
[f g]=tfdata(H8,'v');
N=[f];
NL=length(N);
D=[g];
DL=length(D);
[m n]=tfdata(H8,'v');
r=roots([n]);
r1=r(2)*r(3);
r2= r(4)*r(5);
r3=r(6)*r(7);
%% value of F
Fd=((((r1-r2)/(r1*r3-r2*r3))*(r1*r2-r2*r3)))-(r1-r3);
Dd=(r1-r2);
FN=m(6)*r1*r2*r3/r3-(r1*r2+r1*r3+r2*r3)/r3 - m(4)*(r1*r2*r3) +(r1+r2+r3) + (m(2)*r1*r2*r3-1)*r3;
FD=(r1*r2+r1*r3+r2*r3)/r3 - (r1+r2+r3) + r3;
k=FN/FD
fprintf('-1>K<%6d\n',k)
fprintf('The range of K is between -1 and %d',k)

%%%%%%%%%%%%%8th ORDER%%%%%%%%%%%%%%%
else n==8
```

```
t1=input('Input the shift in t1=')
t2=input('Input the shift in t2=')
t3=input('Input the shift in t3=')
t4=input('Input the shift in t4=')
T1=pi/16+t1;
T2=3*pi/16-t2;
T3=5*pi/16+t3;
T4=7*pi/16-t4;
if T1<0
fprintf('Unstability condition')
break
elseif T1>T2
fprintf('Unstability condition,the range of K cannot be determined')
break
elseif T2<T1
fprintf('Unstability condition,the range of K cannot be determined')
break
elseif T2>T3
fprintf('Unstability condition,the range of K cannot be determined')
break
elseif T3<T2
fprintf('Unstability condition,the range of K cannot be determined')
break
elseif T3>T4
fprintf('Unstability condition,the range of K cannot be determined')
break
elseif T4<T3
fprintf('Unstability condition,the range of K cannot be determined')
break
elseif T4>=pi/2
fprintf('Unstability condition,the range of K cannot be determined')
break
end
a=cos(T1);
b=cos(T2);
e=cos(T3);
h=cos(T4);
H0=tf(1,[1 2*a 1],Ts);
H1=tf(1,[1 2*b 1],Ts);
H2=tf(1,[1 2*e 1],Ts);
H9=tf(1,[1 2*h 1],Ts);
H3=H0*H1*H2*H9;
H4=1/H3;
```

```
[num den]=tfdata(H4,'v');
L=[num];
l=length(L);
j=1;
for i=1:l
if mod(i,2)==0
c(j)=L(i);
else
d(j)=L(i);
end
j=j+1;
end
%Separating the odd and even terms
c;
d;
H5=tf(1,[c 0] ,Ts);
H6=tf(1,d,Ts);
H7=(1/H6);
% Generating Hurwitz polynomial
H8=H7*H5;
[f g]=tfdata(H8,'v');
N=[f];
NL=length(N);
D=[g];
DL=length(D);
H10=1/ tf(1,[N(3)-D(4)/D(2) 0 N(5)-D(6)/D(2) 0 N(7)-D(8)/D(2) 0 1],Ts);
H11=H10*H5;
H12=1/(tf(1,[1 0],Ts)*D(2));
[m n]=tfdata(H11,'v');
r=roots([n]);
r1=r(2)*r(3);
r2= r(4)*r(5);
r3=r(6)*r(7);
FN=(m(6)*r1*r2*r3/r3)-(r1*r2+r1*r3+r2*r3)/r3-m(4)*(r1*r2*r3)+(r1+r2+r3) + (m(2)*r1*r2*r3-1)*r3;
FD=(r1*r2+r1*r3+r2*r3)/r3 - (r1+r2+r3) + r3;
k=FN/FD
fprintf('-1>K<%6d\n',k)
fprintf('The range of K is between -1 and %d',k)
end
%%%End of program
```

Bibliography

[1] Rabiner, R.L. and Gold, B. "Theory and Application of Digital Signal Processing" Prentice Hall, 1975.

[2] Jury, E.I. "Inners and Stability of Dynamic Systems", John Wiley and Sons, 1974.

[3] Gargour, C.S. and Ramachandran, V. "Generation of very strictly Hurwitz polynomials and Applications to 2-D Filter Design", *Control and Dynamic Systems, Academic Press* Inc. vol.69, pp. 211-254, 1995.

[4] Goodman, D. "Some difficulties with Double Bilinear Transformation in 2-D Digital Filter Design" *Proc. IEEE*, vol.66, July 1978.

[5] Tzafestas, S.G. "Multidimensional Systems: Techniques and Applications", 1986.

[6] Kavitharajan, P., and Swamy, M.N.S. "Some results on the nature of a two dimensional filter function possessing certain symmetry in its magnitude response", *IEE Journal on Electronic Circuits and Systems,* 2, (5), pp.147-153, Sept. 1978.

[7] Shanks, J.L., Treitel, S. and Justice, J.H., "Stability of two-dimensional Recursive Filters". *IEEE Trans in Audio-Electro Acoustics*, vol. AU-20, June 1972.

[8] Mitra, S.K., Sagar, A.D. and Pendergrass, N.A. "Realization of two-dimensional Recursive Digital Filters" *IEEE Trans. on Circuits and Systems*, vol. Cas-22, No.3, 1975.

[9] Swamy, M.N.S., Thyagarajan, K.S., and Ramachandran, V., "Two-dimensional wave digital filters using doubly terminated two variable LC-ladder configurations". *Journal of Franklin Institute,* vol.304, No.4/5, pp.201-215.

[10] Mc Clellan, J.H. "The design of two-dimensional digital filters by transformations". *Proc. of the 7th Annual Princeton conference on information sciences and systems*, 1973, pp.247-251.

[11] Bernabli, M., Cappellini, V., and Emiliani, P.M. :"A method for designing 2-D Recursive Digital Filters having Circular Symmetry". *Proc. of Florence conference on digital signal processing, Sept.11th-13th*, 1975, pp.196-203.

[12] Kavitharajan, P., and Swamy, M.N.S. :"Quadrantal symmetry associated with two dimensional digital transfer functions", *ibid.*, vol. CAS-25, pp.340-433, 1978.

[13] Pai, K.R., Murthy, K.V.V., Ramachandran, V., "Complementary Pole-Pair Filters and Pole Parameter Transformations", *J.Circuits and Systems and Computers*, vol.6, No.4, pp.319-350, 1996.

[14] Cappellini, V. and Constantinides, A.G. and Emiliani, P.L., "Digital Filters and their applications", *Academic Press*, New york. 1978.

[15] Goodman, D. "Some stability properties of two-dimensional linear shift-invariant digital filters" *IEEE Trans. on Circuits and Systems.* vol. CAS-24, No.4, pp.201-208, April 1977.

[16] Huang. T.S., "Stability ot two-dimensional recursive filters". *IEEE Trans. in Audio Electro-acoustics*, vol. AU-20, pp.158-163, 1972.

[17] Mersereau, R.M., Mecklenbruker, W.F.G and Quatieri.Jr, T.F., "McClellan transformations for 2-D digital filtering: I.Design", *IEEE Trans. on Circuits and Systems.* vol. CAS-23, No.7, pp.405-414, April 1976.

[18] Hu, J.V. and Rabiner, L.R., "Design techniques for two-dimensional digital filters", *IEEE Trans. in Audio Electro acoustics*, vol. AU-20, No.1, pp.249-257, 1972.

[19] Harris, D.B and Mersereau, R.M., "A comparison of algorithms of minimax design of two-dimensional linear phase FIR digital filters", *IEEE Trans. in Acoustics Speech Signal Processing.*, vol. ASSP-25, No.6, pp.492-500, 1977.

[20] Huang, T.S., "Two-dimensional windows", *IEEE Trans. in Audio Electroacoustics*, vol. AU-20, No.1, pp.88-89, 1972.

[21] Seetharaman, S., "Study of Circularly Symmetrical Two-Dimensional Digital Filters Possessing Separable Denominator Transfer Functions", Thesis, Concordia University, pp.21-25, June 2000.

[22] Costa, J.M. and Venetsanopoulos, A.N., "Design of circularly symmetric two-dimensional filters", *IEEE Trans. in Acoustics Speech Signal Processing*, vol. ASSP-22, No.6, pp.432-443, 1974.

[23] Kavitharajan, P., and Swamy, M.N.S, "Symmetry Constraints on two-dimensional Half-Plane Digital Transfer Functions". *IEEE Trans. On Acoustics, Speech and Signal Processing*, vol. ASSP-27. No.5, pp.506-511, 1979.

[24] Gargour, C.S. and Ramachandran, V. "Generation of stable 2-D Transfer Functions having variable magnitude characteristics", *control and Dynamic Systems, Academic Press Inc.* vol.69, pp.255-297, 1995.

[25] Lavu, K.C. and Ramachandran, V. "Study of Elliptical Symmetry in Two-Dimensional IIR Butterworth Digital Filters", *In Proc. IEEE International Midwest Symposium on Circuits and Systems.* July 2004.

[26] Su, K.L, "Analog Filters", Chapman and Hall, 1996.

[27] Matrox Imaging Library(MIL)-User Guide, Matrox Electronic System Inc. Montreal.